# PROBING A REDOX SWITCH TO SAVE LIVES:

## Development of a Bioassay for Angiotensinogen to Identify Women Prone to Pre-Eclampsia

**Letitia Hayley Gilmour**

A thesis submitted in partial fulfilment of the requirements for the

**Degree of Master of Science in Biochemistry**


**School of Biological Sciences**

**University of Canterbury**

**2014**

# ABSTRACT

Angiotensinogen is a blood protein that plays a critical role in the regulation of blood pressure in the body. This protein exists in two forms, oxidised and reduced, determined by the presence or absence of a disulfide bridge between Cys 18 and Cys 138. The ratio of oxidised to reduced angiotensinogen is 60:40 in the blood of healthy individuals—an equilibrium that is disrupted in women who develop pre-eclampsia, leading to a higher proportion of oxidised angiotensinogen in the blood.[1] Pre-eclampsia, one of the leading causes of premature births, is a severe and potentially fatal pregnancy condition characterised by the sudden onset of symptoms such as high blood pressure and proteinuria typically during the third trimester. This condition is responsible for an estimated 550,000 deaths globally each year, and with no available treatment or cure other than early delivery of the child, there is a desperate need for a reliable and predictive diagnostic test for this condition.

Can we use angiotensinogen as a biomarker for the early diagnosis of pre-eclampsia? Being able to distinguish between reduced and oxidised angiotensinogen and determine the relative amounts of each in blood samples would be of a huge diagnostic value for this condition. This thesis outlines the expression and purification of recombinant human angiotensinogen in *Escherichia coli*, and the development of an antibody-based SPR assay for angiotensinogen that was subsequently used to probe whether reduced and oxidised angiotensinogen can be distinguished experimentally. The assay developed was sensitive and reproducible, and demonstrated that the reduced and oxidised forms can be distinguished experimentally. The antibody bound the two forms with differential affinity, due to differences in both the association and dissociation rates of the two forms with the monoclonal antibody.

Finally, in an attempt to further elucidate the differences between the two redox states of angiotensinogen, molecular dynamic simulations were carried out on angiotensinogen in the presence or absence of the disulfide bond between Cys 18 and Cys 138. These simulations revealed some quite striking differences in the dynamics between the two forms. Reduced angiotensinogen was found to be more dynamic in regions critical for binding to renin, providing a possible explanation for the reported differential affinity that renin displays for the two forms.[1] Thus, reduced and oxidised angiotensinogen show some quite distinct differences and can be distinguished in an SPR-based assay, highlighting their potential for use as a biomarker in a diagnostic bioassay.

# ACKNOWLEDGEMENTS

*"If I have seen further, it is by standing on the shoulders of Giants"*

- Sir Isaac Newton [2]

This project has been a huge undertaking, and there are many people I wish to extend my gratitude towards for their contributions, and without whom completing this thesis simply would not have been possible. It has been a long and challenging road, but I can now see how truly rewarding this journey has been. I am sincerely thankful for all your help along the way and greatly indebted to all of you.

Firstly, I would like to say a huge thank you to my supervisors for supporting me throughout this project. To Professor Conan Fee, for originally taking me on as a summer student with very little experience, and letting me stick around. Also, a big thank you to Dr Renwick Dobson for letting me join the Dobson research gang even though my project had nothing to do with crystallography, and for your unending enthusiasm for my project.

Secondly, I would have been so lost in the CAPE lab and with the SPR had it not been for Rayleen Fredericks and her wealth of helpful advice, thank you so much for everything you taught me along the way! Also, postgraduate life would not have been so enjoyable had it not been for the great group of people on the 6th floor, particularly those residing in office 630, and the Dobson research group. A big thanks to all of you for answering questions, helping to proofread my thesis, and providing much needed distractions—you certainly made the days much more interesting!

I am very grateful to the team at Canterbury Scientific, especially Maurice Owen and Neil Pattinson, for being involved every step of the way throughout this project, for not only providing financial support, but also for helping to find solutions to problems as they arose, and for looking over my thesis drafts. It was great to have input from outside of the university and to get a taste of the industry perspective. This project truly would not have been possible without your continued support.

Also, I cannot forget those who had a huge input from further afield. I would like to extend a big thank you to Yahui Yan at the University of Cambridge for sending me DNA and protein, and answering my seemingly unending list of questions. Also to Tim Yandle and Darrell Wang at Canterbury Endolab for providing me with protein and answering yet even more questions. And finally, a huge thanks needs to be extended to Ben Porebski at Monash University for all his help with the molecular dynamics simulations—these simply would not have been possible without your dedicated help!

And lastly, but by no means least, I would not have made it through to the end of this journey had it not been for the help and support of all my family and friends, who were there for me every step of the way. A huge thank you needs to go to my parents for being so supportive, and for a putting a roof over my head for the last two years, even when I sometimes only came home to sleep, and for forever asking if I had finished my lab work yet. To Emma and Sian, I'm going to miss the countless coffee and lunch dates that certainly brightened the long days over the last few years. And finally, thank you to all my friends who provided much needed distraction to the, at times, monotonous thesis life—I really couldn't have made it to the end without you!

# TABLE OF CONTENTS

# ABBREVIATIONS

| | |
|---|---|
| A | Adenine |
| Å | Angstrom |
| $A_{280}$ | Absorbance of light at 280 nm |
| ACE | Angiotensin converting enzyme |
| ACE2 | Angiotensin converting enzyme 2 |
| ADAM-12s | A disintegrin and metalloprotease domain-containing protein 12s |
| AGT | Angiotensinogen |
| Amp | Ampicillin |
| anti-AGT mAb | Anti-angiotensinogen monoclonal antibody |
| anti-IgG mAb | Anti-immunoglobulin G monoclonal antibody |
| Asn | Asparagine |
| Asp | Aspartate |
| atm | Standard atmosphere unit |
| AT1R | Angiotensin type 1 receptor |
| AT2R | Angiotensin type 2 receptor |
| AU | Absorbance unit |
| BlgA | β-lactoglobulin A |
| bp | Base pairs |
| BSA | Bovine serum albumin |
| C | Cytosine |
| °C | Degrees Celsius |
| Cα, C-alpha | Alpha carbon atom |
| Cam | Chloramphenicol |
| cAMP | Cyclic adenosine monophosphate |
| CAT | Chloramphenicol acetyltransferase |
| cDNA | complementary DNA |
| Co | Cobalt |
| Cys | Cysteine |
| Da | Dalton |
| DsbC | Disulfide bond isomerase C |
| DNA | Deoxyribonucleic acid |
| DNase | Deoxyribonuclease |
| dNTPs | Deoxyribonucleotide triphosphates |
| DTT | Dithiothreitol |

| | |
|---|---|
| *E. coli* | *Escherichia coli* |
| EDAC | 1-ethyl-3-(3-dimethylaminopropyl)carbodiimide |
| EDTA | Ethylenediaminetetraacetic acid |
| EtBr | Ethidium bromide |
| Fc | Fragment cystallizable region on antibody |
| fs | Femtosecond |
| g | Gram |
| G | Guanine |
| *gor* | Glutathione reductase gene |
| GST | Glutathione S-transferase |
| hAGT | Human angiotensinogen |
| HELLP Syndrome | Hemolytic anemia, elevated liver enzymes, and low platelet count syndrome |
| HF | High fidelity |
| His | Histidine |
| HCl | Hydrochloric acid |
| HEK cells | Human embryonic kidney cells |
| IgG | Immunoglobulin G |
| IMAC | Immobilised metal ion affinity chromatography |
| INAD | Inactivation no after-potential D visual scaffold protein |
| IPTG | Isopropyl-β-D-thiogalactopyranoside |
| iTRAQ | Isobaric tags for relative and absolute quantitation |
| IUGR | Intrauterine growth restriction |
| K | Degrees Kelvin |
| $k_a$ | Kinetic association rate constant |
| Kan | Kanamycin |
| kb | Kilobase |
| KCl | Potassium chloride |
| $k_d$ | Kinetic dissociation rate constant |
| $K_D$ | Equilibrium dissociation constant |
| kDa | Kilodalton |
| $KH_2PO_4$ | Potassium dihydrogen phosphate |
| $K_2HPO_4$ | Dipotassium hydrogen phosphate |
| kJ | Kilojoule |
| $k_m$ | Initial rate of mass transport of an analyte to a ligand-bound surface |
| $K_m$ | Michaelis-Menten constant |
| L | Litre |
| LB | Luria-Bertani broth |
| LDS | Lithium dodecyl sulfate |
| Lys | Lysine |

| | |
|---|---|
| M | Molar (mol/L, mole per litre) |
| M235T | methionine to threonine polymorphism at position 235 of angiotensinogen |
| mAb | Monoclonal antibody |
| MCS | Multiple cloning site |
| MES | 2-(*N*-morpholino)ethanesulfonic acid |
| MD | Molecular dynamics |
| mg | Milligram |
| mg/mL | Milligram per millilitre |
| $MgCl_2$ | Magnesium chloride |
| $MgSO_4$ | Magnesium sulfate |
| min | Minutes |
| mL | Millilitre |
| mm | Millimetre |
| mM | Millimolar (mmol/L, millimole per litre) |
| mPEG | Methoxy polyethylene glycol maleimido-propionamide |
| MQ water | Milli-Q water |
| mRNA | Messenger RNA |
| mV | Millivolt |
| MW | Molecular weight |
| MWCO | Molecular weight cut-off |
| Na Acetate | Sodium acetate |
| NaCl | Sodium chloride |
| $Na_2HPO_4$ | Disodium hydrogen phosphate |
| $NaIO_4$ | Sodium metaperiodate |
| NaOH | Sodium hydroxide |
| NEM | *N*-ethylmaleimide |
| ng | Nanogram |
| ng/µL | nanogram per microlitre |
| NHS | *N*-hydroxysuccinamide |
| nm | Nanometre |
| nM | Nanomolar (nmol/L, nanomole per litre) |
| NPT | Isothermal–isobaric ensemble (moles (N), pressure (P), and temperature (T)) |
| ns | Nanosecond |
| NVT | Canonical ensemble (moles (N), volume (V), and temperature (T)) |
| $OD_{600}$ | Optical density at 600 nm |
| OPA | *O*-phthalaldehyde |
| PAPP-A | Pregnancy-associated plasma protein A |
| PBS | Phosphate buffered saline |
| PBST | Phosphate buffered saline with Tween-20 |

| | |
|---|---|
| PCR | Polymerase chain reaction |
| PDB | Protein data bank |
| PEG | Polyethylene glycol |
| PES | Polyether sulfone |
| PIGF | Placental growth factor |
| PMSF | Phenylmethanesulfonyl fluoride |
| PP-13 | Placental protein-13 |
| (P)RR | (Pro)renin receptor |
| ps | Picosecond |
| psi | Pound per square inch |
| PVDF | Polyvinylidene difluoride |
| RAS | Renin-angiotensin system |
| εRF | Relative dielectric permittivity constant |
| RMSD | Root Mean Square Deviation |
| RMSF | Root Mean Square Fluctuation |
| RNA | Ribonucleic acid |
| RNase | Ribonuclease |
| rpm | Revolutions per minute |
| RU | Response unit |
| SDS | Sodium dodecyl sulphate |
| SDS-PAGE | Sodium dodecyl sulphate polyacrylamide gel electrophoresis |
| sec | Seconds |
| SEC | Size exclusion chromatography |
| Serpin | Serine protease inhibitor |
| sflt-1 | Soluble fms-like tyrosine kinase 1 |
| SOC | Super optimal broth with catabolite repression |
| SPC | Simple-point-charge |
| SPR | Surface plasmon resonance |
| sST2 | Soluble somatostatin receptor 2 |
| Str | Streptomycin |
| SUMO | Small ubiquitin-like modifier |
| SUMO-AGT | SUMOylated angiotensinogen |
| SUMO-CAT | SUMOylated chloramphenicol acetyltransferase |
| T | Thymine |
| TAE | Tris acetate EDTA |
| *Taq* | *Thermus aquaticus* |
| TB | Terrific Broth |
| Tet | Tetracycline |
| TCEP | Tris(2-carboxyethyl)phosphine |

| | |
|---|---|
| TE | Tris-EDTA |
| tRNA | Transfer RNA |
| *trxB* | Thioredoxin reductase B |
| µg | Microgram |
| µg/mL | Microgram per millilitre |
| µL | Microlitre |
| µL/min | Microlitre per minute |
| Ulp | Ubiquitin-like protein |
| µm | Micrometre |
| µM | Micromolar (µmol/L, micromole per litre) |
| µs | Microsecond |
| UV | Ultraviolet light |
| V | Volt |
| VEGF | Vascular endothethial growth factor |
| vs. | Versus |
| v/v | Volume per volume |
| w/v | Weight per volume |

# LIST OF FIGURES AND TABLES

## CHAPTER ONE



## CHAPTER THREE

**CHAPTER FOUR**

**CHAPTER FIVE**

# *Chapter One*

# INTRODUCTION

## 1.1 PRE-ECLAMPSIA

### *1.1.1 Background*

Pre-eclampsia is a severe and potentially fatal pregnancy condition that occurs in approximately 2% to 7% of all pregnancies and is one of the leading causes of maternal and perinatal morbidity and mortality worldwide. It is estimated that pre-eclampsia is responsible for approximately 50,000 maternal and 500,000 infant deaths globally each year.[3, 4] The condition is characterised by high blood pressure and proteinuria, which develop after the 20$^{th}$ week of gestation,[5, 6] and often displays sudden onset, developing in a matter of days or even hours with no prior warning. Without medical intervention, pre-eclampsia can develop into HELLP syndrome (Hemolytic anemia, Elevated Liver enzymes, and Low Platelet count) or even eclampsia, which causes neurological symptoms and seizures, leading to organ damage, coma, brain damage, and possible death.[5, 7, 8] Although symptoms typically abate rapidly postpartum,[9] both pre-eclampsia and eclampsia have been observed to develop anywhere up to four weeks following delivery.[10] Recently, it has been hypothesized that pre-eclampsia actually exists as two separate conditions that should be treated and managed differently:[11] early onset pre-eclampsia (prior to 34 weeks) and late-onset pre-eclampsia (above 34 weeks gestation). Early onset pre-eclampsia is typically the more severe form of the condition, which represents approximately 5% to 20% of all pre-eclampsia cases and generally results in premature birth; while late-onset pre-eclampsia, representing the majority of pre-eclamptic cases, on the whole tends to be less severe

and is thought, in part, to be due to pre-existing maternal conditions such as obesity, diabetes mellitus, and renal disease.[5, 12]

Pre-eclampsia is thus a major health concern. Up to 65% of perinatal deaths are due to pre-eclampsia and it is also a major cause of maternal mortality.[13, 14] Intrauterine growth restriction (IUGR) and premature birth, along with their associated short- and long-term health conditions, are just a few of the adverse outcomes that result from the condition, which can have severe impacts on the life of the child and are also costly for the healthcare sector.[5, 15] Interestingly, the effects of pre-eclampsia are not only short term—having pre-eclampsia has been associated with a significantly elevated risk of developing cardiovascular disease, stroke and chronic hypertension later in life, not only for the mother but also the child.[16, 17] Whether this association is purely confounded due to the shared risk factors and pathophysiology of these hypertensive diseases, or whether pre-eclampsia actively causes or triggers cardiovascular disease is unknown and, although difficult to tease apart, is something that does need to be investigated. Being a hypertensive disorder, pre-eclampsia shares many risk factors with cardiovascular disease, such as obesity, insulin resistance, hypertension, as well as elevated lipids and coagulation of the blood.[18]

### *1.1.2 Blood Pressure Control, Hypertension, and their Implications on Health*

Blood pressure is the force that is exerted by circulating blood upon the walls of blood vessels[19] and is at the heart of a number of disease states. Blood pressure can vary throughout the day, according to circadian rhythms,[20] and if it gets too high or too low, can have significant impacts on health. Blood pressure is primarily controlled by the Renin-Angiotensin System (RAS), a hormone cascade that is known to regulate blood pressure through alterations in salt and water balance, vascular tone, and the secretion of aldosterone from the adrenal gland.[19, 21]

This multi-step cascade (for an overview of the RAS see Figure 1.1) produces a potent vasoconstricting peptide, angiotensin-II, which activates the angiotensin type I receptor (AT1R), leading to vasoconstriction and secretion of aldosterone. Aldosterone release results in sodium and water retention by the kidney and a subsequent increase in blood pressure.[19]

High blood pressure is particularly harmful as it means that the heart has to work harder to pump blood into the arteries and around the body, and is commonly termed hypertension. Hypertension is a risk factor for the development of atherosclerosis and hardening of the arteries, which, if left untreated, can result in stroke, cardiovascular disease, and kidney failure.[19] Hypertension is becoming increasingly common in the developing world and is a leading cause of morbidity and mortality globally.[22] Hypertension is responsible for nearly 13% of total deaths worldwide, with the World Health Organisation estimating that more than 17 million people die as a result of cardiovascular disease each year.[23] It has been suggested that by 2025 approximately 29% of the adult population worldwide could be suffering from hypertension.[24]

Chronic essential hypertension is a multi-factorial disease, with many risk factors pre-disposing individuals to develop it including an individual's weight, age, sex, ethnicity, smoking status, levels of physical activity, diet, alcohol consumption, stress, as well as other medical conditions.[22, 25] Alongside environmental factors, hypertension also has a strong genetic component. One gene that has been associated with increased hypertension risk in numerous studies is the AGT gene, which encodes the protein angiotensinogen.[26, 27] A polymorphism within the AGT gene, which results in an amino acid substitution at position 235 (M235T), was shown to be significantly associated with hypertension and increased plasma angiotensinogen levels,[27] and has received much interest from researchers. The protein itself is the substrate of the first and rate-limiting step of the RAS cascade,[28] and thus plays an important role in the regulation of blood pressure. Angiotensinogen levels positively correlate with blood pressure;[29] blood pressure will decrease when antibodies specific to angiotensinogen are injected[30] and

increase in response to injection with angiotensinogen,[31] and transgenic mice expressing rat angiotensinogen display elevated blood pressure.[32] It has been postulated that there may have been an evolutionary advantage to having high circulating angiotensinogen levels when our ancestors lived in Sub-Saharan Africa, where there was little salt in the environment. Things have rapidly changed in our modern Western world; salt is readily available and present in high amounts in our diet, making the once advantageous plasma angiotensinogen levels now disadvantageous—evolution just can't keep up with our fast food way of life![22, 33]

Because of the complex interplay of environmental and genetic risk factors that contribute to an individual's risk of developing hypertension and its subsequent complications, it has been a difficult road (and will remain so in the years to come) for clinicians to better come to grips with understanding the underlying factors that contribute to hypertension, in order to prevent and treat the condition more effectively.[22] Lifestyle changes including exercising, reducing weight, and lowering salt intake can be very beneficial for some individuals in lowering hypertensive risk and treating the disorder.[34] However, lifestyle changes alone are often not enough, and anti-hypertensive medications are frequently prescribed to treat and manage this condition. Common hypertensive therapies include α- and β-blockers, calcium channel blockers and diuretics,[19, 34, 35] as well as compounds which target the RAS cascade such as angiotensin-converting enzyme (ACE) inhibitors and angiotensin II receptor blockers.[19, 36] Difficulties arise in targeting the RAS system, however, as patients often differentially respond to the various anti-hypertensive therapies in a seemingly unpredictable manner. In addition, over time the body overcompensates for the inhibition of the RAS by producing more renin,[19] the enzyme responsible for the first and rate-limiting step in the cascade, resulting in a decrease in the therapeutic benefit of the anti-hypertensive agent. Ideally, inhibition of renin at the first step of the RAS cascade would be more effective as it does not lead to a reactive rise in active renin, but producing bioavailable potent renin inhibitors has been challenging.[37] Despite the difficulties,

aliskiren, a potent renin inhibitor has recently been approved for clinical use for the treatment of hypertensive disorders.[36]

### *1.1.3 The Effects of Pregnancy on the Body and How Pre-eclampsia Alters the Balance*

Throughout the course of a normal healthy pregnancy, many physiological changes take place in the mother's body, particularly in the cardiac and renal systems, to adequately enable the body to cope with the growing demands for increased blood supply and nutrients.[38] After falling pregnant, women experience changes to their cardiac output, blood coagulation, and inflammatory responses, as well as alterations to their response to insulin and lipid modifications in the serum.[4, 39, 40] The RAS cascade itself is altered quite considerably from the onset of pregnancy, with most components of the system being upregulated (see Table 1.1). Renin secretion is increased, and as the placenta grows it stimulates higher levels of angiotensinogen to be synthesized, ultimately leading to higher circulating angiotensin II levels.[9, 41-43] Surprisingly, despite these changes, in healthy pregnancies women appear to be less sensitive to angiotensin II levels,[9] with pregnant women requiring double the amount of angiotensin II compared with non-pregnant women to obtain the same increase in blood pressure, and they actually display a slightly decreased blood pressure in the first two trimesters before their blood pressure returns to normal during the final trimester[38]—it seems that the changes that take place in the RAS are crucial for maintaining a healthy state during pregnancy.

This fine balance maintained during a normal pregnancy can, however, be easily upset, leading to the hypertensive pregnancy condition known as pre-eclampsia. Pre-eclamptic women do not experience the same increase in plasma volume that occurs during normal pregnancies and this, coupled with a decrease in the majority of RAS components (Table 1.1) and a heightened sensitivity to the vasopressor effects of angiotensin II, lead to serious dysfunction of

the salt-water balance which is critical for the health of both mother and fetus.[44] It is thought that the altered fluid and salt-water balance severely limits the placental supply, preventing adequate placental perfusion and fetal substrate delivery, and raising blood pressure, ultimately leading to the clinically manifest symptoms of pre-eclampsia.[44-46] Despite the changes in the RAS cascade and the condition being extensively studied for many years, the underlying causative mechanisms of pre-eclampsia still remain elusive.

| RAS COMPONENTS | NORMOTENSIVE PREGNANCY | PRE-ECLAMPTIC PREGNANCY |
|---|---|---|
| **Angiotensinogen** | ⬆ | ↓ |
| **Renin** | ⬆ | ↑ |
| **Renin Activity** | ⬆ | =/↓ |
| **Aldosterone** | ⬆ | ↓ |
| **Angiotensin II** | ⬆ | =/↓ |
| **Angiotensin II Activity** | ↓ | ⬆ |
| **Angiotensin (1 – 7)** | ⬆ | ↓ |
| **ACE** | ↓ | =/↓ |
| **ACE2** | ⬆ | ↓ |
| **ACE2 Activity** | ⬆ | ↓ |
| **AT1R** | = | ⬆ |

*Table 1.1:*

*Serum levels of the RAS components in both normotensive and pre-eclamptic pregnancies compared to non-pregnant controls where ⬆ indicates significantly increased levels compared with non-pregnancy, ↑ indicates slightly increased levels compared with non-pregnancy, = represents same as non-pregnancy, and ↓ represents decreased levels when compared with non-pregnant controls (adapted from Yang et al. 2013 [44] with permission from the Society for Endocrinology © 2013).*

### *1.1.4 Oxidative Stress and Pre-eclampsia*

Pre-eclampsia is commonly described as a condition characterised by oxidative stress.[18, 47, 48] It is thought that placental dysfunction leads to the excessive production of reactive oxygen species, ultimately resulting in endothelial cell dysfunction and the symptoms of pre-eclampsia.[49, 50] One study monitored the levels of selenium in serum and toenails of pregnant women and found that women with pre-eclampsia had significantly reduced selenium levels compared to the normotensive pregnant and non-pregnant controls.[48] Selenium is essential for the activity of the selenoproteins, such as glutathione peroxidases, which display antioxidant activity. Glutathione peroxidases provide protective effects for the endothelial cells by destroying reactive oxygen species such as hydroperoxides and oxidised lipoproteins. Worryingly, the study found that even the normotensive controls had depleted selenium levels below recommended guidelines and were not receiving the full protection from glutathione peroxidases as a result.[48]

Reactive oxygen species can have effects on the RAS as well. Oxidative stress enhances the cleavage of angiotensin I from angiotensinogen and also increases expression of the AT1R receptor, while angiotensin II can exert some of its vasoconstrictor effects through the production of reactive oxygen species also.[51] Changes to both the maternal and fetal antioxidant levels in the circulation have been observed[52, 53] and pre-eclampsia also results in increased levels of lipid peroxidation in the placenta.[54]

### *1.1.5 Treatment and Management of Pre-eclampsia*

There is presently no cure or effective treatment for pre-eclampsia—delivery remains the one and only option in cases of severe pre-eclampsia when the life of the mother or baby is at

risk.[9, 16] Symptoms normally subside within a couple of days after giving birth and by 12 weeks post-delivery a pre-eclamptic woman's blood pressure should have returned to normal.[9, 18] However, early delivery often comes at the expense of the health or even life of the child.[9, 55] Ideally the pregnancy needs to continue for as long as possible to allow the infant's lungs to mature prior to birth, and thus conservative management (typically bed rest and anti-hypertensive therapy) is provided to prolong the pregnancy as long as it is medically safe and possible to do so, while at the same time manage the symptoms and prevent them from worsening.[4, 5]

Magnesium sulfate is commonly employed by clinicians in order to prevent the seizures that can be brought on by pre-eclampsia and eclampsia,[7, 8] and is recommended by the World Health Organisation as the most effective, safe, and low-cost anti-convulsant treatment for severe pre-eclampsia and eclampsia.[8] It has also been found to be the most important action to prevent death from this disease.[56]

Many attempts have been made to treat pre-eclampsia using a variety of medication, supplements, and lifestyle changes with little success. Treating pregnant women who have chronic hypertension with anti-hypertensive agents, while being effective at treating and managing the hypertension, did little to abate the risk of developing pre-eclampsia or reducing its severity.[57] Similarly, little benefit was observed from taking supplements such as fish oil, calcium, or vitamins C and E in terms of reducing pre-eclampsia risk.[58-60]

One promising preventive measure, low-dose aspirin, which was originally thought to be protective against developing pre-eclampsia, has been hotly debated, with multiple studies finding it provides no preventive benefit.[58] One meta-analysis did find that low-dose aspirin does have some preventive measure, but if and only if treatment is started before 16 weeks gestation, while a recent review and analysis of over 20 studies found that low dose aspirin from the end of the first trimester could result in risk reduction of developing pre-eclampsia by an

estimated 10% in high-risk women.[61] Advances in treating pre-eclampsia have been limited due to complex nature of the pathogenesis of the disease which is not yet fully understand.[4, 9]

### *1.1.6 Pre-eclampsia and Genetics*

Like hypertension, pre-eclampsia is a multifactorial disease comprised of a strong genetic component[4] with an estimated heritable genetic component likely to be somewhere in the range of 20% to 40%, which is comparable to the genetic heritability of hypertension.[18] Pre-eclampsia, too, has been associated with the M235T angiotensinogen polymorphism, but only in some populations.[62-64] Residue 235 is located on the surface of the angiotensinogen protein[25] and having a methionine or threonine residue at this position does not appear to have any effect on the kinetics of the reaction between renin and angiotensinogen.[6] Thus, it is yet to be elucidated whether the M235T polymorphism is responsible for playing a direct role in hypertension and pre-eclampsia, or if it is a purely a neutral marker in linkage disequilibrium to another marker which is yet to be identified.[6, 25] In fact, M235T is associated with increased plasma angiotensinogen levels, but it has been postulated that this phenotype is due to M235T being associated with the G–6A substitution in the promoter region of the AGT gene.[65]

Another missense mutation at position 10 of angiotensinogen, which results in a leucine residue being substituted for a phenylalanine (L10F), has also been implicated in the inherited predisposition to pre-eclampsia. This mutation gives rise to a doubling of the catalytic efficiency of the reaction between renin and angiotensinogen[6] and, in the reported case, resulted in the affected woman suffering from severe pre-eclampsia, requiring delivery of the fetus at only 28 weeks. Clearly, polymorphisms present in the angiotensinogen protein can have large ramifications, particularly during pregnancy, on the tightly controlled RAS, which can have serious health implications.

Aside from the mother's contribution to the development of pre-eclampsia, it was recently shown that the fetus can also contribute to the risk of developing pre-eclampsia through the genes it inherits from the father.[18, 66] Women who had children either with a man who was born of a pre-eclamptic birth,[67, 68] or a man who had himself previously had a child with another women who developed pre-eclampsia during the course of her pregnancy,[69] were shown to be at a significantly increased risk of developing pre-eclampsia. Thus, the father's genetic contribution also has a role to play in the development of this condition. Furthermore, it has been suggested that genomic imprinting, which gives rise to the preferential expression of either the maternal or paternal genes, may also be involved in the manifestation of this disorder.[70]

## 1.2 THE RENIN-ANGIOTENSIN SYSTEM

### *1.2.1 Overview*

The Renin-Angiotensin System (RAS), as already outlined, is a critical player in salt and water homeostasis, and in the regulation of blood pressure in the body (see Figure 1.1).[19, 21] This hormone system is thought to have its origins in the early stages of vertebrate evolution and is present across the majority of vertebrate species including elasmobranchs and cyclostomes.[71-74] The RAS has been shown to also play diverse roles in several processes in the body including inflammation, thrombosis, development, and growth and remodelling.[75-78] In addition to being present in the circulation, there is now a wealth of evidence in support of local RAS systems existing in the tissues,[79, 80] particularly in the heart,[79] brain,[81] adrenal gland,[82] liver, ovaries,[83] testes,[84] retina,[85] salivary glands,[86] vascular endothelium,[87] smooth muscle cells,[88] and adipose tissue,[89] as well being present in the placenta.[90] The existence of a local RAS is interesting as it suggests that the local RAS may exert its effects independent of the circulation

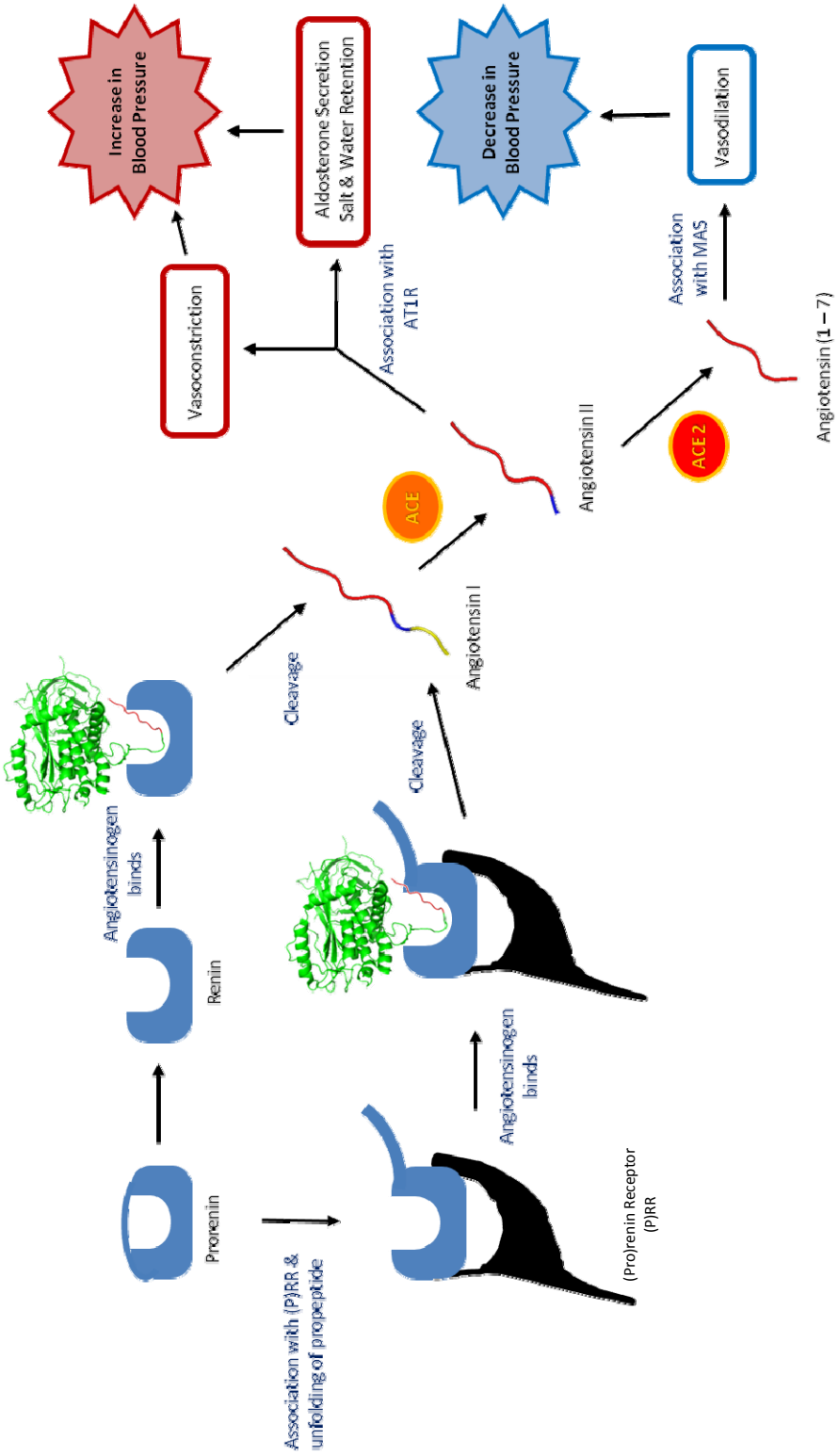


*Figure 1.1:*

*Schematic overview of the Renin-Angiotensin System cascade and the proposed routes to changes in blood pressure (PDB file 2X0B[1] was used to generate the angiotensinogen and angiotensin molecules).*

RAS in a tissue-specific manner.[22] A complete functioning RAS was also found to be present in human glioblastomas and thus inhibition of this local RAS may be one way to treat and control glioblastoma progression.[91]

### *1.2.2 Renin, Prorenin and the (Pro)renin Receptor*

Renin (EC 3.4.23.15), first cloned in 1984, is an aspartic protease which catalyses the first and rate-limiting step of the RAS cascade.[92] Cleavage of angiotensinogen releases the decapeptide angiotensin-I through the action of renin's two catalytic aspartate residues Asp 38 and Asp 226 (Figure 1.2, numbering according to Imai *et al.* 1983).[93, 94]

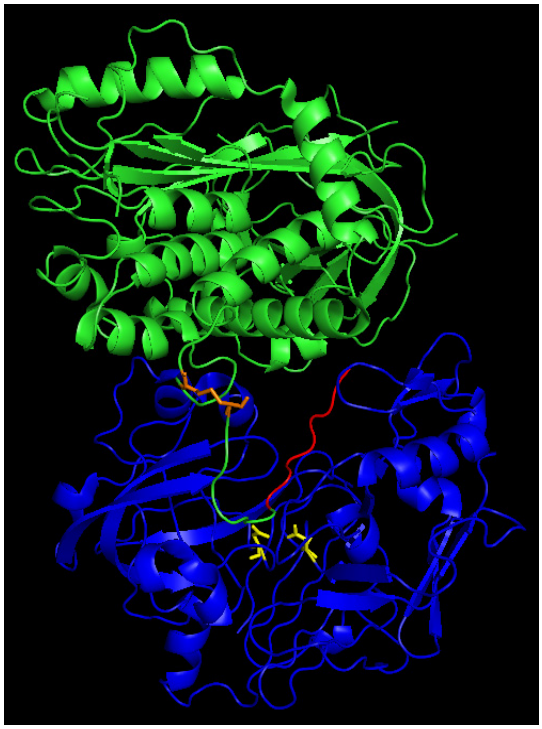

*Figure 1.2:*

*The crystal structure of the complex formed when human renin (blue) binds human angiotensinogen (green). Renin's two catalytic aspartate residues (Asp 38 and Asp 226, in yellow) cleave the N-terminal 10 amino acid peptide, angiotensin I (red), from angiotensinogen. The two cysteine residues, Cys 18 and Cys 138, responsible for angiotensinogen's redox switch are shown in orange (PDB file 2X0B [1]).*

Aspartic proteases are a structurally homologous family of enzymes of which the digestive enzymes pepsin, gastricsin, and chymosin, as well as some retroviral proteinases are members.[95] Most non-retroviral aspartic proteases are synthesized as an inactive zymogen state characterised by a highly basic prosegment that blocks access to the active site, and renin is no

exception.[96] Prorenin, or inactive renin, contains a 5 kDa propeptide (43 amino acids in length) on the N-terminus that tucks into the enzymatic cleft preventing renin from binding its substrate.[35] Under physiological conditions, less than 2% of prorenin is the open active form and activation can either occur proteolytically or non-proteolyically (see Figure 1.3).[35, 97]

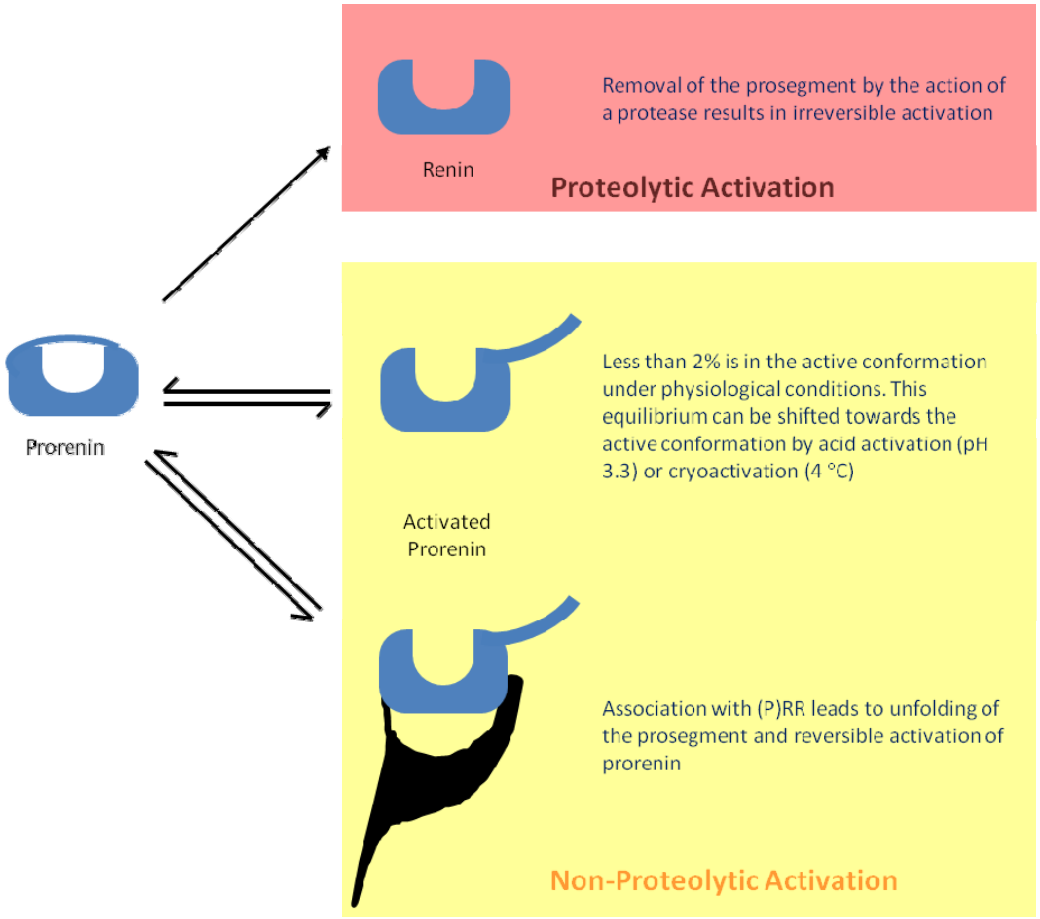


*Figure 1.3:*

*Schematic diagram showing how prorenin can be activated either proteolytically and irreversibly, giving rise to active renin, or non-proteolytically in a reversible manner with the unfolding of the propeptide revealing renin's active site.*

Proteolytic activation involves the physical removal of the propeptide by the action of a protease. Trypsin is typically used *in vitro*, but the protease responsible for the *in vivo* activation of prorenin has not yet been identified.[35] In contrast, non-proteolytic activation is a reversible process which involves the unfolding of the prosegment, followed by the enzyme assuming its

enzymatically active conformation. This equilibrium can be driven in favour of the open active conformation by exposure to low pH (optimally pH 3.3, termed acid activation, which leads to complete activation of prorenin), or alternatively low temperatures (typically 4 °C, commonly referred to as cryoactivation, which results in partial activation of prorenin of approximately 15% of total activity).[35]

(Pro)renin is expressed in the juxtaglomerular cells of the kidney, where it is secreted toward the renal interstitium.[35, 98] Prorenin is expressed constitutively, but active renin is thought to be stored and then released in response to acute stimuli, without any change in prorenin levels.[35] Despite being enzymatically inactive, prorenin circulates in the plasma at high concentrations (sometimes at levels which are 100 times greater than active renin),[99] and it puzzled researchers for some time as to the physiological role that prorenin may play, particularly considering that high prorenin levels are associated with pregnancy and several medical conditions.[85] A piece of this puzzle was solved when in 2002, Nguyen *et al.*[100] cloned a 350 amino acid receptor which binds to both renin and prorenin. Binding to this receptor does not result in the degradation or internalisation of the (pro)renin, as is the case when (pro)renin associates with the mannose-6-phosphate clearance receptors.[97] Rather, the catalytic activity of renin is increased four-fold, and prorenin, while showing little activity in solution, gains full activity on association with the receptor which has become known as the (pro)renin receptor or (P)RR.[1, 100] The idea that a receptor is able to non-proteolytically activate a zymogen is not a new one; urokinase undergoes similar activation, and exhibits enhanced catalytic activity when bound to its receptor.[101] The (P)RR may provide a physiological role for circulating prorenin, particularly in tissues,[102, 103] and is thought to be implicated in the pathogenesis of conditions such as diabetic retinopathy, where prorenin levels are very high.[85] It is noteworthy, though, that the physiological role that the (P)RR may play *in vivo* is hotly debated by researchers. The (P)RR may bear little physiological relevance as the nanomolar affinity with which the receptor

binds (pro)renin could prove insufficient to bind the picomolar concentrations of (pro)renin in biological fluids found *in vivo*.[104]

### *1.2.3 Angiotensinogen and Angiotensin Production*

Angiotensinogen is the only known physiological substrate for renin.[105] Angiotensinogen is classified as a serpin (serine protease inhibitor) due to its similarity in terms of genetic structure[106] and overall structural homology to other serpins such as α1-antitrypsin, and ovalbumin.[107] Despite these characteristics, angiotensinogen shares a low sequence similarity to members of the superfamily,[106] and has lost its inhibitory function.[108] First cloned in 1984,[109] angiotensinogen is 452 amino acids in length[107] and is synthesized in the liver[110] and secreted constitutively to circulate in the plasma at concentrations which are close to the $K_m$ of the renin-catalysed reaction.[111, 112] Thus, being the substrate of the regulatory point in the RAS cascade, the concentration of angiotensinogen is the rate-determining factor and facilitates the fine-tuned regulation of the system, as small changes in angiotensinogen concentrations will affect the levels of angiotensin I being produced. Reaction of angiotensinogen with renin results in the cleavage of the N-terminal decapeptide to produce angiotensin I. This reaction is species-specific—human renin will cleave canine, rat, and sheep angiotensinogens, but human angiotensinogen is not cleaved by renins other than human renin.[113] The remainder of the angiotensinogen molecule after cleavage by renin is often called 'spent angiotensinogen' or 'des-angiotensin I renin substrate' and is not known to have any physiological role.[114]

Angiotensin Converting Enzyme (ACE), the second enzyme in the RAS cascade, is found in the lungs and other vascular beds and is responsible for converting angiotensin I to the vasoactive octapeptide angiotensin II.[9] Angiotensin II exerts most of its biological effects, including vasoconstriction, and sodium and water retention, through binding the angiotensin

receptors, AT1R and AT2R. Angiotensin II may also exert effects independent of blood pressure.[115] Angiotensin Converting Enzyme 2 (ACE2), a relatively newly described member of the RAS cascade, accepts both angiotensin I and angiotensin II as a substrate, and cleaves off a single amino acid residue to produce the vasoactive angiotensin (1 – 9) and angiotensin (1 – 7) respectively.[44, 46, 116] Angiotensin (1 – 7) exerts vasodilatory action, providing counter-regulation of the vasoconstricting properties of angiotensin II, by binding to MAS receptors.[116]

## 1.3 REDOX SWITCHES

### *1.3.1 Background*

Cells are constantly being exposed to changes in environmental redox states and have evolved multiple ways to sense and cope with these changes.[117, 118] Although implicated in various diseases in biological systems such as pre-eclampsia, oxidative species may play a more general role in the cell by regulating various functions and acting as signalling molecules.[119] By reacting with biomolecules, oxidants serve as a marker of the redox environment, allowing the cell to sense alteration in the redox state.[117, 118] Small changes to the fine balance between the rates of reactive oxygen species production and breakdown can result in oxidative stress.[120] Oxidative stress can lead to covalent modification of protein side-chains, allowing the cells to sense and respond to the changing environment. Cysteine residues in proteins are particularly poised to be sensitive to these oxidative changes and can act as redox sensors. The p$K_a$ of the cysteine sulfydryl group is 8.3, and thus under unstressed physiological conditions normally exists as the reduced free thiol protonated form (—SH) in the cytoplasm.[117] However, changes in the redox environment can lead to the reversible oxidation of cysteine residues to several states including disulfide bond formation (—S—S—) with another nearby cysteine residue. Not all

cysteine residues can act as redox sensors, as the surrounding micro-environment in the protein can alter the p$K_a$ of the residue such that the thiolate ion (—$S^-$) is either stabilised or destabilised, or alternatively the oxidant may not have access to the cysteine residue if it is buried inside the protein.[118, 120] The dynamic process of disulfide bond breakage and formation in key cellular proteins, as a result of exposure to oxidative changes, is known as redox signalling.[117]

Cysteine residues can play crucial roles in contributing to the structure and stability of proteins.[121] As such, disulfide bond formation due to the surrounding redox environment can trigger switches in protein structure and activity, changes that can be even more profound than those induced by phosphorylation.[122, 123] Several redox switch proteins have been identified to date, proteins which have evolved to carry out vital roles depending on the surrounding redox state, and these protein cysteine-mediated redox switches have several themes in common including a structural transition-mediated functional switch, as well as conformation strain-driven switch mechanism, and a transition time between redox states in the millisecond range.[123] Examples of such redox switches include the OxyR protein,[124] the *Drosophila* 'inactivation, no after-potential D' (INAD) visual scaffold protein,[125] and angiotensinogen,[1] which as we have already seen plays a significant role in the control of blood pressure.

### *1.3.2 Angiotensinogen*

Angiotensinogen contains four cysteine residues, but only Cys 18 and Cys 138 (Figure 1.4), which form a disulfide bridge, are conserved across all species.[105, 126] The reduction potential for the free thiol/disulfide bond equilibrium between these residues was shown to be –230 V at pH 7 and 25 °C,[1] and it is this disulfide bond which is thought to be crucial for constraining the N-terminus in order for the angiotensinogen molecule to adopt a favourable conformation for reaction with renin.[126] Transferring the N-terminal portion of angiotensinogen

to the protein framework of α1-antitrypsin significantly altered the kinetics of the reaction with renin, thus the angiotensinogen body contributes to the reaction rather than being purely a passive carrier of the angiotensin I peptide.[126]

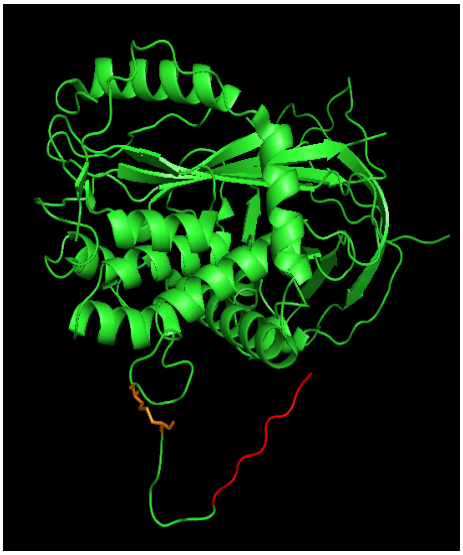

*Figure 1.4:*

*Crystal structure of human angiotensinogen with the N-terminal angiotensin I peptide (cleaved by renin) shown in red. Cys 18 and Cys 138 residues, present as a disulfide in the oxidised form or as free thiols in the reduced form are shown in orange (PDB file 2X0B).*

Angiotensinogen is secreted in the oxidised bridged form from the endoplasmic reticulum and then is subsequently reduced in the plasma, resulting in a consistent ratio of 60:40 of oxidised to reduced forms in the circulation regardless of gender or age.[1] On incubation with renin and the (P)RR, the reaction of renin with the reduced form of angiotensinogen was not significantly altered by the presence of the (P)RR, but the oxidised form displayed a four-fold increase in the catalytic release of angiotensin I when reacting with renin in the presence of the (P)RR[1] This is significant, as with the stable ratio in the plasma pool of the two forms, the redox switch between the two forms would be particularly poised to take place in the tissues and vascular beds, providing a redox-sensitive regulation of angiotensin I release in a tissue-specific manner. Interestingly, the stable ratio between the two redox forms of angiotensinogen was shown to be altered in women with pre-eclampsia—pre-eclamptic women display a much higher proportion of the oxidised form compared with the reduced form in their plasma. This apparent switch to an oxidised-dominated plasma pool of angiotensinogen is predicted to be even more

pronounced in the tissues and, given the higher catalytic efficiency of renin for the oxidised form of angiotensinogen,[1] may provide clues as to how the hypertension associated with pre-eclampsia develops. It is thus conceivable, and attractive to postulate that this difference between the two redox states could be used as a biomarker for early detection of pre-eclampsia.

## 1.4 Recent Advances in Pre-eclampsia Diagnosis and the Search for Potential Biomarkers

Early diagnosis of pre-eclampsia is critical, allowing better monitoring and management plans to be put in place before the onset of symptoms, and can lead to better outcomes for both mother and child. Despite much research having been done to identify potential biomarkers which could be used as an early diagnosis for pre-eclampsia, we still have no accurate predictive biomarkers or validated screening tests to identify women who are prone to developing this condition, and to date, the only predictive information available to doctors when predicting risk is maternal history and risk factors.[5, 127-129] Table 1.2 shows some of the biomarkers which have been investigated thus far with limited success. It has been suggested that a combinatorial approach, combining environmental and maternal risk factors with biomarkers, could be used for better success at a screening approach for pre-eclampsia, given that so far no single biochemical marker has been identified that is capable of detecting this condition early.[5, 45]

One difficulty in the search for predictive biomarkers is the ability for these markers to arise in time for intervention to be put in place. Some of these markers only appear at the onset of symptoms or shortly beforehand, and thus are not of great value as an early diagnostic tool.[129] The recent discovery of pre-eclamptic women having higher levels of oxidised angiotensinogen provides further hope that a biomarker, or combination of biomarkers, that will be useful as a diagnostic tool could soon be at hand. As with the reduced selenium levels observed in pre-

eclamptic women,[47] the increased levels of oxidised angiotensinogen was observed in women who already had clinical manifestation of symptoms.[1] Further longitudinal studies, following women the full length of their pregnancy term, will need to be carried out to determine at what stage these markers develop as to whether they are causative or of value in a diagnostic setting, allowing for an improved management plan to be put in place.

| MARKER OR DIAGNOSTIC TOOL | REFERENCE |
|---|---|
| ADAM-12s | 130 |
| Adiponectin | 131 |
| Angiotensinogen levels | 129 |
| Cell-free fetal nucleic acid in maternal circulation | 132 |
| Doppler ultrasonography | 128 |
| Homocysteine | 131 |
| iTRAQ (isobaric tags for relative and absolute quantification) | 129 |
| microRNA<br>- miR-210<br>- miR-34a | <br>133<br>134 |
| Placental Growth Factor (PIGF) | 128, 135 |
| Platelets Flow Cytometry | 136 |
| Placental Protein-13 (PP-13) | 137 |
| Pregnancy-Associated Plasma Protein A (PAPP-A) | 138 |
| Soluble fms-like Tyrosine Kinase 1 (sflt-1) | 128, 139 |
| Soluble ST2 (sST2) | 135 |
| Vascular Endothelial Growth Factor (VEGF) | 140 |

*Table 1.2:*

*Markers or techniques that have been investigated for their potential to be predictive of development of pre-eclampsia.*

## 1.5 SCOPE OF THIS THESIS

Pre-eclampsia is a severe pregnancy condition that often develops suddenly with huge detrimental ramifications for the health of both mother and child. With no effective treatment or cure to date (Section 1.1.5), it is crucial that this condition is identified early on in the pregnancy before any life-threatening symptoms develop in order that better monitoring and management plans can be put in place. Such a feat would ultimately lead to better outcomes for both the mother and child, especially considering pre-eclampsia is one of the leading causes of maternal and perinatal morbidity and mortality worldwide. Unfortunately, despite much research interest in this field (Section 1.4) and many potential biomarkers being identified, there has been limited success to date in identifying a biomarker that is able to predictably and easily identify women who are likely to develop pre-eclampsia much in advance of the onset of symptoms.

As mentioned in Sections 1.3.2 and 1.4 above, the recent discovery by Zhou and colleagues in 2010[1] that, compared to normal healthy persons and healthy pregnant women, pre-eclamptic women display far greater levels of oxidised angiotensinogen and significantly decreased levels of the reduced form, provides renewed hope that there may be a predictive biomarker for pre-eclampsia on the horizon. The attractiveness of angiotensinogen's redox switch as a predictive biomarker will only hold if a sensitive, high throughput diagnostic test can be developed which will allow distinction between the two forms of this plasma protein. This in itself would be an accomplishment given the intrinsic similarity of the two forms that differ only in the absence or presence of a disulfide bond between Cys 18 and Cys 138.[1] Thus, the big question remains as to whether a sensitive bioassay can be developed to distinguish between the two redox forms of angiotensinogen.

One technique which may be a way forward to developing such a bioassay to distinguish between reduced and oxidised angiotensinogen is surface plasmon resonance. Surface plasmon

resonance (SPR) is an optical label-free technique commonly used to quantify the interactions between biomolecules such as proteins, whereby the interactions between a ligand immobilised on a gold-plated chip and a second free-flowing biomolecule (analyte) are measured as a change in the refractive index on the chip surface.[141] In itself, or complemented with other techniques, SPR is a powerful technique as it allows the characterisation of multiple interactions simultaneously, as well as the calculation of many kinetic and binding parameters, thus it is not surprising that this is one of the preferred methods to report the kinetics of protein-protein interactions in the literature.[141, 142]

Utilising this technique, it may be possible to develop a bioassay for angiotensinogen by immobilising angiotensinogen-specific ligands, such as antibodies raised against human angiotensinogen or renin itself, onto a chip surface and measuring the interactions that occur following injection of angiotensinogen across the surface. One or more functional assays for angiotensinogen, if developed, would then open the door to address the ultimate goal: to probe whether the two redox forms of angiotensinogen, reduced and oxidised, can indeed be distinguished experimentally in such a way to facilitate a functional bioassay which could then prove to be a way to identify women prone to developing pre-eclampsia, a challenge which is continuing to stumble clinicians and researchers alike.

This thesis presents an investigation into angiotensinogen ranging from the recombinant expression and purification of human angiotensinogen described in Chapter Three, the development of methods to detect angiotensinogen using surface plasmon resonance (Chapter Four), to the probing of angiotensinogen's redox switch and the differences between the two redox forms which is described in Chapter Five. Details of methods used throughout the research outlined in this thesis can be found in Chapter Two, while a discussion of the results and concluding remarks can be found in Chapter Six and Chapter Seven, respectively.

*Chapter Two*

# MATERIALS AND METHODS

## 2.1 MATERIALS

### *2.1.1 Chemicals and Reagents*

All buffers, reactions, or solutions requiring water throughout the work detailed in this thesis utilised Milli-Q water (MQ water; pyrogen-free, DNase-free, RNase-free ultrapure type 1 Milli-Q water) dispensed from a Milli-Q Reference fitted with a BioPak Polisher (Merck Millipore, Billerica, Massachusetts, USA). General chemicals used to make buffers and solutions, unless mentioned specifically below, were purchased from a variety of suppliers including Amersham Biosciences, Bioline, Life Technologies, Merck, Sigma-Aldrich, and Thermo Fisher Scientific.

Luria-Bertani (LB) media was prepared using LB Broth Base (Lennox L Broth Base; Invitrogen, Carlsbad, California, USA) as per directions and autoclaved before use. LB for LB agar plates was prepared with 1% w/v agar added prior to autoclaving. Stock solutions of 20% (w/v) glucose (BDH Chemicals, VWR International, Readnor, Pennsylvania, USA) were prepared with MQ water and filter sterilised prior to use. Stock solutions of 1 M isopropyl-β-D-thiogalactopyranoside (IPTG; A & A Biotechnology, Gdynia, Poland) were prepared with MQ water and filter sterilised prior to aliquots being frozen and stored at –20 °C.

Antibiotics used for all bacterial work were prepared according to the following:

- Ampicillin (Amp) was made at 100 mg/mL (ampicillin sodium salt; AppliChem, Darmstadt, Germany) with MQ water and filter sterilised. Aliquots were stored at –20 °C, and Amp was used in media at a concentration of 100 μg/mL.
- Chloramphenicol (Cam; Roche, Indianapolis, Indiana, USA) was made at 30 mg/mL in 100% ethanol. Aliquots were stored at –20 °C and Cam was used in media at 30 μg/mL.
- Kanamycin (Kan) stock solutions were prepared at 50 mg/mL (kanamycin sulphate, Roche, Indianapolis, Indiana, USA) with MQ water and filter sterilised. Aliquots were stored at –20 °C, and Kan was used in media at a concentration of 50 μg/mL for kanamycin-resistant plasmids or at 15 μg/mL for the kanamycin-resistant origami (DE3) cells.
- Tetracycline (Tet) was made at 12.5 mg/mL (tetracycline HCl, NBL Gene Sciences Limited, Northumberland, UK) in 100% methanol. Aliquots were stored at –20 °C, and Tet was used in media at a concentration of 12.5 μg/mL.
- Streptomycin (Str) was prepared at a concentration of 50 mg/mL (streptomycin sulphate, Sigma-Aldrich, St. Louis, Missouri, USA) with MQ water and filter sterilised. Aliquots were stored at –20 °C and Str was used at a concentration of 50 μg/mL in media

### *2.1.2 Vectors, DNA Constructs, and Primers*

The pET_16b_AGT plasmid (ampicillin resistant), which contains the gene for His-tagged human angiotensinogen, was a kind gift from Yahui Yan and Robin Carrell at the University of Cambridge. The pETDuet_DsbC_BlgA plasmid (ampicillin resistant), a construct used in our laboratory, contains the gene for disulfide bond isomerase (DsbC) protein which aids in correct disulfide bond formation. The cloning vector, pCR™ 2.1-TOPO®, was supplied as part of the TOPO® TA Cloning® Kit (Invitrogen™ by Life Technologies™, Carlsbad, California,

USA). Meanwhile, the pET-SUMO expression vector was supplied as part of the Champion™ pET SUMO Protein Expression System Kit (Invitrogen™ by Life Technologies™, Carlsbad, California, USA). All primers were ordered from Integrated DNA Technologies (IDT, Singapore).

### *2.1.3 Bacterial Strains*

The following chemically competent *Escherichia coli* (*E. coli*) bacterial cells were used for all cloning and protein expression work:

| ***E. coli* Bacterial Cell Strain** | **Strain Genotype** | **Antibiotic Resistance (if any)** |
|---|---|---|
| **Cloning Strains:** | | |
| DH5α | *F⁻φ80lacZΔM15 Δ(lacZYA-argF) U169 recA1 endA1 hsdR17 (rk-, mk+) phoA supE44 λ⁻ thi⁻1 gyrA96 relA1* | n/a |
| **Expression Strains:** | | |
| BL21 (DE3) | *F⁻ ompT hsdS$_B$* ($r_B^- m_B^-$) *gal dcm* (DE3) | n/a |
| BL21 (DE3) star | *F⁻ompT hsd*$S_B$ ($r_B^- m_B^-$) *gal dcm rne*131 (DE3) | n/a |
| Rosetta (DE3) | *F⁻ ompT hsdS$_B$* ($r_B^- m_B^-$) *gal dcm* (DE3) pRARE ($Cam^R$) | Chloramphenicol |
| Origami (DE3) | *Δ(ara–leu)7697 ΔlacX74 ΔphoA PvuII phoR araD139 ahpC galE galK rpsL* F'[$lac^+$ $lacI^q$ *pro*] (DE3) *gor522::Tn10 trxB* ($Kan^R$, $Str^R$, $Tet^R$) | Kanamycin, Tetracycline, Streptomycin |

### *2.1.4 Proteins*

The restriction enzymes NdeI and KpnI-HF, as well as the cutsmart buffer, were purchased from New England Biolabs Inc. (NEB, Ipswich, Massachusetts, USA). Bovine Serum Albumin (BSA; Albumin Fraction V pH 7.0), used as a protein standard, was purchased from AppliChem (Darmstadt, Germany). Lysozyme from chicken egg white, and Trypsin from bovine pancreas were obtained from Sigma-Aldrich (St. Louis, Missouri, USA).

Recombinant His-tagged reduced and oxidised angiotensinogen (expressed in *E. coli*, derivatised by reaction with *N*-ethylmaleimide (NEM) in the presence or absence of reducing agent) was a gift from Tim Yandle and Darrell Wang at Endolab (Canterbury Health Laboratories, Christchurch, New Zealand). Recombinant His-tagged human angiotensinogen, and recombinant human glycosylated renin with a C-terminal His-tag (expressed in HEK 293 cells, activated with trypsin) was a kind gift from Yahui Yan and Robin Carrell at the University of Cambridge. Finally, recombinant human glycosylated prorenin with a C-terminal His-tag (REN-317H) was purchased from Creative Biomart (Shirley, New York, USA).

### *2.1.5 Antibodies*

Mouse Anti-Human IgG Fc-specific monoclonal IgG Antibody (Clone 7QD) was obtained from General Bioscience Corporation (Brisbane, California, USA). Antibodies raised against angiotensinogen were purchased from R & D Systems (Clone #369439; Minneapolis, Minnesota, USA) and from Santa Cruz Biotechnology (sc-7419; Dallas, Texas, USA).

### *2.1.6 Other Equipment*

All Eppendorf tubes and pipette tips used throughout all experiments were sterilised by autoclaving at 121 °C for 20 minutes and were allowed to cool prior to use. Large cultures were centrifuged in the Sorvall™ RC 6 Plus Centrifuge (Thermo Scientific, Waltham, Massachusetts, USA) using the fixed angle F10S-6x500y rotor, while samples of 50 mL or less were centrifuged using the Eppendorf Centrifuge 5810R (Eppendorf, Hamburg, Germany) with the fixed angle rotors F34-6-38 and F45-30-11.

A Minitron incubator shaker (Infors HT, Bottmingen, Switzerland) was used for the incubation of all bacterial cell cultures. DNA and some protein concentrations were measured using a Nanodrop Spectrophotometer ND-1000 (Thermo Scientific, Wilmington, Delaware,

USA). Buffers were filtered either through a Whatman™ Klari-Flex™ 250 mL 0.22 μm PES Filter Funnel (Fisher Scientific, Loughborough, UK) or through a 33 mm Millex-GV 0.22 μm PVDF syringe filter (Merck Millipore, Billerica, Massachusetts, USA). Finally, all pH measurements were performed using the UltraBasic pH/mV meter (Denver Instrument, Bohemia, New York, USA).

## 2.2 General Procedures

### *2.2.1 Transformation*

Chemically competent *E. coli* cells were transformed according to the following protocol. See appropriate sections below for details of which strains were transformed with which plasmid.

One vial containing 50 μL of competent cells was thawed on ice. The thawed cells were then transferred to a pre-chilled tube containing 1 μL (~100 ng) of plasmid DNA, and flicked to mix. Subsequently, the cells were incubated on ice for ten minutes, and then heat shocked for 60 seconds at 42 °C, before being immediately returned to ice, where they were left to recover for a further five minutes. If the DNA construct being transformed contained a kanamycin resistance gene, 250 μL of SOC media was added to the cells and then the tube was incubated, shaking at 180 rpm, in a Minitron incubator for 1 hour at 37 °C. Cells were then plated using aseptic techniques on pre-warmed LB agar plates containing the appropriate antibiotics, with either the entire 50 μL of transformed cells or 100 μL of transformed cells in SOC media (for kanamycin resistant plasmids only) being spread on the plate with a disposable sterile plastic spreader. Cells which had not been transformed were plated on an LB agar plate containing the same antibiotics as a negative control. Once plates were dry, they were sealed with parafilm and incubated upside down overnight at 37 °C in a controlled temperature room.

### *2.2.2 Plasmid Purification*

Using aseptic techniques, an autoclaved pipette tip was used to pick a single colony of DH5α cells from the transformation plate (Section 2.2.1), and the colony was then transferred to 10 mL of sterile LB media containing the antibiotic appropriate to the transformed plasmid. Cells were cultured overnight at 37 °C, shaking at 180 rpm in a Minitron incubator. Following overnight culturing, 5 mL of culture was harvested by centrifuging at 4 °C, 10,000 rpm for five minutes, and the media (supernatant) was discarded leaving the harvested cells in the pellet. The plasmid was extracted from the cells and purified using the Purelink® Quick Plasmid Miniprep Kit (Invitrogen™ by Life Technologies™, Carlsbad, California, USA) according to the kit's purification procedure by centrifugation. Plasmid DNA was eluted with 50 µL Tris-EDTA (TE) buffer (supplied with kit) and the concentration of plasmid was checked by Nanodrop at 230 nm. All purified plasmid DNA was stored at –20 °C.

### *2.2.3 DNA Gel Electrophoresis*

Agarose gels were prepared by adding 0.5 g of agarose to 50 mL of Tris acetate EDTA (TAE) buffer (1% w/v agarose), and microwaving the solution for approximately two minutes until the agarose was completely dissolved. SYBR® Safe DNA Gel Stain (Invitrogen™, Carlsbad, California, USA), 3 µL, was added to the dissolved agarose solution and swirled to mix, to allow visualisation of DNA in the gel following electrophoresis. The 1% agarose TAE solution was then poured into a gel cast box, and the comb to form wells was inserted. The gel was left to set at room temperature.

Once set, the agarose gel was removed from the gel casting box and placed in a Minnie Gel Unit (Hoefer Inc., San Francisco, California, USA) and sufficient TAE buffer (1X, see recipe in Appendix) was added so that the gel was just covered. DNA loading dye (6X, see recipe in Appendix) was added at 1/6 of the sample volume (samples which contained GoTaq®

Green Master Mix (Promega Corporation, Madison, Wisconsin, USA) required no loading dye) and, once mixed, were loaded into each well. HyperLadder™ 1 kb (Bioline USA Inc., Taunton, Massachusetts, USA), 3 µL, was loaded into one of the wells as a molecular weight marker. DNA gels were run for 30 minutes at 160 volts (BioRad PowerPac Basic, BioRad Laboratories, Hercules, California, USA).

Once electrophoresis was complete, DNA was visualised by taking an image of the gel using the SynGene Chemi Genius 2 Bio Imaging System and GeneSnap (SynGene, Cambridge, UK) using the transilluminator darkroom lighting and the EtBr/UV filter.

### *2.2.4 Polymerase Chain Reaction (PCR)*

PCR amplification of the human angiotensinogen gene was carried out using Platinum® *Taq* DNA Polymerase High Fidelity (Invitrogen™ by Life Technologies™, Carlsbad, California, USA). High Fidelity PCR Buffer (10X) and 50 mM magnesium sulfate was supplied with Platinum® *Taq* DNA Polymerase, while the 50 mM dNTP mix was supplied with Champion™ pET SUMO Protein Expression System Kit (Invitrogen™ by Life Technologies™, Carlsbad, California, USA). PCR reactions were set up in PCR tubes according to the following:

| PCR COMPONENTS | VOLUME | FINAL CONCENTRATION |
|---|---|---|
| DNA Template (pET_16b_AGT, 100 ng/µL) | 1 µL | 2 ng/µL |
| 10X PCR Buffer | 5 µL | 1X |
| 50 mM $MgSO_4$ | 2 µL | 2 mM |
| 50 mM dNTPs | 1 µL | 1 mM (0.25 mM each) |
| Forward Primer (10 µM) | 1 µL | 0.2 µM |
| Reverse Primer (10 µM) | 1 µL | 0.2 µM |
| Platinum® *Taq* Polymerase High Fidelity | 0.2 µL | 1 unit |
| Autoclaved MQ water | 38.8 µL | |
| Total Volume | 50 µL | |

The PCR reaction was then run according to the following cycling parameters using a MultiGene™ PCR Thermal Cycler (LabNet International Inc., Edison, New Jersey, USA):

| STEP | TIME | TEMPERATURE | CYCLES |
|---|---|---|---|
| Initial Denaturation | 2 min | 94 °C | 1X |
| Denaturation | 1 min | 94 °C | 25X |
| Annealing | 1 min | 53 °C | |
| Extension | 1.5 min | 72 °C | |
| Final Extension | 7 min | 72 °C | 1 X |

A final extension time of at least 7 minutes at 72 °C was required to ensure all PCR products were full length and 3' adenylated (required for TA cloning). Following the final cycle of PCR amplification, the reaction was maintained at 4 °C. PCR amplification products were analysed by DNA electrophoresis by loading 5 µL of each PCR reaction with DNA loading dye (6X, see recipe in Appendix) into each well of a 1% w/v agarose gel (Section 2.2.3).

### *2.2.5 Colony PCR*

Colony PCR was carried out on *E. coli* DH5α colonies produced as a result of ligation and transformation to check for the presence and correct size of DNA insert (i.e. human angiotensinogen gene) within the DNA plasmid of interest. Using aseptic techniques, each colony was picked from an LB agar plate with an autoclaved toothpick and resuspended in 20 µL of sterile MQ water. If many colonies were present on the plate, ten colonies were randomly picked and screened for the correct DNA insert. PCR amplification was carried out using GoTaq® Green Master Mix (Promega Corporation, Madison, Wisconsin, USA). PCR reactions were set up in PCR tubes according to the following:

| PCR COMPONENTS | VOLUME |
|---|---|
| GoTaq® Green Master Mix | 7.5 µL |
| Forward Primer (10 µM) | 0.5 µL |
| Reverse Primer (10 µM) | 0.5 µL |
| Resuspended DH5α colony | 2 µL |
| Autoclaved MQ water | 4.5 µL |
| Total Volume | 15 µL |

The PCR reaction was then run according to the following cycling parameters using a MultiGene™ PCR Thermal Cycler (LabNet International Inc., Edison, New Jersey, USA):

| STEP | TIME | TEMPERATURE | CYCLES |
|---|---|---|---|
| Initial Denaturation | 3 min | 95 °C | 1X |
| Denaturation | 45 sec | 95 °C | 30X |
| Annealing | 15 sec | 53 °C | |
| Extension | 105 sec | 72 °C | |
| Final Extension | 5 min | 72 °C | 1 X |

Following the final cycle of PCR amplification, the reaction was maintained at 4 °C. PCR amplification products were analysed by DNA electrophoresis by directly loading the entire 15 µL of each colony PCR reaction into each well of a 1% w/v agarose gel (Section 2.2.3).

The remaining 18 µL of each resuspended colony was stored at 4 °C. Each colony containing a plasmid with the correctly sized DNA insert was directly added to 10 mL of sterile LB media containing the appropriate antibiotic. Cells were cultured overnight at 37 °C, shaking at 180 rpm in a Minitron incubator in preparation for plasmid purification (Section 2.2.2) the following day.

### *2.2.6 Sodium Dodecyl Sulfate Polyacrylamide Gel Electrophoresis (SDS-PAGE)*

SDS-PAGE gels were run to analyse protein samples, or cell samples for protein expression. Samples were prepared by adding a volume of sample reducing dye (see recipe in Appendix) equivalent to half the sample volume, and mixing well before being heated for 5 minutes at 95 °C using the Accublock Digital Dry Bath (LabNet International Inc., Edison, New Jersey, USA). Samples were then briefly centrifuged for 30 seconds at 12,000 rpm. If SDS-PAGE analysis was not immediately being carried out, samples were stored at –20 °C.

All SDS-PAGE analysis was performed using Bolt® Pre-cast 4-12% Bis-Tris Plus 10 well or 15 well gels (Novex® by Life Technologies™, Carlsbad, California, USA). Gels, with white strip and comb removed, were placed in a Bolt™ Mini Gel Tank (Life Technologies™, Carlsbad, California, USA), and then the anode and cathode chambers were filled with 1X Bolt® MES SDS Running Buffer (supplied as 20X, Life Technologies™, Carlsbad, California, USA), ensuring that the wells of the gel were filled with buffer. Samples were loaded into each well; Novex® Sharp Pre-stained Protein Standard (Novex® by Life Technologies™, Carlsbad, California, USA) was used as a molecular weight (MW) marker by loading 5 µL into one of the wells of the gel. SDS-PAGE gels were run for 35 minutes at 165 volts (BioRad PowerPac Basic, BioRad Laboratories, Hercules, California, USA).

Once electrophoresis was complete, gels were removed from the plastic gel cassettes and rinsed with water to remove excess salts and SDS before being stained with Coomassie Blue stain (see recipe in Appendix) on a shaker for 15 minutes. The stain was discarded and the gel was rinsed with water to remove excess stain before being placed in destain solution (see recipe in Appendix) and left on a shaker until sufficiently destained so that a picture could be taken.

### *2.2.7 OPA Fluorescence Assay*

The *o*-phthalaldehyde (OPA) fluorescent assay was one of the methods that were employed to quantify protein concentrations. In the presence of mercaptoethanol, *o*-phthalaldehyde reacts with primary amines to produce a blue fluorescent product which has maximum excitation at 340 nm and maximum emission at 455 nm.[143, 144]

The OPA reagent was prepared as outlined in the Appendix. A stock solution of 1 mg/mL bovine serum albumin (BSA) was made by dissolving 10 mg of BSA in approximately 700 µL of PBS pH 7.4, then making the volume up to 1 mL with PBS, and mixing well. Solutions of 0.5 mg/mL BSA in PBS, 0.5 mg/mL BSA in PBS with 1.1 mM NEM, and 0.5 mg/mL BSA in PBS with 0.33 mM DTT and 1.1 mM NEM were then prepared (as outlined below) to approximate the concentrations of NEM and DTT (taking into account dilution factors), which were present in the protein samples supplied, to ascertain whether these molecules, separately or combined, affect the assay and alter the generation of standard curves in any way.

| | **0.5 mg/mL BSA** | **0.5 mg/mL BSA + NEM** | **0.5 mg/mL BSA + DTT & NEM** |
|---|---|---|---|
| 1 mg/mL BSA in PBS | 100 µL | 100 µL | 100 µL |
| 5 mM NEM in PBS | - | 43.75 µL | - |
| 1.5 mM DTT, 5 mM NEM in PBS | - | - | 43.75 µL |
| PBS pH 7.4 | 100 µL | 56.25 µL | 56.25 µL |
| Total Volume | 200 µL | 200 µL | 200 µL |

A dilution series for each of the three sets of the BSA standards was prepared, such that a range of concentrations from 0 µg/mL to 500 µg/mL was obtained. 10 µL of each standard/ sample (samples diluted if necessary) was pipetted in duplicate into the wells of a 96 well µClear® flat-bottomed, black chimney well microplate (Greiner Bio-One, Frickenhausen, Germany). Subsequently, 200 µL of fresh OPA reagent was added to each well, and the reagent

and samples were mixed well using a multi-channel pipette, taking care that no bubbles were present in the wells. The plate was allowed to incubate at room temperature for 15 minutes to allow adequate formation of the fluorescent product before the fluorescence in each well was measured with the SpectraMax® M5 Multimode Microplate Reader (Molecular Devices, Sunnyvale, California, USA) using SoftMax Pro 5.4.1 software with the excitation wavelength set to 340 nm and the emission wavelength at 455 nm. Standard curves were generated using Microsoft Excel and the equations of the standard curves were used to extrapolate the concentration of protein samples, taking into account any dilution factors if necessary.

## 2.3 CLONING OF THE HUMAN ANGIOTENSINOGEN GENE INTO PETDUET_DSBC VECTOR

The pETDuet_DsbC_BlgA contains two multiple cloning sites (MCS). DsbC, a disulfide bond isomerise protein is cloned into MCS1 between NcoI and HindIII, while β-lactoglobulin A (BlgA) had already been cloned into MCS2, which was subsequently replaced with the human angiotensinogen (hAGT) gene, between the NdeI and KpnI restriction sites. Fortunately, pET_16b_AGT already contained an NdeI restriction site at the 5' terminus of the hAGT sequence but a KpnI restriction site required at the 3' end of the gene was engineered through primer design and PCR.

### *2.3.1 PCR of hAGT Gene from pET_16b_AGT*

The hAGT gene was PCR amplified with the addition of a 3' KpnI restriction site (underlined in primer sequence) as outlined in Section 2.2.4. PCR products were assessed by DNA gel electrophoresis (Section 2.2.3) with 5 μL of the completed PCR reaction. The primers used for amplification were as follows:

| | | |
|---|---|---|
| Forward Primer: | T7 Promoter | 5'-TAA TAC GAC TCA CTA TAG GG-3' |
| Reverse Primer: | pETDuet_hAGT_KpnI | 5'-CGA GGT ACC TTG TTA GCA GCC GGA TCA T-3' |

### *2.3.2 Cloning of hAGT Gene into TOPO Vector*

The following reaction was set up to ligate the hAGT gene into the pCR™ 2.1-TOPO® vector (both vector and salt solution were supplied with the TOPO® TA Cloning® Kit (Invitrogen™ by Life Technologies™, Carlsbad, CA, USA)):

| LIGATION COMPONENTS | VOLUME |
|---|---|
| Fresh PCR Product | 4 µL |
| Salt Solution | 1 µL |
| pCR™ 2.1-TOPO Vector | 1 µL |
| Total Volume | 6 µL |

The reaction was mixed with a pipette, and left to incubate for five minutes at room temperature. Following incubation, 2 µL of the ligation reaction was used to transform DH5α cells as described in Section 2.2.1. Transformed cells were plated on a LB + Kan agar plate. Note that the TOPO vector confers resistance to both ampicillin and kanamycin, but kanamycin was chosen for selection as any residual pET_16b_AGT plasmid (ampicillin resistant) from the PCR reaction would result in a false positive on LB + Amp agar plates.

### *2.3.3 Colony PCR to Check for Presence of hAGT Gene in TOPO Vector*

Ten DH5α colonies were randomly picked and subjected to colony PCR as described in Section 2.2.5 using the M13 forward and M13 reverse sequencing primers (supplied with the TOPO® TA Cloning® Kit). Colonies that contained a discrete band corresponding to the expected insert size of 1733 bp were grown overnight in LB + Kan media and the plasmid was purified as per Section 2.2.2.

| | | |
|---|---|---|
| Forward Primer: | M13 Forward | 5'-GTA AAA CGA CGG CCA G-3' |
| Reverse Primer: | M13 Reverse | 5'-CAG GAA ACA GCT ATG AC-3' |

### *2.3.4 Restriction Digest of TOPO_hAGT and pETDuet_DsbC_BlgA*

A double restriction digest of the TOPO_hAGT plasmid (to isolate the hAGT gene) and pETDuet_DsbC_BlgA (to remove the BlgA gene from the plasmid) using the restriction enzymes NdeI and KpnI-HF was set up, and left to incubate 2 hours at 37 °C, according to the following:

| TOPO_hAGT RESTRICTION DIGEST | VOLUME |
|---|---|
| TOPO_hAGT (200 ng/µL) | 10 µL |
| NdeI | 1 µL |
| KpnI-HF | 1 µL |
| Cutsmart Buffer (10X) | 5 µL |
| Autoclaved MQ water | 33 µL |
| Total Volume | 50 µl |

| pETDUET_DSBC_BLGA RESTRICTION DIGEST | VOLUME |
|---|---|
| pETDuet_DsbC_BlgA (45 ng/µL) | 43 µL |
| NdeI | 1 µL |
| KpnI-HF | 1 µL |
| Cutsmart Buffer (10X) | 6 µL |
| Autoclaved MQ water | 9 µL |
| Total Volume | 60 µL |

### *2.3.5 Gel Purification of Restricted pETDuet_DsbC Vector and hAGT Gene*

Following restriction digest, the entire restriction digest of both plasmids was loaded into separate wells of an agarose gel and underwent DNA gel electrophoresis according to

Section 2.2.3. Because of the large volume of the digest reactions (50 µL and 60 µL), each digest reaction was split between two wells. Undigested pETDuet_DsbC_BlgA and TOPO_hAGT were run on the same gel as controls. Gel bands corresponding to the restricted hAGT gene (1380 bp) and restricted pETDuet_DsbC vector (6130 bp) were excised from the gel using a scalpel blade and a Dark Reader® Transilluminator (Clare Chemical Research, Dolores, Colorado, USA) to visualise the bands, and the restricted DNA was purified from the gel pieces with the Agarose Gel DNA Extraction Kit (Roche, Indianapolis, Indiana, USA). Recovery of DNA was checked using the Nanodrop spectrophotometer.

### *2.3.6 Ligation of hAGT Gene into pETDuet_DsbC Vector and Transformation*

Ligation was carried out using T4 DNA Ligase, supplied in Enzyme Solution I (DNA Ligation Kit Version 2.1, TaKaRa Bio Inc., Otsu, Shiga, Japan). The following reaction was set up to ligate the hAGT gene into the pETDuet_DsbC vector:

| LIGATION COMPONENTS | VOLUME |
|---|---|
| pETDuet_DsbC Vector (restricted) | 0.25 µL |
| hAGT Gene Insert (restricted) | 2.25 µL |
| Enzyme Solution I | 2.5 µL |
| Total Volume | 5 µL |

The reaction was mixed with a pipette, and left to incubate for 15 minutes at room temperature. Following incubation, the entire 5 µL of the ligation reaction was used to transform DH5α cells as described in Section 2.2.1. Transformed cells were plated on an LB + Amp agar plate.

### *2.3.7 Colony PCR to Check for Presence of hAGT Gene in pETDuet_DsbC*

All DH5α colonies resulting from ligation and transformation were picked and subjected to colony PCR as described in Section 2.2.5 using the plasmid-specific Duet UP2 and T7 Terminator primers. Colonies that contained a discrete band corresponding to the expected insert size of 1620 bp were grown overnight in LB + Amp media and the plasmids were purified as per Section 2.2.2.

| | | |
|---|---|---|
| Forward Primer: | Duet UP2 | 5'-TTG TAC ACG GCC GCA TAA TC-3' |
| Reverse Primer: | T7 Terminator | 5'-TAG TTA TTG CTC AGC GGT GG-3' |

### *2.3.8 Sequencing of pETDuet_DsbC_hAGT plasmid*

Sequencing was carried out at the Canterbury Sequencing and Genotyping Facility (School of Biological Sciences, University of Canterbury, Christchurch, New Zealand) to check that the hAGT gene was in the correct frame of the pETDuet plasmid for expression and that no mutations had been introduced through the cloning procedures. The plasmid specific Duet UP2 and T7 Terminator, forward and reverse primers respectively (see Section 2.3.7), were used for sequencing the pETDuet_DsbC_hAGT plasmid.

## 2.4 CLONING OF THE HUMAN ANGIOTENSINOGEN GENE INTO PET-SUMO VECTOR

The pET-SUMO vector uses the TA cloning approach to provide quick, one-step cloning of the PCR product directly into the expression vector immediately after the sequence coding for a N-terminal 6X His tag and SUMO (Small Ubiquitin-like Modifier) fusion protein.

### *2.4.1 PCR of hAGT Gene from pET_16b_AGT*

The hAGT gene, including 3' adenylation overhangs, was PCR amplified as outlined in Section 2.2.4. PCR products were assessed by DNA gel electrophoresis (Section 2.2.3) with 5 µL of the completed PCR reaction. The primers used for amplification were as follows:

| | | |
|---|---|---|
| Forward Primer: | pET-SUMO_hAGT_F | 5'-GAC CGG GTG TAC ATA CAC-3' |
| Reverse Primer: | pET-SUMO_hAGT_R | 5'-TCA TGC TGT GCT CAG C-3' |

### *2.4.2 Ligation of hAGT Gene into pET-SUMO Vector*

The following reaction was set up to ligate the hAGT gene into the pET-SUMO vector (pET-SUMO vector, 10X ligation buffer, and T4 ligase were supplied with the Champion™ pET SUMO Protein Expression System Kit (Invitrogen™ by Life Technologies™, Carlsbad, California, USA)):

| LIGATION COMPONENTS | VOLUME |
|---|---|
| Fresh PCR Product | 1 µL |
| 10X Ligation Buffer | 1 µL |
| pET-SUMO Vector | 2 µL |
| T4 Ligase (4.0 Weiss units/µL) | 1 µL |
| Autoclaved MQ Water | 5 µL |
| Total Volume | 10 µL |

The reaction was mixed with a pipette, and left to incubate for 30 minutes at room temperature. Following incubation, aliquots of 2 µL of the ligation reaction were used to transform five vials of DH5α cells as described in Section 2.2.1. Transformed cells were plated on LB + Kan agar plates.

### *2.4.3 Colony PCR to Check for Presence of hAGT Gene in pET-SUMO Plasmid*

All DH5α colonies resulting from ligation and transformation were picked and subjected to colony PCR as described in Section 2.2.5 using the plasmid-specific SUMO Forward and T7 Terminator primers. Colonies which contained a discrete band corresponding to the expected insert size of 1612 bp were grown overnight in LB + Kan media and the plasmids were purified as per Section 2.2.2.

| | | |
|---|---|---|
| Forward Primer: | SUMO Forward | 5'-AGA TTC TTG TAC GAC GGT ATT AG-3' |
| Reverse Primer: | T7 Terminator | 5'-TAG TTA TTG CTC AGC GGT GG-3' |

### *2.4.4 Sequencing of pET-SUMO_hAGT plasmid*

Sequencing was carried out at the Canterbury Sequencing and Genotyping Facility (School of Biological Sciences, University of Canterbury, Christchurch, New Zealand) to check that the hAGT gene was in the correct frame of the pET-SUMO plasmid for expression and that no mutations had been introduced through the cloning procedures. The plasmid specific SUMO Forward and T7 Terminator sequencing primers (see Section 2.4.7) were used for sequencing the pET-SUMO_hAGT plasmid.

## 2.5 RECOMBINANT HUMAN ANGIOTENSINOGEN EXPRESSION TRIALS

Extensive expression trials were undertaken to ascertain suitable conditions to obtain soluble, native, and pure recombinant human angiotensinogen. A range of *E. coli* strains, expression conditions, media types, and lysis conditions were trialled as outlined in the following sections.

### *2.5.1 General Expression Protocol*

Using aseptic techniques, an expression strain of *E. coli* cells was transformed with the constructs detailed below, according to the protocol in Section 2.2.1, and cells were plated on LB agar plates with appropriate antibiotics and left at 37 °C to grow overnight. The following day, a single colony was picked with an autoclaved pipette tip and resuspended in a vial containing 10 mL LB media with the appropriate antibiotics. This pre-culture was incubated at 37 °C in a Minitron incubator shaking at 250 rpm overnight. The next day, the optical density at 600 nm ($OD_{600}$) of the pre-culture was measured using the Smart Spec$^{TM}$ Plus Spectrophotometer (Bio-Rad Laboratories, Hercules, California, USA) and then the appropriate amount of pre-culture was added to a conical flask containing 50 mL LB (with appropriate antibiotic) so that the starting $OD_{600}$ of the expression flask was 0.1 Absorbance Units (AU).

This 50 mL culture was incubated at 37 °C in a Minitron incubator shaking at 250 rpm, and, with the $OD_{600}$ being monitored, the culture was left to grow until an $OD_{600}$ of 0.6 to 0.8 AU was reached. An uninduced sample was then taken by removing a sample with a volume equivalent to an $OD_{600}$ of 1.0 AU (i.e. $1.0/OD_{600}$ x 1 mL = volume of sample to be taken). The uninduced cell sample was harvested by centrifuging the sample at 4 °C for 5 minutes at 12,000 rpm to pellet the cells. The supernatant was discarded and the cell pellet was frozen and stored at –20 °C.

The culture flask was cooled down and induced by adding 50 µL of 1 M IPTG to give a final concentration of 1 mM IPTG. The flask was returned to the shaking Minitron incubator to express at the desired temperature of 26 °C or 37 °C. After four hours of expression, and again after overnight expression, the $OD_{600}$ was measured and samples were taken, with the volume of sample taken being equivalent to an $OD_{600}$ of 1.0 AU as with the uninduced samples above. Cell samples were harvested as described above by centrifuging the samples for 5 minutes at 4 °C and 12,000 rpm. The supernatants were discarded and cell pellets were frozen and stored at –20 °C.

In order to analyze the cells to check expression levels and solubility of the expressed protein, cell pellets were removed from the freezer and thawed on ice. If cells were to be lysed by sonication, 200 µL of the desired buffer was added to the cell pellet before the cells were sonicated using the Stepped Titanium Microtip (3.9 mm diameter) of the Sonic Ruptor 400 Ultrasonic Homogenizer (Omni International Inc., Kennesaw, Georgia, USA). Sonication was carried out on ice for 5 second intervals until cells were completely resuspended and the solution was homogenous.

Alternatively, cells were lysed using CelLytic$^{TM}$ B Bacterial Cell Lysis Extraction Reagent (10X concentrate, Sigma-Aldrich, St. Louis, Missouri, USA), a lysis reagent that contains a combination non-denaturing zwitterionic detergents which gently lyse the cells with the help of lysozyme. CelLytic B lysis solution was prepared by combining 100 µL of 10X CelLytic B concentrate with 20 µL of 10 mg/mL lysozyme (to give a final concentration of 0.2 mg/mL lysozyme), and 880 µL of the desired buffer. 200 µL of this 1X CelLytic B lysis solution was added to the thawed cell pellet, and the solution was gently pipetted up and down until the pellet was completely resuspended. The cells were then mixed by gently inverting the tube for 10 to 15 minutes.

Once lysis was complete, either by sonication or CelLytic B, 100 µL of the lysed cells was transferred to a clean tube and kept as a sample of total cell lysate. The remaining 100 µL was then centrifuged for 5 minutes at 4 °C, 12,000 rpm to separate the soluble fraction from the insoluble fraction which forms a pellet at the bottom of the tube. Following centrifugation, the soluble supernatant was removed and placed in a clean tube, and kept as a sample of the soluble fraction. The remaining pellet was completely resuspended in 100 µL of the buffer used for lysis—this is the insoluble fraction. These samples were analysed by SDS-PAGE by loading 5 µL of each sample in wells of a gel and run as described in Section 2.2.6 above. This expression

protocol was carried out for the expression trials detailed in Sections 2.5.2, 2.5.3, and 2.5.4 below.

### *2.5.2 His-tagged Human Angiotensinogen (pET_16b_AGT plasmid)*

BL21 (DE3) star competent cells were transformed with the pET_16b_AGT plasmid and cultured in three different media types (LB, TB, and 2*TY, see Appendix for recipes) with ampicillin as the selective antibiotic. The cells were induced with either 0.1 mM or 1 mM IPTG, and were left to express at 26 °C and 37 °C, for four hours and overnight (16 hours). Cells were lysed by sonication or CelLytic B with PBS, PBS + 1% Triton X-100, Tris, and Lysis Buffer (see Appendix for recipes) as the buffer used for lysis.

Rosetta (DE3) competent cells were transformed with the pET_16b_AGT plasmid and cultured in two different media types (LB and TB) with ampicillin and chloramphenicol as the selective antibiotics. The cells were induced with 1 mM IPTG, and were left to express at 26 °C and 37 °C, for four hours and overnight (16 hours). Cells were lysed by sonication or CelLytic B with PBS, PBS + 1% Triton X-100, Tris, and Lysis Buffer as the buffer used for lysis.

Origami (DE3) competent cells were transformed with the pET_16b_AGT plasmid and cultured in LB media with ampicillin, kanamycin, streptomycin, and tetracycline as the selective antibiotics. The cells were induced with 1 mM IPTG and were left to express at 26 °C and 37 °C for four hours and overnight (16 hours). Cells were lysed with CelLytic B (Lysis Buffer was the buffer used for lysis).

### *2.5.3 Human Angiotensinogen (pETDuet_DsbC_hAGT plasmid)*

BL21 (DE3) competent cells were transformed with the pETDuet_DsbC_hAGT plasmid and cultured in LB media with ampicillin as the selective antibiotic. The cells were induced with 1 mM IPTG and were left to express at 26 °C and 37 °C, for a period of four hours

and overnight (16 hours). Cells were lysed by CelLytic B with Lysis Buffer (see recipe in Appendix) used as the buffer for lysis.

Origami (DE3) competent cells were transformed with the pETDuet_DsbC_hAGT plasmid and cultured in LB media with ampicillin, kanamycin, streptomycin, and tetracycline as the selective antibiotics. The cells were induced with 1 mM IPTG and were left to express at 26 °C and 37 °C, for four hours and overnight (16 hours). Cells were lysed by CelLytic B with Lysis Buffer used as the buffer for lysis.

### *2.5.4 SUMO-tagged Human Angiotensinogen (pET-SUMO_hAGT plasmid)*

BL21 (DE3) competent cells were transformed with the pET-SUMO_hAGT plasmid and cultured in LB media (supplemented either in the presence or absence of 1% glucose) with kanamycin as the selective antibiotic. If the media was supplemented with 1% glucose, glucose was added to the media in both the pre-culture and expression culture flasks. The cells were induced with 1 mM IPTG and were left to express at 26 °C and 37 °C, for four hours and overnight (16 hours). Cells were lysed by either sonication or CelLytic B with Lysis Buffer used as the buffer for lysis.

## 2.6 EXPRESSION AND PURIFICATION OF RECOMBINANT HUMAN ANGIOTENSINOGEN

Following extensive expression trials and optimization of the expression and lysis conditions, recombinant human angiotensinogen was expressed and purified according to the following protocol:

### *2.6.1 Expression*

Using aseptic techniques, BL21 (DE3) competent *E. coli* cells were transformed with the pET-SUMO_hAGT plasmid according to the protocol described in Section 2.2.1, and cells

were plated on LB + Amp agar plates and left at 37 °C to grow overnight. The following day, a single colony was picked and resuspended in a flask containing 50 mL LB + Amp + 1% glucose media. This pre-culture was incubated at 37 °C in a Minitron incubator shaking at 250 rpm overnight. The next day, the $OD_{600}$ of the pre-culture was measured using the Smart Spec™ Plus Spectrophotometer (Bio-Rad Laboratories, Hercules, California, USA) and then the appropriate amount of pre-culture was added to a 2 L baffled conical flask containing 500 mL LB + Amp + 1% glucose so that the starting $OD_{600}$ of the expression flask was 0.1 AU.

This 500 mL expression culture was incubated at 37 °C in a Minitron incubator shaking at 250 rpm, and, with the $OD_{600}$ being monitored, the culture was left to grow until an $OD_{600}$ of 0.6 to 0.8 AU was reached (typically 2 to 3 hours). The culture flask was cooled down and then induced by adding 500 µL of 1 M IPTG to give a final concentration of 1 mM IPTG. The flask was returned to the shaking Minitron incubator to express at 26 °C for 16 hours (overnight). Cells were harvested by splitting the culture in two and centrifuging cells at 4 °C for ten minutes at 8,000 rpm. The supernatants were discarded, and the cell pellets were resuspended in 10 mL PBS buffer (to wash pellet and remove any residual media) and transferred to 50 mL Falcon tubes (Corning®, Tewksbury, Massachusetts, USA), before being centrifuged for a further 20 minutes at 4 °C and 10,000 rpm to pellet the cells. The supernatant was removed and discarded, and the cell pellets were frozen and stored at –20 °C.

### *2.6.2 Cell Lysis*

A 250 mL cell pellet was removed from the freezer and thawed on ice, before being completely resuspended in 20 mL Lysis Buffer containing a small spatula of lyophilised DNase I (to reduce viscosity of cell lysate; Roche, Indianapolis, Indiana, USA), Cells were lysed using the Microfluidics M-110P Cell Homogenizer® (Microfluidics, Westwood, Massachusetts, USA) at 17,000 psi and 4 °C. Cell samples were passed through the homogenizer twice to ensure

complete lysis, which results from the shear stresses and decompression that occur when the cells are passed through a needle valve at high pressure, causing cell disruption when cells return to normal atmospheric pressure. Following lysis, the cell lysate was centrifuged at 10,000 rpm for 20 minutes at 4 °C to pellet any insoluble material. The supernatant was transferred to a clean 50 mL tube and kept on ice ready for purification.

### *2.6.3 His-tag Purification*

Purification by means of immobilised metal ion affinity chromatography (IMAC) was carried out using HisPur™ Cobalt (Co) Resin (Thermo Scientific, Rockford, Illinois, USA). A 5 mL gravity flow column (Pierce Biotechnology, Rockford, Illinois, USA) was packed with 2 mL resin, and the storage buffer was allowed to flow through and was discarded. The resin was then washed with 20 mL MQ water (10 column volumes), before being equilibrated with 10 column volumes of Lysis Buffer. The equilibrated resin was then transferred to the tube containing the soluble fraction of the cell lysate, and incubated for 30 minutes in a 4 °C controlled temperature room on a rotary wheel at a slow speed. This was then repacked into the gravity flow column and the flow through collected. The flow through was applied to the column once more to ensure maximum binding of the His-tagged SUMO fusion protein to the resin. The bound resin was then washed with 10 column volumes of PBS 10 mM imidazole pH 7.4 to remove any extraneous, weakly bound proteins. SUMO-AGT was then eluted with 10 mL of PBS 50 mM imidazole pH 7.4, collected in 1 mL fractions. Fractions were analysed by SDS-PAGE (Section 2.2.6) and those fractions containing SUMO-AGT were pooled and concentrated using a Vivaspin® 6 30,000 Da MWCO PES spin concentrator (Sartorius, Goettingen, Germany).

### *2.6.4 Size Exclusion Chromatography*

As a second and final step of purification, size exclusion chromatography (SEC) was performed to separate proteins by size in order to remove unwanted proteins that co-eluted with SUMO-AGT in the first IMAC step of purification. A 24 mL Superdex 200 gel filtration pre-packed column (GE Healthcare Life Sciences, Uppsala, Sweden) was connected to the AKTA Express (GE Healthcare Life Sciences, Uppsala, Sweden) and washed with three column volumes of MQ water before being equilibrated with 75 mL of PBS pH 7.4 buffer at a flow rate of 0.3 mL/min. The concentrated protein sample was then loaded onto the column and run, for a total buffer volume of 30 mL, at a flow rate of 0.25 mL/min at 4 °C, and collected in a 96 well plate in 1 mL fractions. Fractions that corresponded to the $A_{280}$ peak on the chromatograph (UniCorn 5.11 Workstation, GE Healthcare Life Sciences, Uppsala, Sweden) were analysed by SDS-PAGE (Section 2.2.6) and fractions containing pure SUMO-AGT were pooled and concentrated using a Vivaspin® 6 10,000 Da MWCO PES spin concentrator (Sartorius, Goettingen, Germany). Pure protein was snap frozen with liquid nitrogen and stored at –80 °C.

### *2.6.5 Cleavage of SUMO Tag*

Cleavage using SUMO Protease (1 U/µL, supplied with SUMO Protease Buffer as part of the Champion™ pET SUMO Protein Expression System Kit (Invitrogen™ by Life Technologies™, Carlsbad, California, USA)) was carried out to remove the His-tag and SUMO fusion protein from the N-terminus of angiotensinogen. For every 20 µg of SUMO-AGT fusion protein to be cleaved, 10 units of protease (10 µL) was added to the protein solution with 4 µL of 10X SUMO Protease Buffer (– salt), and made up to a total volume of 40 µL with MQ water and mixed well. The reaction was left to incubate for 3 hours at room temperature, before being flowed through a pre-equilibrated 1 mL Co resin gravity column to remove the cleaved SUMO

tag and the SUMO protease from the solution. The flowthrough was collected and contained pure recombinant human angiotensinogen.

## 2.7 Expression and Purification of SUMOylated Chloramphenicol Acetyltransferase

The expression control protein, SUMO-chloramphenicol acetyltransferase (SUMO-CAT; pET-SUMO/CAT plasmid supplied with the Champion™ pET SUMO Protein Expression System Kit (Invitrogen™ by Life Technologies™, Carlsbad, California, USA) was expressed and purified as a SUMOylated protein to be used as a negative control in surface plasmon resonance experiments. Using aseptic techniques, BL21 (DE3) competent *E. coli* cells were transformed with the pET-SUMO/CAT plasmid according to the protocol described in Section 2.2.1, and cells were plated on LB + Amp agar plates and left at 37 °C to grow overnight. The SUMO-CAT protein was then expressed and purified according to the same protocol described for SUMO-AGT in Sections 2.6.1, 2.6.2, and 2.6.3 above. SUMO-CAT protein was eluted from the Co resin using PBS 150 mM imidazole pH 7.4 as the elution buffer, concentrated with a Vivaspin® 6 10,000 Da MWCO PES spin concentrator (Sartorius, Goettingen, Germany), and then subjected to size exclusion chromatography as described in Section 2.6.4. Pure protein was snap frozen with liquid nitrogen and stored at –80 °C.

## 2.8 Surface Plasmon Resonance Experiments

All surface plasmon resonance (SPR) experiments were carried out on the ProteOn™ XPR36 Protein Interaction Array System using ProteOn™ GLC Sensor Chips at 25 °C using ProteOn™ 0.35 mL, or 2 mL deep well 96 well plates (all purchased from Bio-Rad Laboratories, Hercules, California, USA). Following much optimisation of ligand immobilisation levels, buffer

conditions, analyte concentrations, injection parameters, and regeneration conditions, SPR experiments were carried out as described in Sections 2.8.1 to 2.8.6 below:

### *2.8.1 Buffer and Protein Solution Preparation*

All buffers and solutions run on the SPR were prepared fresh and filtered using 0.2 μm syringe-driven, or vacuum-driven filters, before being sonicated for 20 minutes (Digitech Ultrasonic Cleaner, Digitech Systems, Kolkata, India) to degas and break apart any remaining particulate in solution. Activation and deactivation solutions for amine coupling were supplied as part of the ProteOn$^{TM}$ amine coupling kit (Bio-Rad Laboratories, Hercules, California, USA). All protein samples were centrifuged at 4 °C for 5 minutes at 12,000 rpm to pellet any aggregate that may be present in the sample, prior to the concentration being checked in triplicate by Nanodrop $A_{280}$ (protein concentration was calculated by dividing the $A_{280}$ by the protein's extinction coefficient) and/or by OPA fluorescent assay in order to obtain accurate protein concentrations. Phosphate buffered saline with Tween-20 (PBST, see recipe in Appendix) was used as the running buffer in all experiments and in the blank buffer injections.

### *2.8.2 Sensor Chip Initialisation and Pre-Conditioning*

Each time a new or used sensor chip was inserted into the SPR machine, a wet initialisation (50% v/v glycerol) was performed. Following several system flushes with the running buffer, the sensor chip surface of a new chip was conditioned prior to any immobilisations by carrying out successive 30 μL pulses of 0.25% Tween-20, 50 mM NaOH, and 100 mM HCl for 60 seconds each at a flow rate of 30 μL/min, first in the vertical direction (ligand) followed by the horizontal direction (analyte). Eight blank buffer runs in the analyte direction followed by an additional eight blank buffer runs in the ligand direction were then carried out to remove all traces of the pre-conditioning solutions and equilibrate the chip surface

prior to any experiments taking place (100 µL of PBST injected at a flow rate of 100 µL/min for 60 seconds for each blank buffer run).

### *2.8.3 Interaction of Recombinant Human Angiotensinogen with Anti-Angiotensinogen Antibody*

A multiplex approach was taken to investigate the interactions that take place between recombinant human angiotensinogen and the human serpin A8/angiotensinogen monoclonal antibody (mouse $IgG_1$ clone #369439; R & D Systems, Minneapolis, Minnesota, USA)—henceforth referred to as 'anti-AGT mAb'. Mouse anti-human IgG Fc specific monoclonal IgG antibody (clone 7QD; General Bioscience Corporation, Brisbane, California, USA)—referred to as 'anti-IgG mAb'—was immobilised to one ligand channel to serve as a reference channel while anti-AGT mAb was immobilised to a further four channels at the same level of ligand density to serve as replicates.

#### *2.8.3.1 Immobilisation*

The sensor chip surface of the ligand channels was activated by a 150 µL injection of a 1:1 mixture of 0.4 M 1-ethyl-3-(3-dimethylaminopropyl)carbodiimide (EDAC) and 0.1 M *N*-hydroxysuccinamide (NHS) for 300 seconds at a flow rate of 30 µL/min to activate the carboxymethyl dextran on the sensor chip surface, to produce reactive succinimide esters. Ligand was then immobilised on each channel by injecting 150 µL of 0.75 µg/mL antibody (in 10 mM sodium acetate buffer pH 4) for 300 seconds at a flow rate of 30 µL/min—anti-IgG mAb was immobilised across ligand channel 1 (L1, reference channel), while anti-AGT mAb was immobilised across ligand channels (L2 to L5). Ligand immobilisation was directly followed by deactivation with 1 M ethanolamine HCl pH 8 at a flow rate of 30 µL/min for 300 seconds to deactivate any unreacted succinimide esters.

Following two blank buffer injections, four stabilisation steps were performed in the ligand direction to stabilise the ligand surface and remove any weakly bound ligand molecules. Two 30 µL pulses of 10 mM sodium acetate pH 3.0 were followed by two 30 µL pulses of 10 mM glycine HCl pH 2.0, with each 18 second injection having a flow rate of 100 µL/min. Multiple blank buffer injections, first in the ligand direction and then the analyte direction, were performed until a stable baseline was achieved across all channels.

#### *2.8.3.2 Interaction with SUMO-AGT*

A dilution series of pure SUMO-AGT with a dilution factor of two was prepared in PBST to give SUMO-AGT concentrations of 3 µM, 1.5 µM, 0.75 µM, 0.375 µM, 0.1875 µM, and 0.0938 µM. A 409 µL injection of each SUMO-AGT concentration was flowed across the chip in the analyte direction at a flow rate of 25 µL/min and allowed to associate with the anti-AGT mAb for a total contact time of 981 seconds (16 minutes 21 seconds). At the end of the injection, running buffer was flowed across all analyte channels for 600 seconds to allow dissociation. This was then followed with regeneration of the ligand surface—a 30 µL pulse of glycine HCl pH 2.0 for a total of 18 seconds at a flow rate 100 µL/min to remove any undissociated analyte. At least four blank buffer injections were performed to allow the ligand to recover and ensure a stable baseline was re-established. This interaction run was also repeated using pure SUMO-CAT as a negative control.

#### *2.8.3.3 Interaction with Reduced and Oxidised Angiotensinogen*

A dilution series of pure oxidised angiotensinogen (derivatised with NEM) with a dilution factor of two was prepared in PBST to give oxidised angiotensinogen concentrations of 2 µM, 1 µM, 0.5 µM, 0.25 µM, 0.125 µM, and 0.0625 µM. A 409 µL injection of each oxidised angiotensinogen concentration, in descending order, was flowed simultaneously across the chip

in the analyte direction at a flow rate of 25 µL/min and allowed to associate with the anti-AGT mAb for a total contact time of 981 seconds (16 minutes 21 seconds). At the end of the injection, running buffer was flowed across all analyte channels for 1800 seconds (30 minutes) to allow dissociation. This was then followed with regeneration of the ligand surface—a 30 µL pulse of glycine HCl pH 2.0 for a total of 18 seconds at a flow rate 100 µL/min to remove any undissociated analyte. At least four blank buffer injections were performed to allow the ligand to recover and ensure a stable baseline was re-established. The order of the concentration series of oxidised angiotensinogen was then randomised and the interaction run was repeated such that each concentration of oxidised angiotensinogen was flowed across a different analyte channel to the previous interaction run.

A dilution series of pure reduced angiotensinogen (derivatised with DTT, followed by NEM) was prepared identically to oxidised angiotensinogen to give the same concentrations listed above. A 409 µL injection of each reduced angiotensinogen concentration, in descending order, was flowed simultaneously across the chip in the analyte direction at a flow rate of 25 µL/min and allowed to associate with the anti-AGT mAb for a total contact time of 981 seconds (16 minutes 21 seconds). At the end of the injection, running buffer was flowed across all analyte channels for 1800 seconds (30 minutes) to allow dissociation. This was then followed with regeneration of the ligand surface—a 30 µL pulse of glycine HCl pH 2.0 for a total of 18 seconds at a flow rate 100 µL/min to remove any undissociated analyte. At least four blank buffer injections were performed to allow the ligand to recover and ensure a stable baseline was re-established. The order of the concentration series of reduced angiotensinogen was then randomised and the interaction run was repeated such that each concentration of reduced angiotensinogen was flowed across a different analyte channel to the previous interaction run.

Finally, the three highest concentrations of oxidised and reduced angiotensinogen were injected simultaneously across all channels in the same run, first in a ordered fashion, and then as

a repeat in a randomised order in the second interaction run, such that in each run oxidised angiotensinogen was flowed across three channels and reduced angiotensinogen was flowed across the other three channels.

### *2.8.4 Interaction of Recombinant Human Angiotensinogen with Recombinant Glycosylated Human Renin via Amine Coupling*

Recombinant human glycosylated renin was immobilised directly onto the chip surface *via* amine coupling using several approaches, to measure the kinetic parameters of the interactions between renin and angiotensinogen.

#### *2.8.4.1 Immobilisation of Prorenin and Renin*

Prorenin was proteolytically activated to renin by trypsin digest—0.1 mg/mL prorenin was digested with trypsin at a concentration of 5 μg/mL for 2 minutes at 37 °C, before the reaction was quenched with 0.5% formic acid or 2 mM phenylmethanesulfonyl fluoride (PMSF). SDS-PAGE analysis was used to confirm complete cleavage of the prosegment.

The sensor chip surface was activated by a 150 μL injection of a 1:1 mixture of 0.4 M EDAC and 0.1 M NHS for 300 seconds at a flow rate of 30 μL/min. Ligand was then immobilised on each channel by injecting 150 μL of 0.01 mg/mL prorenin or renin (in 10 mM sodium acetate buffer pH 4) for 300 seconds at a flow rate of 30 μL/min. Ligand immobilisation was directly followed by deactivation with 1 M ethanolamine HCl pH 8 at a flow rate of 30 μL/min for 300 seconds. Multiple blank buffer injections, first in the ligand direction and then the analyte direction, were performed until a stable baseline was achieved across all channels.

*2.8.4.2 Immobilisation of Prorenin and Renin on a Spacer*

Immobilisation of prorenin and renin was performed exactly as described above, except that the activation/immobilisation/deactivation steps described in Section 2.8.4.1 above were preceded by an additional three steps. Firstly, the carboxymethyl dextran sensor chip surface was activated with a 1:1 mixture of 0.4 M EDAC and 0.1 M NHS (30 µL/min for 300 seconds), which was then followed by the immobilisation of 150 µL of a spacer molecule, hexamethylenediamine (Sigma-Aldrich, St. Louis, Missouri, USA), at a concentration of 11 mg/mL in PBST pH 7.4 for a contact time of 300 seconds. The surface was then deactivated with 1 M ethanolamine pH 8.5 before the immobilisation of prorenin or renin, as described in Section 2.8.4.1.

*2.8.4.3 Interaction with Angiotensinogen*

A dilution series of pure angiotensinogen (reduced or oxidised) with a dilution factor of two was prepared in PBST pH 7.4 to give angiotensinogen concentrations of 200 nM, 100 nM, 50 nM, 25 nM, 12.5 nM, and 6.25 nM. A 100 µL injection of each angiotensinogen concentration was flowed simultaneously across the chip in the analyte direction at a flow rate of 50 µL/min and allowed to associate with the prorenin or renin for a total contact time of 120 seconds. At the end of the injection, running buffer was flowed across all analyte channels for 600 seconds to allow dissociation. This was then followed with regeneration of the ligand surface—a 30 µL pulse of glycine HCl pH 2.0 for a total of 18 seconds at a flow rate 100 µL/min to remove any undissociated analyte.

#### *2.8.4.4 Activation of Prorenin by Trypsin Digest on Sensor Chip*

Prorenin, already immobilised on the sensor chip surface at a concentration of 0.01 mg/mL, was proteolytically digested by flowing trypsin across the ligand channel. Trypsin, 208 µL at a concentration of 0.5 mg/mL in MQ water, was injected, across the ligand channel that contained immobilised prorenin at a flow rate of 25 µL/min for 500 seconds. The reaction was quenched by a 30 µL pulse of 0.5% formic acid for 18 seconds at a flow rate of 100 µL/min. Multiple blank buffer injections, first in the ligand direction and then the analyte direction, were performed until a stable baseline was achieved across all channels, before interaction runs with angiotensinogen, as described in Section 2.8.4.3, were repeated.

### *2.8.5 Interaction of Recombinant Human Angiotensinogen with Recombinant Glycosylated Human Renin via Aldehyde Coupling*

As an alternative approach to the amine coupling immobilisation of renin described in Section 2.8.4, renin was immobilised onto the sensor chip surface using aldehyde coupling, which tethers proteins to the chip surface by their glycosylation residues rather than by amine residues (such as lysines).

#### *2.8.5.1 Immobilisation*

The sensor chip surface was activated by a 180 µL injection of a 1:1 mixture of 0.4 M EDAC and 0.1 M NHS for 180 seconds at a flow rate of 25 µL/min to activate the carboxymethyl dextran on the sensor chip surface to produce reactive succinimide esters. A 175 µL injection of 5 mM carbohydrazide (in MQ water; Sigma-Aldrich, St. Louis, Missouri, USA) was flowed across the surface for 420 seconds at a flow rate of 25 µL/min to introduce hydrazide groups to the sensor chip surface, which was then subsequently followed by deactivation with

175 µL of 1 M ethanolamine HCl pH 8 injected at a flow rate of 25 µL/min for 420 seconds to deactivate any unreacted succinimide esters. Renin (oxidised with 1 mM sodium meta periodate (Sigma-Aldrich, St. Louis, Missouri, USA) according to the protocol in the Biacore Sensor Surface Handbook (BR-1005-71 Edition AB) was then immobilised at a concentration of 0.01 mg/mL (in 10 mM sodium acetate buffer pH 4 or pH 5) by injecting 210 µL of protein solution across two ligand channels for 420 seconds at a flow rate of 30 µL/min. Two 250 µL injections of 0.1 M sodium triacetoxyborohydride (Sigma-Aldrich, St. Louis, Missouri, USA dissolved in 0.1 M sodium acetate pH 4) were performed for 10 minutes each at a flow rate 25 µL/min to reduce and stabilise the covalent bond formed between the ligand and surface. An unmodified surface was used as a reference channel. Multiple blank buffer injections, first in the ligand direction and then the analyte direction, were performed until a stable baseline was achieved across all channels.

#### *2.8.5.2 Interaction with SUMO-AGT*

A dilution series of pure SUMO-AGT with a dilution factor of two was prepared in PBST to give SUMO-AGT concentrations of 3 µM, 1.5 µM, 0.75 µM, 0.375 µM, 0.1875 µM, and 0 µM. A 250 µL injection of each SUMO-AGT concentration was flowed across the chip in the analyte direction at a flow rate of 50 µL/min and allowed to associate with the immobilised renin for a total contact time of 300 seconds. At the end of the injection, running buffer was flowed across all analyte channels for 600 seconds to allow dissociation. This was then followed with regeneration of the ligand surface—a 30 µL pulse of glycine HCl pH 2.0 for a total of 18 seconds at a flow rate 100 µL/min to remove any undissociated analyte. At least four blank buffer injections were performed to allow the ligand to recover and ensure a stable baseline was re-established. This interaction run was repeated using pure SUMO-CAT as a negative control.

### *2.8.6 Data Analysis*

All data were exported from the ProteOn™ Manager (Bio-Rad Laboratories, Hercules, California, USA). The data were processed using Scrubber 2 (Prot version, Biologic Software, Campbell, Australian Capital Territory, Australia) and fit to a simple 1:1 Langmuir binding model (or a more complex binding model if necessary) using ClampXP software[145] to obtain kinetic association and dissociation constants. Monte Carlo analysis was also performed using ClampXP for each dataset by performing 50 independent rounds of model fitting with a maximum iteration of 25 cycles per fit, a variation of 1000%, and added noise of 4 RU.

Statistical analysis was carried out on the mean anti-AGT mAb surface kinetic constant values for oxidised and reduced angiotensinogen by performing independent sample *t*-tests (two-tailed, 95% confidence level) to test whether the kinetic values for the two forms of angiotensinogen differed significantly. Minitab 16 (Lead Technologies, Inc., Charlotte, North Carolina, USA) was used to perform the statistical analysis, and the data were checked for normality using the normality test prior to analysis.

## 2.9 REACTION OF RECOMBINANT HUMAN ANGIOTENSINOGEN WITH MPEG 5000/10000

Polyethylene glycol (PEG) with a maleimide functionality (methoxy polyethylene glycol maleimido-propionamide, mPEG) was used to demonstrate that the angiotensinogen protein could be derivatised in either the reduced or oxidised form. Stock solutions of mPEG 5000 and mPEG 10000 (Chirotech Technology Ltd., Cambridge, UK) were prepared fresh immediately prior to use in PBS pH 7.2 at concentrations of 30 mM and 20 mM respectively. A stock solution of tris(2-carboxyethyl)phosphine (TCEP; Sigma-Aldrich, St. Louis, Missouri, USA) was also prepared freshly, just prior to use, in PBS pH 7.2 at a concentration of 100 mM.

Pure SUMO-AGT at a concentration of 1.4 mg/mL (in PBS pH 7.2) was incubated in either the presence or absence of 10 mM TCEP for one hour at 25 °C shaking in an Eppendorf

Thermomixer® Comfort (Eppendorf, Hamburg, Germany). TCEP did not need to be removed prior to the mPEG incubation as the compound does not contain any free thiols that could react with the maleimide functionality. Subsequently, mPEG 5000 or mPEG 10000 was added to the protein solution to give a final mPEG concentration of 10 mM, and was mixed well. Upon mixing, a 20 μL sample of each reaction was immediately taken and prepared for SDS-PAGE analysis (see Section 2.2.6) and samples were stored at –20 °C for later analysis.

The SUMO-AGT mPEG reactions were returned to the thermomixer and left to incubate at 25 °C while shaking and protected from light. Further 20 μL samples were taken after 1.5 hours, 4 hours, and overnight incubation and prepared for SDS-PAGE analysis. As a control, a sample of SUMO-AGT in the presence or absence of reducing agent was also run on the same SDS-PAGE gel, so that any changes in molecular weight that occurred would be clearly shown.

## 2.10 MOLECULAR DYNAMIC SIMULATIONS

Molecular dynamic simulations were performed at Monash University (Melbourne, Australia). Molecular dynamics simulations were carried out on human angiotensinogen (PDB structure 2WXW), in both the reduced form (Cys 18 and Cys 138 reduced) and oxidised form (Cys 18 and Cys 138 disulphide bonded). Missing loops and side chain residues were modeled using MODELLER.[146] All chain termini were capped with neural groups (acetyl and methylamide). With completed structures, the simulations were solvated in a cubical simulation box with a minimum distance of 1.4 nm from the protein to the box wall, followed by the addition of 150 mM NaCl to the aqueous phase. Simulations initially measured at 11.19 nm x 11.19 nm x 11.19 nm containing 133,011 water molecules, 139 sodium ions and 127 chloride ions for a total of 136,910 atoms.

All simulation systems were subjected to energy minimization, followed by a three stage equilibration protocol with positional restrains holding all protein atoms with 1,000 kJ

$mol^{-1}$ $nm^{-2}$ for 100 ps, restraints on all backbone atoms with 1,00 kJ $mol^{-1}$ $nm^{-2}$ for 100 ps and restraints on C-alpha atoms with 100 kJ $mol^{-1}$ $nm^{-2}$ for 100 ps, respectively. Each system was then subjected to free simulation with configurations stored every 10 ps for analysis.

The prepared reduced and oxidised systems were run at 300 K for 500 ns, in triplicate, with each replicate starting from a different distribution of initial velocities. All simulations were performed using GROMACS version 4.0.7,[147] in conjunction with the GROMOS 54A7 united-atom force field.[148] Ionizable residues were set to their standard protonation states at pH 7. Water was represented explicitly using the simple-point-charge (SPC) model.[149] All simulation systems were equilibrated in an NVT ensemble and production runs performed in an NPT ensemble under periodic conditions. Temperature was maintained close to its reference value of 300 K by V-rescale temperature coupling. Pressure was maintained close to a reference value of 1 atm by isotropic coupling with a berensden pressure bath.[150] Non-bonded interactions were evaluated using a twin-range cut-off scheme: interactions falling within the 0.8 nm short-range cutoff were calculated every 2 fs whereas interactions within the 1.4 nm long cutoff were updated every 10 fs, together with the pair list. A generalized reaction-field correction was applied to the electrostatic interactions beyond the long-range cutoff,[151] using a relative dielectric permittivity constant of $\varepsilon RF = 62$ as appropriate for SPC water.[152]

All bond lengths to hydrogen atoms were constrained using the P-LINCS algorithm[153] and water geometry was constrained using the SETTLE algorithm.[154] The time step used for integrating the equations of motion was 2 fs.

Analyses of the simulations were performed using the tools provided in the GROMACS package 4.0.7,[147] and custom scripts in conjunction with ProDy.[155] Graphs and plots were produced using Matplotlib.[156] Molecular graphics were prepared with PyMol version 1.3.2[157] and Visual Molecular Dynamics (VMD) 1.9.2.[158]

*Chapter Three*

# EXPRESSION AND PURIFICATION OF RECOMBINANT HUMAN ANGIOTENSINOGEN

## 3.1 INTRODUCTION

Prior to the introduction of recombinant protein expression, angiotensinogen could only be studied by purifying it from the plasma of humans and other animals in multi-step purification schemes with generally low yields. For instance, Bouhnik *et al.* purified rat angiotensinogen in a six step procedure involving ammonium sulphate precipitation, and multiple chromatography steps, followed by isoelectric focussing, with an overall yield of only 7%.[159] Similarly, Grisé *et al.* reported the partial purification of angiotensinogen from human plasma in a five step process including ammonium sulphate precipitation, followed by four chromatographic steps resulting in a 100-fold purification with a yield of only 15.9%.[160] More recently, human angiotensinogen was elegantly immunopurified from plasma in a one-step process with a yield of approximately 90% by using an immunoaffinity column containing anti-angiotensinogen monoclonal antibodies immobilised on cyanogen bromide-activated Sepharose.[25] Despite advances in purification of angiotensinogen from plasma, plasma purification is limited by the amount of angiotensinogen present in plasma, with a large volume of plasma required to obtain a substantial amount of angiotensinogen.

The publication of the cDNA sequence of the human angiotensinogen gene in 1984 heralded the move towards recombinant expression of angiotensinogen.[109] With advances in fusion protein technology for enhanced solubility and affinity purification purposes, as well as many expression hosts now readily at our disposal, the expression of recombinant

angiotensinogen has been described in both bacterial and mammalian expression systems,[1, 161, 162] allowing far greater amounts of angiotensinogen to be more readily available to be studied. For instance, Zhou *et al.* reported the expression of recombinant glycosylated angiotensinogen in human embryonic kidney cells, and these researchers also made use of the SUMO-fusion system to facilitate recombinant bacterial expression of angiotensinogen.[1] Recombinant technology has facilitated the simple isolation and purification of proteins, often in only one or two steps, through the introduction of affinity fusion tags such as polyhistidine (His), and glutathione-s-transferase (GST) tags, which can be removed following purification, allowing for quick, low-cost purification of recombinant proteins and high yields.[163]

Compared with eukaryotic expression systems, expression using the bacterial host *E. coli* provides a simple, rapid and inexpensive method of protein expression, but it does also have its drawbacks.[163-165] Proteins produced using *E. coli* as the expression host lack post-translational modifications, such as glycosylation—modifications that could be important for protein structure or function.[164] In addition, recombinant proteins (particularly of eukaryotic origin) overexpressed in *E. coli* have the propensity to form insoluble inclusion bodies, further complicating the expression and purification procedure.[163-165] These are all factors that need to be taken into consideration when choosing expression and purification strategies.

This chapter describes the construction of two expression plasmids containing the human angiotensinogen gene, and the screening and optimisation of angiotensinogen expression in *E. coli* cells in order to ascertain the best expression conditions for recombinant production of human angiotensinogen. Large-scale expression and purification was subsequently carried out to obtain pure recombinant human angiotensinogen and is described in detail.

## 3.2 CLONING OF THE HAGT GENE INTO PETDUET_DSBC VECTOR

PCR amplification of the human AGT gene (from the pET_16b_AGT plasmid) to include the addition of the KpnI restriction site at the 3' end of the gene led to the generation of a 1533 bp sized fragment of DNA which, when subjected to DNA gel electrophoresis, migrated as a discrete band (Figure 3.1).

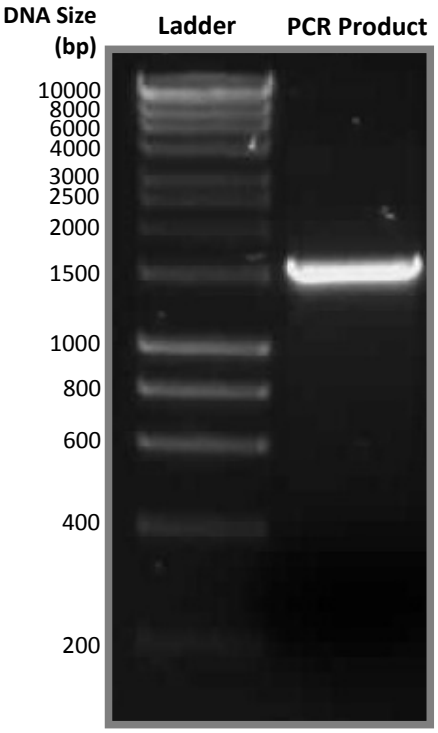


*Figure 3.1:*

*DNA gel electrophoresis analysis of PCR amplification of the human angiotensinogen gene from the pET_16b_AGT plasmid (with the addition of the KpnI restriction site) to be cloned into pETDuet_DsbC vector via the TOPO vector.*

Many colonies were obtained as a result of the amplified gene being ligated into the pCR™ 2.1-TOPO vector and subsequent transformation of the ligation mixture into DH5α cells. Screening of ten of these colonies by colony PCR revealed that ligation of the hAGT gene into the TOPO vector was successful with eight of the ten colonies screened containing a discrete band of the expected gene insert size of 1733 bp (when amplified using the M13 forward and reverse primers) as shown in Figure 3.2. Colonies that did not contain the hAGT gene had a band of approximately 200 bp, which is consistent with the size of PCR product expected when the

region between the forward and reverse primer sites is amplified in an empty plasmid (i.e. no insert present).

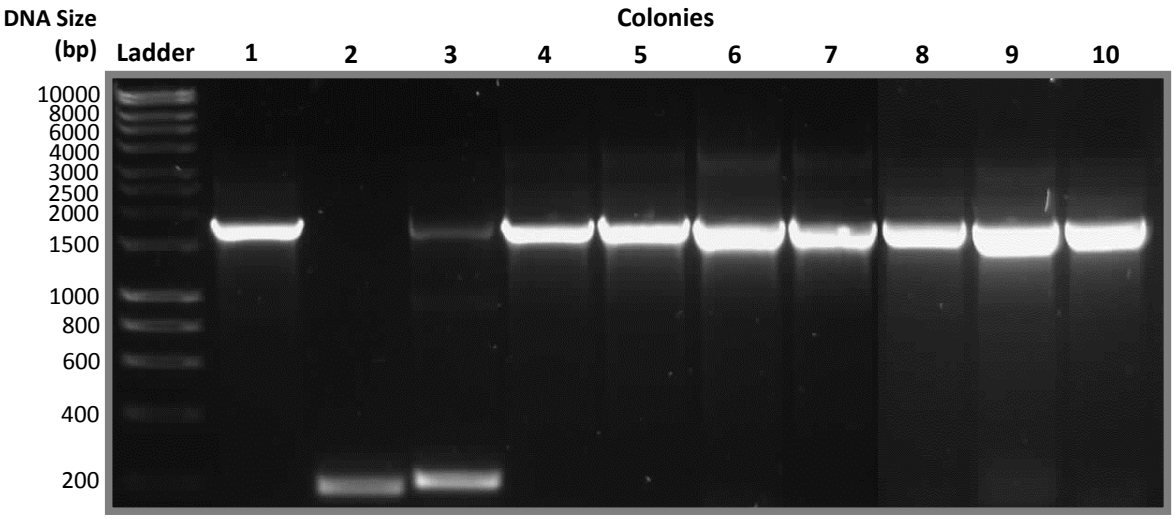


*Figure 3.2:*

*DNA gel electrophoresis analysis of colony PCR to check for the presence of the hAGT gene insert, carried out on ten of the colonies obtained following ligation of the hAGT gene into the pCR™ 2.1-TOPO vector. Colonies 1 and 4 – 10 all contained the correctly sized hAGT gene insert. Colonies 2 and 3 were false positives and contained no gene insert.*

Following plasmid purification, both the TOPO-hAGT plasmid and the pETDuet_DsbC_BlgA plasmid were subjected to a double restriction digest using the restriction enzymes NdeI and KpnI-HF. A double digest of the pETDuet_DsbC_BlgA plasmid was performed to remove the BlgA gene from the plasmid, while the TOPO-hAGT plasmid was digested to cut the hAGT gene out of the plasmid ready for ligation into the pETDuet_DsbC plasmid. Following the digestion, both restricted DNA plasmids were run on an agarose gel (Figure 3.3) so that the hAGT gene insert and the restricted vector pETDuet_DsbC vector could be purified. As a control, the unrestricted plasmid DNA was also run on the same gel so that restriction would be clearly observable and could be differentiated from unrestricted plasmid.

The intact TOPO_hAGT and pETDuet_DsbC_BlgA plasmids (prior to restriction) did not migrate to the expected sizes of 5464 bp and 6610 bp respectively, due to circular DNA having a different electrophoretic mobility to linear DNA—it is clear, however, from this gel that restriction had indeed taken place, with the restricted TOPO vector and pETDuet_DsbC vectors migrating to the expected sizes of 4084 bp and 6130 bp respectively. The hAGT gene insert is shown as a discrete band at 1380 bp, as expected, while the BlgA gene was only just visible on the gel migrating to a size of approximately 600 bp.

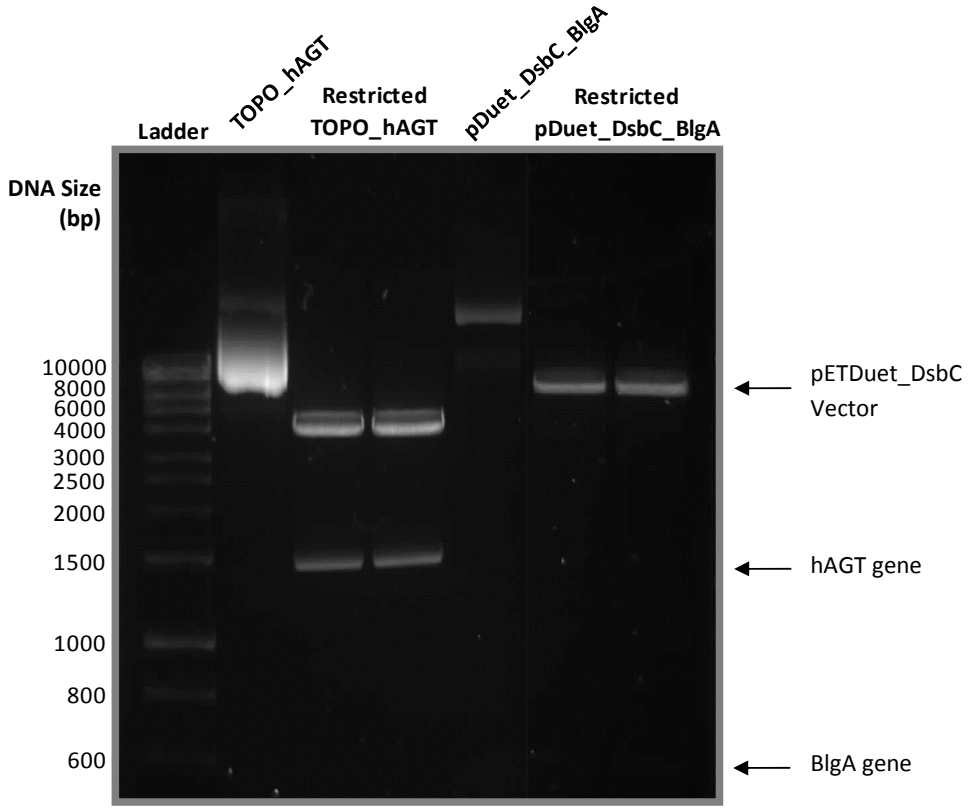


*Figure 3.3:*

*DNA gel electrophoresis analysis of the double restriction digest of the TOPO_hAGT and pETDuet_DsbC_BlgA plasmids to isolate the hAGT gene insert and the pETDuet_DsbC plasmid ready for ligation. Unrestricted TOPO_hAGT and pETDuet_DsbC_BlgA were also run as a control.*

Following gel purification and ligation of the hAGT gene into the pETDuet_DsbC vector, cells were transformed with the ligation mixture resulting in a total of 15 colonies being obtained. Colony PCR screening of these colonies revealed that ten of these colonies contained the hAGT gene (confirming successful ligation of the hAGT gene into pETDuet_DsbC), with the insert DNA migrating to the expected insert size of 1620 bp, while the remaining five colonies were false positives. Five of the colonies screened by colony PCR are shown in Figure 3.4 below.

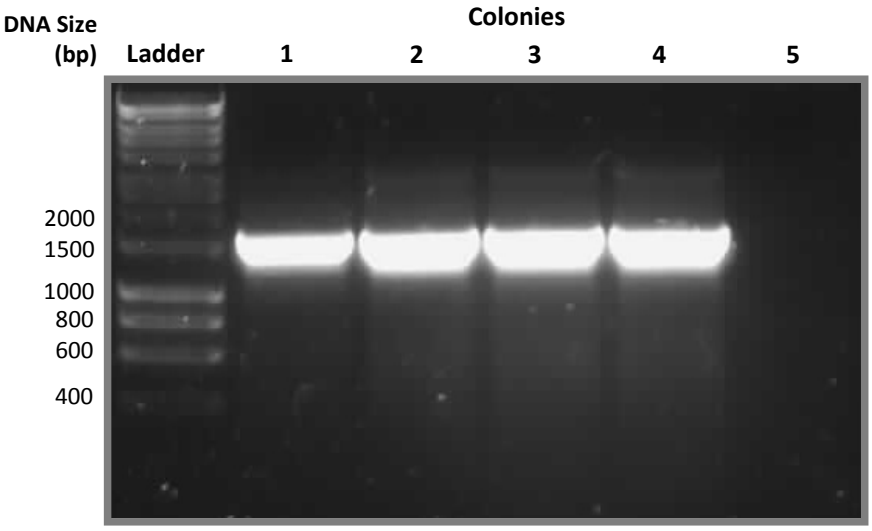


*Figure 3.4:*

*DNA gel electrophoresis analysis of colony PCR to check for the presence of the hAGT gene insert, following ligation of the hAGT gene into the pETDuet_DsbC vector. Colony PCR screening of five of the fifteen colonies obtained is shown. Colonies 1 – 4 contained the correctly sized hAGT gene insert. Colony 5 was a false positive and contained no gene insert.*

The pETDuet_DsbC_hAGT plasmid was purified from each of the ten colonies, and sequencing confirmed that the hAGT gene had the correct sequence (i.e. no mutations were introduced as a result of the cloning procedures) and the gene was in the correct frame of the plasmid for expression.

## 3.3 CLONING OF THE HAGT GENE INTO PET-SUMO VECTOR

PCR amplification of the human AGT gene (from the pET_16b_AGT plasmid), ready for ligation into the pET-SUMO vector, resulted in the generation of a 1359 bp sized fragment of DNA (as expected) which, when subjected to DNA gel electrophoresis, migrated as a discrete band (Figure 3.5).

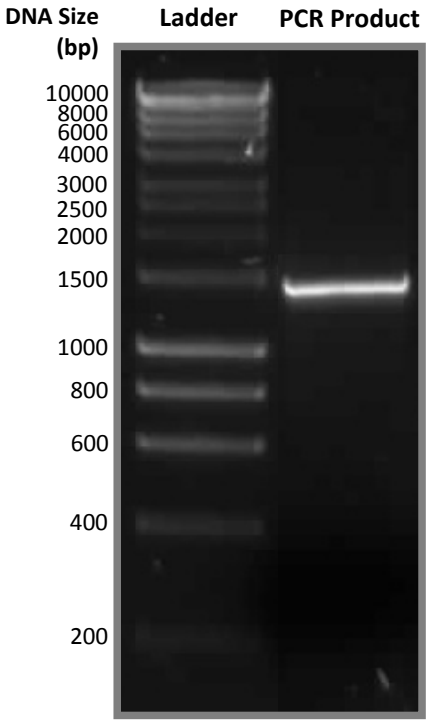


*Figure 3.5:*

*DNA gel electrophoresis analysis of PCR amplification of the human angiotensinogen gene from the pET_16b_AGT plasmid ready for cloning into pET-SUMO vector.*

In total, seven colonies were obtained as a result of the amplified gene being ligated into the pET-SUMO vector and the subsequent transformation of the ligation mixture into DH5α cells. Screening of these seven colonies by colony PCR revealed that ligation of the hAGT gene into the pET-SUMO vector was successful with four of the seven colonies screened containing a discrete band of the expected gene insert size of 1612 bp (when amplified using the plasmid specific SUMO forward and T7 reverse primers) as shown in Figure 3.6. Colonies that did not contain the hAGT gene had a band of approximately 200 bp, which is consistent with the size of

PCR product expected when the region between the forward and reverse primer sites is amplified in an empty plasmid (i.e. no insert present).

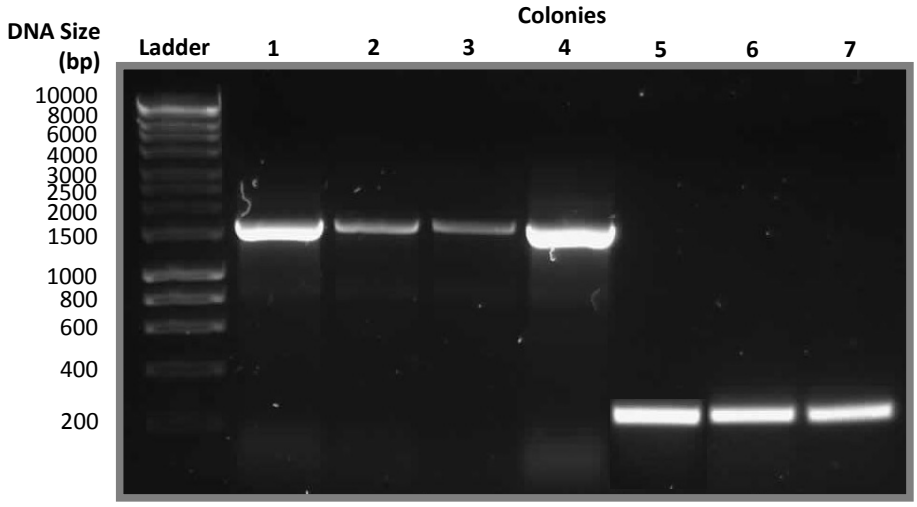


*Figure 3.6:*

*DNA gel electrophoresis analysis of colony PCR to check for the presence of the hAGT gene insert, following ligation of the hAGT gene into the pET-SUMO vector. Colony PCR screening of all seven colonies obtained is shown. Colonies 1 – 4 contained the correctly sized hAGT gene insert. Colonies 5 - 7 were false positives and contained no gene insert.*

The plasmid was purified from each of the four colonies, and sequencing was performed to check whether the hAGT gene had the correct sequence (i.e. no mutations were introduced as a result of the cloning procedures) and the gene was in the correct frame of the plasmid for expression. It was also particularly important to check the orientation of the hAGT gene in the pET-SUMO vector. This was because the pET-SUMO cloning system makes use of the TA cloning technique, whereby the single 3'-adenylated overhangs, produced by *Taq* polymerase during the extension cycle of PCR, ligate efficiently into the linearised vector containing 3'-thymidine overhangs. Thus, unlike cloning mediated by restriction enzymes, which provide orientation-specific ligation of the gene of interest into the destination plasmid, TA cloning results in ligation of the gene insert into the plasmid in either orientation. Sequencing revealed

that only one of the four colonies contained the hAGT gene in the correct orientation, the other three positive clones contained the hAGT gene ligated into the pET-SUMO vector in the reverse orientation.

## 3.4 EXPRESSION TRIALS

Having created two different plasmids containing the hAGT gene, in addition to obtaining the pET_16b_AGT construct, extensive expression trials were subsequently carried out to ascertain the optimum conditions required to overexpress and purify recombinant human angiotensinogen to maximise the yield of native pure protein.

Several *E. coli* cell strains were used during expression trials. BL21 (DE3) star cells contain a mutation in the RNaseE gene (*rne*131) that confers enhanced stability of mRNA transcripts, compared to the standard BL21 (DE3) strain, leading ultimately to higher yields of protein. It was thought that Rosetta (DE3) cells, which supply genes for tRNAs of rare codons on the pRARE plasmid, may have helped with the expression of the hAGT gene as it contains several codons that are rarely used in *E. coli*. As another approach, Origami (DE3) cells were also trialled as it was thought that these cells may have provided some benefit by aiding in the correct folding of the angiotensinogen protein. Mutations in the thioredoxin reductase (*trxB*) and glutathione reductase (*gor*) genes of these cells have the ability to greatly enhance the formation of disulfide bonds in the cell's cytoplasm. Given that angiotensinogen contains four cysteine residues, any misfolding could lead to aberrant disulfide bond formation, and ultimately aggregation and insolubility of the recombinant protein.

Firstly, the pET_16b_AGT construct, which codes for the N-terminally deca-His-tagged angiotensinogen protein, was transformed into the three *E. coli* strains BL21 (DE3) star, Rosetta (DE3), and Origami (DE3). SDS-PAGE analysis of these cells, when induced, showed good overexpression of the angiotensinogen protein, which migrated to a size of approximately

52 kDa on the gels. Unfortunately irrespective of cell strain, growth temperature, expression time, or growth media, the angiotensinogen protein was shown to be largely insoluble and was found only in the insoluble pellet fraction. Trials with different buffer conditions for lysis, or lowering of the IPTG concentration for expression induction (lower IPTG levels may have slowed protein expression, increasing the yield of soluble protein), did little to improve the solubility of His-tagged angiotensinogen.

Secondly, the pETDuet_DsbC_hAGT construct was transformed into BL21 (DE3) and Origami (DE3) cells. This construct encodes the gene for untagged human angiotensinogen (49.9 kDa) which is co-expressed with DsbC, a 23 kDa protein that acts as a disulfide bond isomerise and chaperone to facilitate correct disulfide bond formation.[166] Despite DsbC expressing well on induction with IPTG, no overexpression of angiotensinogen could be observed on SDS-PAGE analysis in either *E. coli* cell strain, regardless of expression temperature or time. Sequencing confirmed that the pETDuet_DsbC_hAGT construct contained the hAGT gene in the correct frame for expression and the sequence was correct, ruling out any nonsense mutations that could result in premature termination of translation. Thus it was unclear as to the reason for the failure of this construct to overexpress angiotensinogen, and it was not pursued any further.

Finally, the pET-SUMO_hAGT plasmid was transformed into BL21 (DE3) cells. This construct, which confers kanamycin resistance, was not trialled in the Origami (DE3) strain due this strain's intrinsic resistance to kanamycin. The pET-SUMO_hAGT plasmid encodes the gene for angiotensinogen, with an N-terminal His-tag followed by the SUMO fusion tag prior to the start of the angiotensinogen sequence. The SUMO protein, an 11 kDa *Saccharomyces cerevisae* Smt3 protein, has been shown to both increase expression levels and enhance protein solubility, and can subsequently be removed by the specific SUMO Protease, Ulp, following expression and purification[167, 168] and was an approach undertaken successfully by Zhou *et al*.[1] SDS-PAGE analysis of cells transformed with this construct showed good overexpression of the SUMO-

AGT protein following overnight expression, with the SUMO-AGT protein migrating to a size of just above 60 kDa (consistent with its expected molecular weight of 63.1 kDa). Although insoluble when expressed at 37 °C, what was surprising was the effect that the addition of 1% glucose to the growth media had on the solubility of the SUMO-AGT protein when expressed at 26 °C, as shown in Figure 3.7. Transformed cells cultured and induced in LB media alone led to the production of SUMO-AGT which was almost completely insoluble and present in the pellet fraction. Addition of 1% glucose to the growth media dramatically enhanced the solubility of the SUMO-AGT protein, so much so that the SUMO-AGT protein was now completely soluble and present in the soluble fraction.

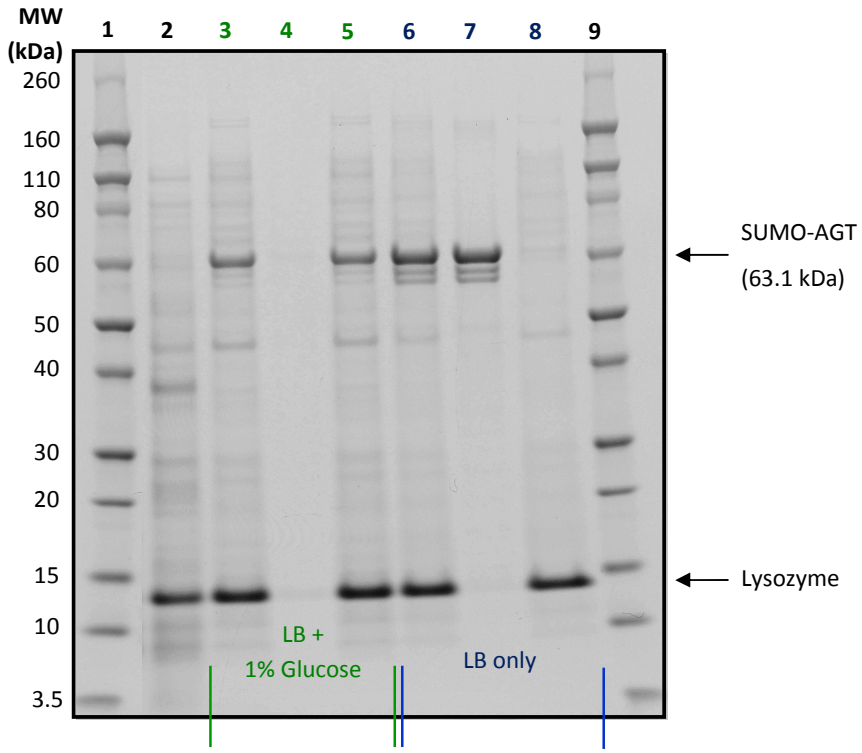


*Figure 3.7:*

*SDS-PAGE analysis of BL21 (DE3) cells expressing the SUMO-AGT protein at 26 °C. The molecular weight marker (Novex® Sharp Pre-stained Protein Standard) was loaded in lanes 1 and 9. Uninduced cells were run in lane 2. Lanes 3, 4, and 5 contain the total cell lysate, pellet, and soluble fractions, respectively, of cells induced with IPTG and grown in LB media supplemented with 1% glucose. Lanes 6, 7, and 8 contain the total cell lysate, pellet, and soluble fractions, respectively, of cells induced with IPTG and grown in LB media alone. Cells were lysed with CelLytic B and 0.2 mg/mL lysozyme, which can be seen on the gel at a MW of 14.3 kDa.*

How can glucose make such a difference to the solubility of the SUMO-AGT protein? Glucose appears to play a modulative role in the regulation of recombinant protein expression. Expression of the SUMO-AGT protein from the pET-SUMO_hAGT plasmid is under the regulatory control of the $T7_{lac}$ promoter. Until induction, expression of the T7 RNA polymerase (regulated by the *lacUV5* promoter of the host strain) is repressed because the Lac repressor, LacI, is bound to the promoter region preventing its transcription by other RNA polymerases.[169-171] When allolactose, or its synthetic mimic IPTG, is added to the bacterial culture, it binds to the Lac repressor and alleviates repression, paving the way for the transcription and expression of T7 RNA polymerase, which, now unregulated, is free to bind to the T7 promoter on the pET-SUMO_hAGT plasmid and transcribe the hAGT gene, inducing expression of the SUMO-AGT protein. In a perfect system, the repression of expression would be complete such that no leaky expression of the desired protein would occur. However, this is rarely the case. Despite the increased level of repression of the $T7_{lac}$ promoter over the standard T7 promoter, some leaky expression of the desired protein prior to induction will often be observed due to the occasional expression and high activity of T7 RNA polymerase[169, 171]—which is where glucose comes in. The addition of 1% glucose is able to maintain tight regulation of the promoter and reduce basal or leaky protein expression by preventing the accumulation of cyclic adenosine monophosphate (cAMP) within the cell.[171] cAMP accumulation, in the absence of glucose, initiates transcription of the gene for T7 RNA polymerase from the *lacUV5* promoter, even in the absence of inducer, by activating the catabolite gene activator protein (CAP).[169, 171] Thus glucose plays a role in catabolite repression, greatly decreasing any undesired expression of the protein of interest prior to induction.

Although, little to no basal expression of the SUMO-AGT protein was evident in the uninduced cells by SDS-PAGE analysis (Figure 3.7), this does not rule out that small levels of expression of SUMO-AGT may be occurring prior to induction. Cells cultured in the presence or

absence of glucose showed very little difference in their rates of growth, thus it appears that glucose might simply be slowing down the rate of transcription and expression of the SUMO-AGT protein by maintaining cAMP levels to a minimum until all the glucose is used up. With glucose slowing protein expression so that SUMO-AGT is not being produced at a breakneck pace within the cell on induction, there appears to be a higher yield of soluble protein possibly by allowing more time for correct folding, as well as by slowing the huge accumulation of the SUMO-AGT protein intracellularly, since aggregation and inclusion body formation is far more likely as protein concentrations increase within the cell.[163, 164]

With expression conditions optimised, several lysis methods were trialled to ascertain the best and most facile way to lyse the cells for larger scale expression to obtain the highest yield of soluble SUMO-AGT for purification. The three means of cell lysis trialled were sonication, cell homogenization, and CelLytic B. Sonication is a common method of bacterial cell lysis that is carried out by immersing a probe in the cell suspension that gives off pulses of high frequency sound waves which shear cells.[165, 172] Although commonly employed for cell lysis, it has the disadvantage of generating heat, resulting in denatured protein, and thus sonication is carried out on ice to minimise heat generation. A much gentler alternative to sonication is to use a cell homogenizer that uses high pressure to lyse cells by shear forces, which, depending on the protein of interest, can result in higher yields of soluble protein than sonication[165, 172]—the only disadvantage being that much larger volumes of cell suspensions (>20 mL) are required for this lysis method. Lastly, CelLytic B is another method of cell lysis (employed during expression trials) that facilitates the gentle lysis of bacterial cells by the action of non-denaturing zwitterionic detergents aided by the addition of lysozyme. As opposed to sonication and the cell homogenizer, CelLytic B tends to result in much higher yields of the protein of interest,[173] but although it will not solubilise inclusion bodies, CelLytic B does tend to solubilise a larger amount of the other proteins present in the cell lysate compared to other lysis methods, which

could complicate downstream purification strategies, and it also adds a substantial amount of detergent to the protein extract, which would need to subsequently be removed.

The results of lysis trials are shown in the SDS-PAGE gel in Figure 3.8. Sonication led to mostly insoluble SUMO-AGT, although a small proportion was present in the soluble fraction. Lysis by the cell homogenizer also led to a large amount of insoluble SUMO-AGT, but there was still a substantial amount present in the soluble fraction. CelLytic B lysis, on the other hand, led to completely soluble SUMO-AGT protein; in fact lysis by this method resulted in virtually no insoluble material at all with only a very small pellet obtained following centrifugation of the cell lysate. Due to CelLytic B's propensity to solubilise everything in the cell lysate, including two protein bands that sit just below the band of SUMO-AGT on the gel (Figure 3.8) which also overexpress on induction with IPTG, it was decided that cell homogenization would be used as the method of cell lysis prior to purification despite its lower yield of soluble protein. Although the nature of these two proteins with a similar molecular weight to SUMO-AGT was not known, given that their expression was induced by IPTG, it is possible that these are truncated SUMO-AGT proteins, shortened either due to early termination of transcription/translation or through proteolytic degradation following lysis. If this is the case, then their presence in the soluble fraction of the cell-lysate could unnecessarily complicate purification. Thus, cell homogenization was chosen as the preferred method for cell lysis.

## 3.5 Expression and Purification of Human Angiotensinogen

With expression and lysis conditions for the SUMO-AGT protein optimised, larger-scale expression and purification could now be carried out. Cells expressing SUMO-AGT overexpressed the protein just as well in larger culture volumes (500 mL) as they did in smaller cultures. Cells were lysed by cell homogenisation in a buffer containing 50 mM potassium

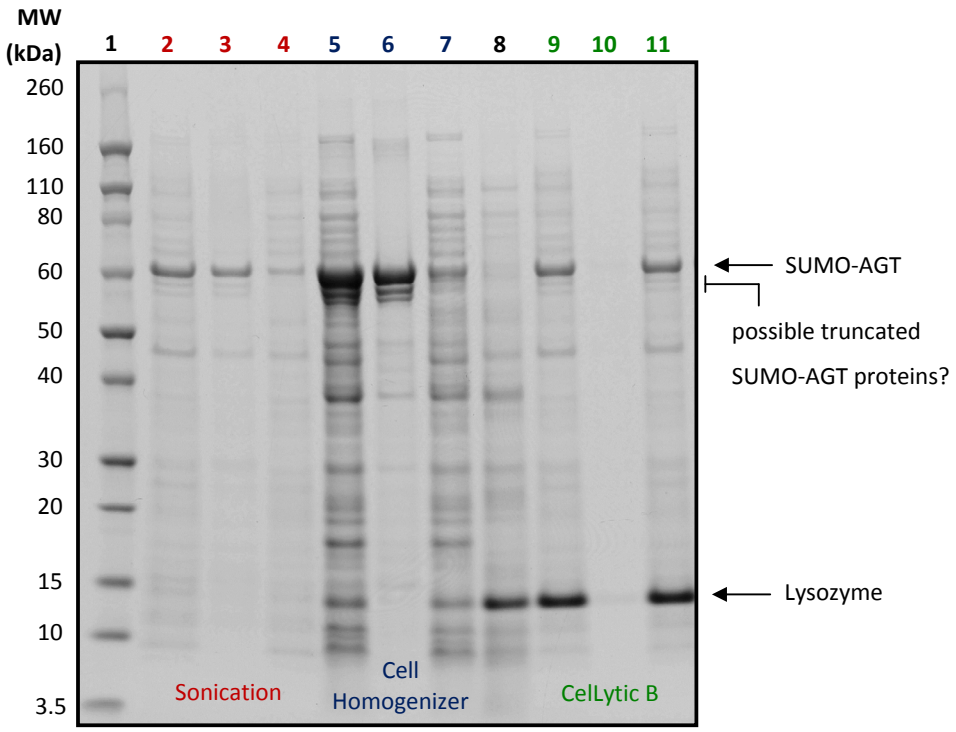


*Figure 3.8:*

*SDS-PAGE analysis of BL21 (DE3) cells expressing the SUMO-AGT protein at 26 °C lysed by three different methods. The molecular weight marker (Novex® Sharp Pre-stained Protein Standard) was loaded in lane 1 while uninduced cells were loaded in lane 8. Lanes 2, 3, and 4 contain the total cell lysate, pellet, and soluble fractions, respectively, of cells lysed by sonication. Lanes 5, 6, and 7 contain the total cell lysate, pellet and soluble fractions, respectively, of cells lysed using the cell homogenizer. Lysis by CelLytic B and lysozyme is displayed in the last three lanes, with lanes 9, 10, and 11 containing the total cell lysate, pellet and soluble fraction, respectively. All samples were lysed in Lysis Buffer.*

phosphate, 400 mM sodium chloride, 100 mM potassium chloride, 10% glycerol, 0.5% Triton X-100, and 10 mM imidazole at pH 7.8 (Lysis Buffer, see Appendix). Protein was purified by IMAC (cobalt resin) followed by size exclusion chromatography resulting in highly pure SUMO-AGT. Figure 3.9 shows the various fractions resulting from the His-tag affinity purification (IMAC) step. SUMO-AGT (63.1 kDa) bound well to the resin and eluted at an imidazole concentration of 50 mM with a couple of other protein species which had a MW of 30 kDa or less. Spin concentration, with a 30,000 MWCO concentrator, of the pooled fractions

containing SUMO-AGT served not only to concentrate the protein but also to remove the majority of the smaller proteins which co-eluted with SUMO-AGT.

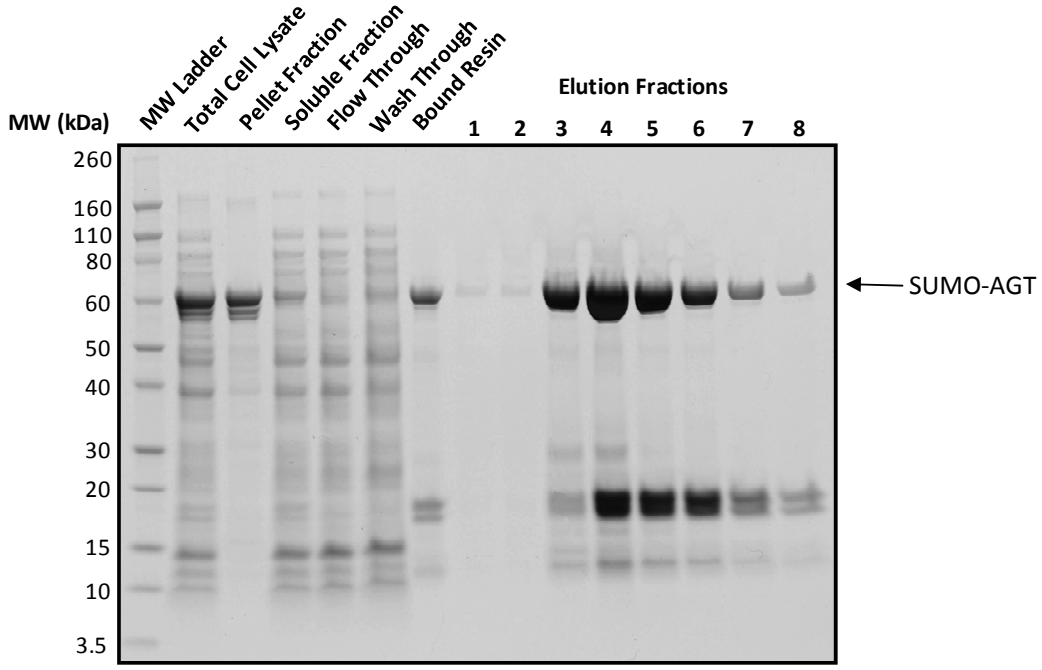


*Figure 3.9:*

*SDS-PAGE analysis of IMAC purification of SUMO-AGT from cell lysate using HisPur cobalt resin. The first lane contains the molecular weight marker (Novex® Sharp Pre-stained Protein Standard). Subsequent lanes contain the total cell lysate, the pellet fraction, and the soluble fraction (what was loaded onto the column), followed by the flow through and wash fractions as labelled. The lane containing the bound resin shows SUMO-AGT bound well to the resin. The SUMO-AGT protein was eluted in PBS pH 7.4 containing 50 mM imidazole and collected in 1 mL fractions.*

Size exclusion chromatography using a gel filtration column (24mL Superdex 200) was used as a final polishing purification step. By separating proteins according to size,[165] gel filtration allowed the removal of the smaller proteins from the purified protein resulting in a pure sample of SUMO-AGT. This step was also used as a means of buffer exchange to remove the imidazole from the protein buffer. Elutions were collected in 1 mL fractions and SDS-PAGE analysis revealed that SUMO-AGT eluted as the first big peak (see Figures 3.10 and 3.11) with a shoulder that contained smaller protein species. Fractions that corresponded to the second

smaller peak with a maximum at approximately 26 mL were also subjected to SDS-PAGE analysis but no protein was present in these fractions at concentrations visible on the gel. Seven elution fractions corresponding to the elution from 10 mL to 16 mL in Figure 3.10 and 3.11 were pooled and concentrated as they contained the majority of the SUMO-AGT protein and negligible amounts of the smaller protein species. This constituted pure SUMOylated human angiotensinogen.

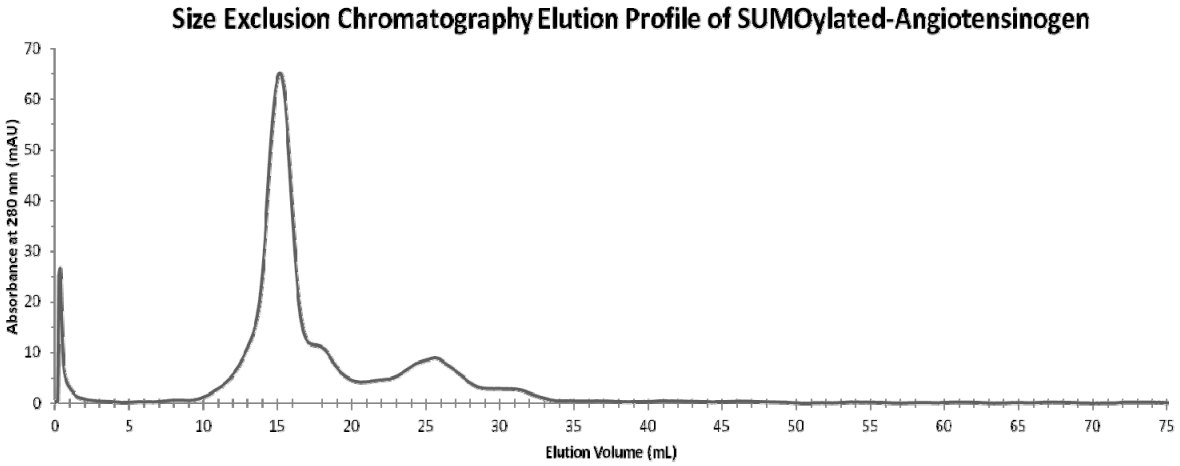


*Figure 3.10:*

*Size exclusion chromatograph of SUMO-AGT purified on a 24 mL Superdex 200 gel filtration column at 4 °C at a flow rate of 0.25 mL/min. Elutions were collected in 1 mL fractions. The main peak from 10 mL of elution contained pure SUMO-AGT, while smaller protein species began to elute from approximately 16 mL onwards corresponding to the shoulder of the main peak.*

Finally, cleavage of the SUMO fusion tag, including the N-terminal His-tag, was carried out using SUMO Protease to release native untagged recombinant human angiotensinogen. By running the cleavage reaction through an IMAC column, the pure untagged angiotensinogen was collected in the flow through, while the SUMO tag, SUMO Protease, and any uncleaved SUMO-AGT remained bound to the resin. Figure 3.12 summarises the entire purification of SUMO-AGT including the final cleavage and purification step which gave rise to pure recombinant human angiotensinogen (49.8 kDa).

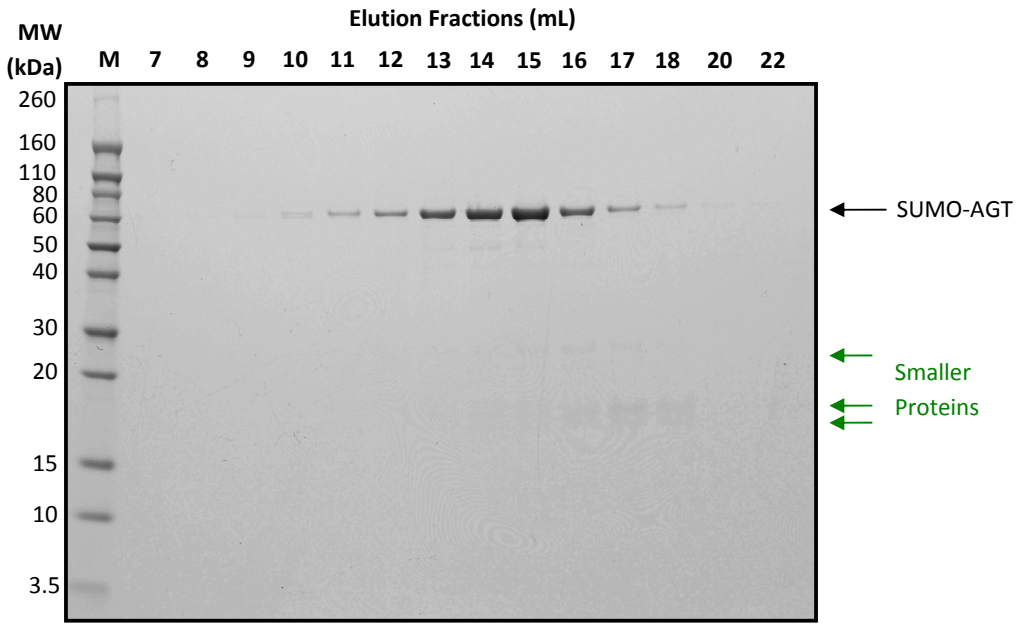


*Figure 3.11:*

*SDS-PAGE analysis of size exclusion chromatography elution peak fractions from the purification of SUMO-AGT. The MW ladder (M; Novex® Sharp Pre-stained Protein Standard) is in the first lane and subsequently each SEC fraction is labelled to correspond to the elution fraction (in mL) displayed on the elution profile in Figure 3.10 above. Smaller protein species are indicated by the green arrows (← ) on the right of the gel.*

Although cleavage of the SUMO tag results in pure untagged angiotensinogen which was the ultimate goal, a large amount of protease would be required to obtain sufficient amounts of angiotensinogen since 1 unit of SUMO Protease is defined as the amount of protease required to cleave 2 µg of fusion protein in 1 hour at 30 °C. Thus, 500 units of SUMO Protease would be required to generate only 1 mg of native recombinant angiotensinogen, assuming 100% cleavage, which sharply raises the cost of producing angiotensinogen recombinantly. In addition, an undesired outcome of the cleavage reaction is the reduction of angiotensinogen's Cys 18 and Cys 138 disulfide bond due to the dithiothreitol (DTT) present in the protease buffer, required for the activity of SUMO Protease—meaning that the angiotensinogen would no longer be present in the oxidised disulfide bonded form needed for further experiments. Because of this, it was decided that pure recombinant angiotensinogen would be left with the SUMO fusion tag

intact, greatly reducing the costs of recombinant production of the human angiotensinogen protein, as well as preventing the unintentional reduction of the disulphide bond between the two cysteine residues involved in angiotensinogen's redox switch.

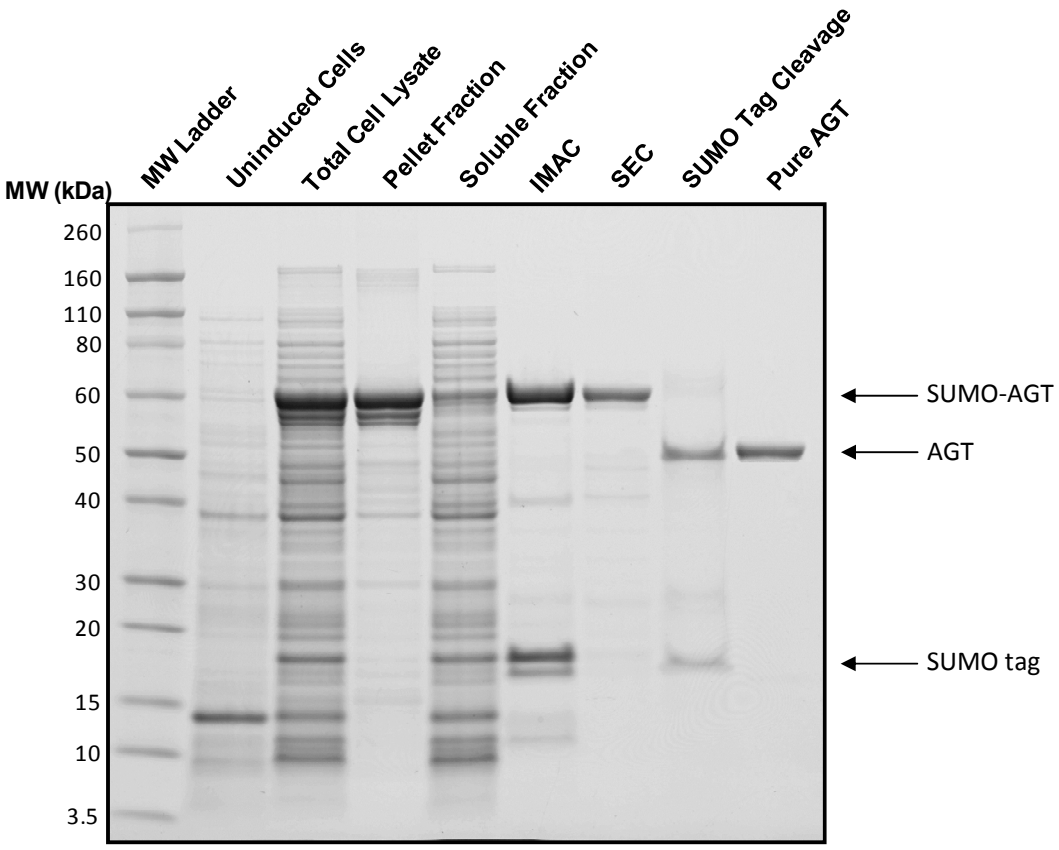


*Figure 3.12:*

*SDS-PAGE analysis of the entire expression and purification of recombinant human angiotensinogen. Each lane is labelled appropriately from the cell lysate fractions of BL21 (DE3) cells expressing SUMO-AGT to the protein following His-tag purification (IMAC) and subsequent gel filtration (SEC) purification steps, and finally tag cleavage resulting in pure angiotensinogen. The MW ladder (Novex® Sharp Pre-stained Protein Standard) was loaded in the first lane and uninduced cells were loaded in the second lane.*

## 3.6 EXPRESSION AND PURIFICATION OF SUMO-CAT

The decision to leave the SUMO tag intact on recombinant human angiotensinogen meant that it was important to have another SUMOylated protein as a negative control for SPR experiments to ensure that the SUMO fusion protein was not responsible for any interactions observed. For this reason, SUMOylated chloramphenicol acetyltransferase (SUMO-CAT), encoded by the pET SUMO/CAT plasmid that was supplied with the pET SUMO Protein Expression System kit as an expression control, was expressed and purified for use as a SUMOylated negative control. CAT is the enzyme responsible for bacterial resistance to the antibiotic chloramphenicol, serving to inactivate the antibiotic by catalysing the *O*-acetylation of chloramphenicol, which prevents the antibiotic binding to its site of action on the ribosome.[174]

The SUMO-CAT fusion protein expressed well following induction with IPTG, migrating to a size of just below 40 kDa on an SDS-PAGE gel which is consistent with its molecular weight of 39 kDa. The fusion protein is highly soluble, with only a very small amount of the protein present in the insoluble pellet on centrifugation to clarify the cell lysate following lysis by cell homogenization (see Figure 3.13). Figure 3.13 summarises the entire expression and purification of the SUMO-CAT protein. Purification of SUMO-CAT was carried out in the same way as purification for SUMO-AGT, the only difference being the concentration of imidazole required in the elution buffer to elute the protein from the HisPur cobalt resin during His-tag purification. In contrast to SUMO-AGT, which eluted at a concentration of 50 mM imidazole, the majority of SUMO-CAT did not elute until a concentration of 150 mM imidazole was flowed through the column. IMAC purification resulted in reasonably pure SUMO-CAT, and the subsequent gel filtration step did little to further purify the protein, but since this protein was required as a negative control only, additional purification steps were deemed unnecessary.

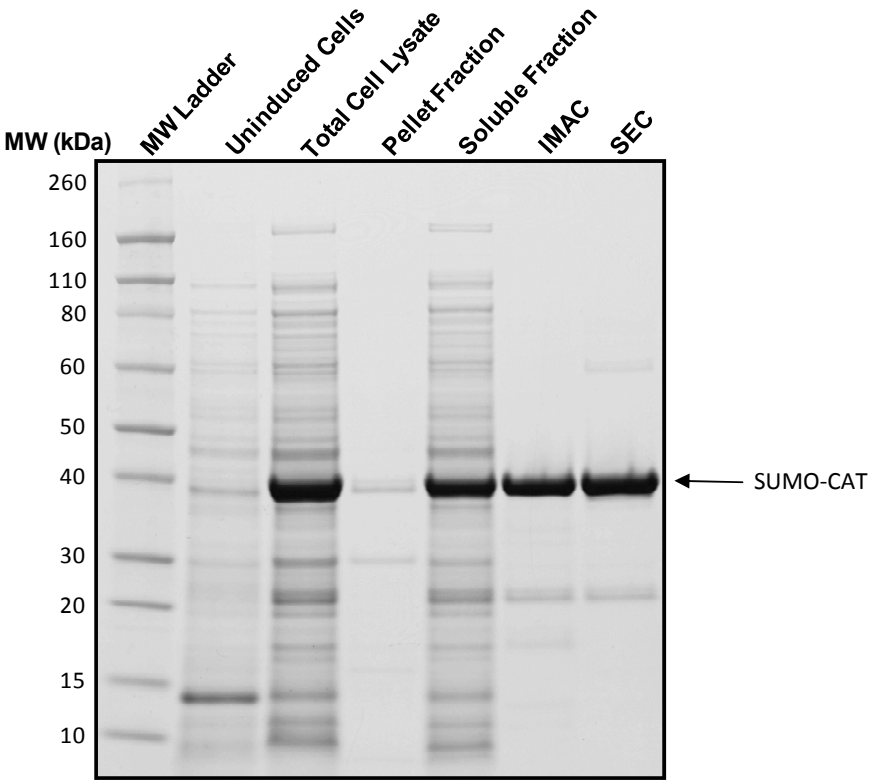


*Figure 3.13:*

*SDS-PAGE analysis of the entire expression and purification of recombinant SUMO-CAT fusion protein. Each lane is labelled appropriately from the cell lysate fractions of BL21 (DE3) cells expressing SUMO-CAT to the protein following His-tag purification (IMAC) and subsequent gel filtration (SEC) purification steps. The MW ladder (Novex® Sharp Pre-stained Protein Standard) was loaded in the first lane and uninduced cells were loaded in the second lane.*

## 3.7 SUMMARY

Recombinant human angiotensinogen was successfully expressed and purified from BL21 (DE3) *E. coli* cells. Extensive expression trials with three different plasmids encoding the human angiotensinogen gene, several expression hosts, and different expression conditions revealed that soluble protein could be obtained when angiotensinogen was expressed with the SUMO fusion tag at 26 °C in LB media supplemented with 1% glucose. Cell homogenization was deemed to be the most appropriate means to carry out cell lysis, and the SUMO-AGT

protein was subsequently purified from the cell lysate by a two-step purification involving firstly immobilised metal ion affinity chromatography to isolate the His-tagged protein, followed by size exclusion chromatography to remove any proteins that co-eluted with SUMO-AGT in the first purification step, resulting in pure recombinant SUMOylated human angiotensinogen.

The SUMO fusion tag could then be cleaved off the purified fusion protein with SUMO Protease to produce pure recombinant human angiotensinogen. It was decided to leave the angiotensinogen protein tagged, however, not only to minimise recombinant protein costs, but also to prevent the reduction of the disulphide bond between Cys 18 and Cys 138, which came hand in hand with tag cleavage due to the reducing agent present in the protease buffer that was essential for the protease's activity. Lastly, another SUMOylated protein, SUMO-CAT, was expressed and purified in a similar manner in order that it could be used as a negative SUMOylated control protein in SPR experiments.

*Chapter Four*

# DEVELOPMENT OF AN SPR-BASED BIOASSAY FOR ANGIOTENSINOGEN

## 4.1 INTRODUCTION

Surface plasmon resonance (SPR) is an optical technique that has provided a versatile tool for researchers as they attempt to understand, characterise, and marvel at the diverse, numerous, and at times unpredictable interactions between biomolecules that exist in our natural world. Although the technique itself was first described in 1968,[175] it wasn't until the 1990's that SPR biosensors became available in a commercial capacity for research purposes.[176] SPR biosensors offer the advantage of being able to monitor biomolecular interactions in real-time, and are versatile, sensitive, and automated,[176-179] ultimately providing the ideal platform for the rapid label-free analysis of the interactions that take place between a diverse range of biomolecules including proteins, DNA, antibodies, and small molecules.[176, 179] Carefully designed SPR experiments can yield a large amount of information about the interaction being investigated, including whether the molecules do indeed interact, the elucidation of kinetic association and dissociation constants, and information in support of proposed binding mechanisms.[141, 142, 179, 180] It is no wonder, therefore, that this technique is commonly used to characterise interactions between biomolecules with over 1400 articles published annually describing experiments involving biosensors.[141, 142, 177]

SPR biosensors such as the Biacore™ (GE Healthcare) and Biorad's ProteOn™ XPR36 make use of chip-based technology, an autosampler, a microfluidics system and an optics system that communicates with a computer so that the interactions can be monitored in real-time.[179, 180] To investigate the interaction between two proteins, one protein (termed the ligand) is typically

immobilised covalently on the surface of a sensor chip by making use of one of many surface chemistries available.[176] The second protein, known as the analyte, is then injected, flowed across the sensor chip surface in aqueous solution, and allowed to interact with the immobilised ligand. Analyte molecules accumulate on the sensor chip surface as the binding phase proceeds, and this increase in mass, at or close to the surface of the chip (within approximately 100 nm), results in an increase in refractive index.[141, 179, 181] This change in refractive index is measured and plotted in real-time as response units (RU) vs time,[180] resulting in the generation of a sensorgram as depicted in Figure 4.1.

Following this association phase where the two proteins interact, running buffer is flowed continuously across the immobilised ligand surface to allow the bound complex to dissociate, and this is typically referred to as the dissociation phase (see Figure 4.1). If the sensorgram has not returned to baseline following dissociation, some analyte may remain bound to the ligand, and a regeneration step may be needed to remove any remaining bound analyte, typically using short pulses of low or high pH, high salt, or detergents.[180] These biosensors are so sensitive that even small changes in the ionic strength or pH of a buffer will result in a change in the refractive index that will be detected by an SPR machine, thus much care must be taken in the preparation of all buffers and solutions to be used on these machines to prevent aberrant or false responses. In addition, careful consideration must be made to ensure the appropriate control surfaces are used for referencing to correct for differences in the refractive index of the samples, as well as any non-specific binding that may occur.[180, 181]

The ProteOn™ XPR36 is particularly powerful in that it facilitates up to 36 different interactions to be measured simultaneously through the use of a 6 x 6 array of six horizontal and six vertical channels on a single chip.[177, 179] Details of the sensor chip used by the ProteOn™ XPR36 are shown in Figure 4.2. The chip itself is composed of a glass prism with a very thin

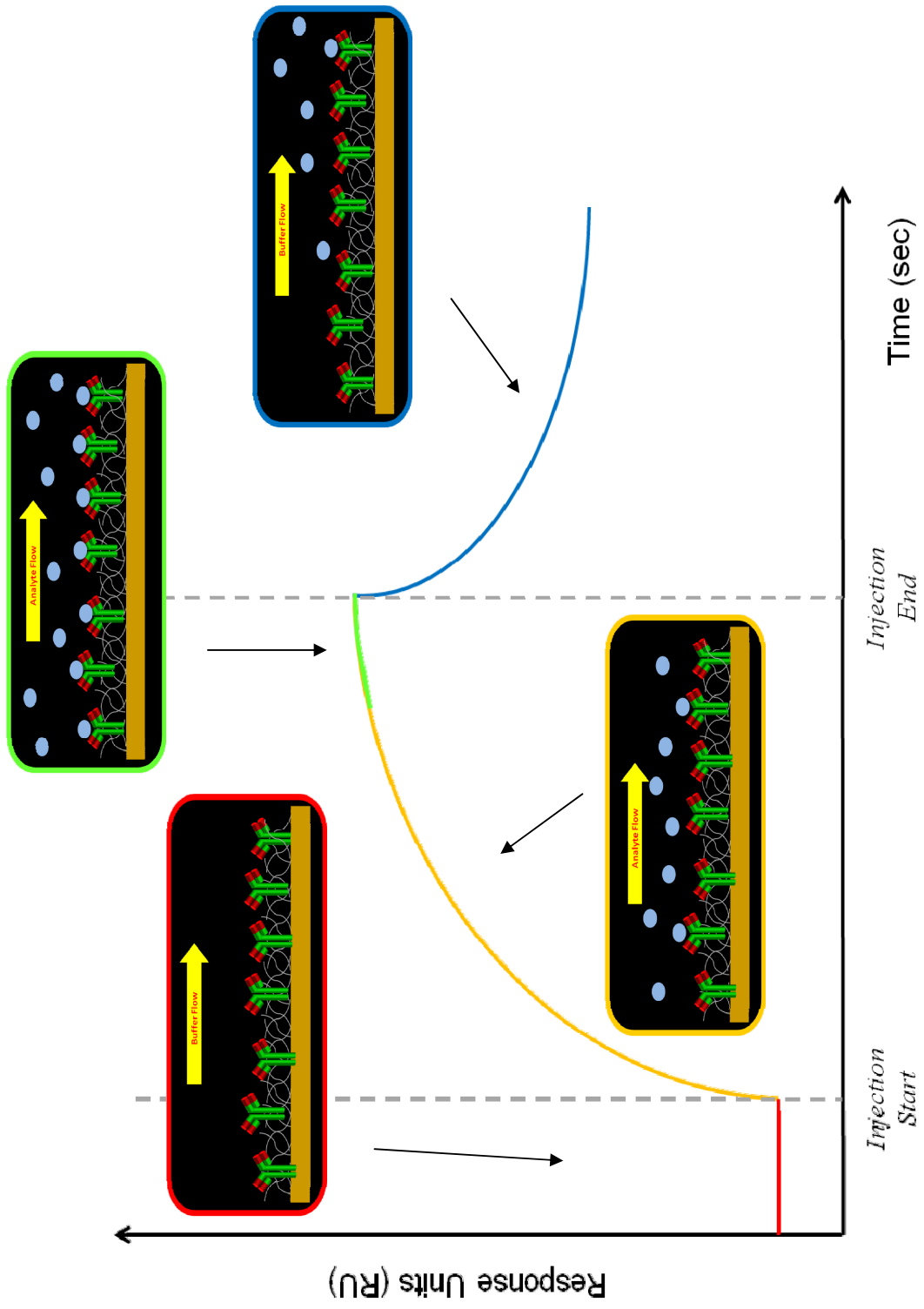


*Figure 4.1: Schematic representation of the typical sensorgram obtained when an analyte interacts with an immobilised ligand on the surface of a sensor chip. In this example, the anaylte is an antibody (green) which is immobilised on the modified alginate polymer layer on the surface of the chip. The yellow arrow indicates the direction of flow, while the analyte is depicted as light blue circles.*

gold layer on the top surface (Figure 4.2a). Above the gold layer, is a thin layer of a carboxylated alginate polymer (much like tangled netting), allowing immobilisation of ligand molecules close to the chip surface via a variety of immobilisation surface chemistries.[179, 180] Ligands can be immobilised in the six vertically-orientated ligand channels, and following a 90° rotation, analyte molecules are flowed through the six parallel horizontally-orientated analyte channels[177, 179] (Figure 4.2b and 4.2c). This 6 x 6 array created by the intersection of the vertical and horizontal channels facilitates a multiplexing approach to data collection, allowing data to be collected at 36 data points simultaneously in one experiment—a technique which is referred to as One-shot Kinetics™.[179] This approach was further extended by Abdiche *et al*. who described a method to create a 36-ligand array,[177] vastly improving high-throughput analysis of analyte-ligand pairs, and streamlining assay development.

Because of the many advantages offered by the ProteOn™ XPR36, in addition to the SPR technique's sensitivity and ability to probe biomolecular interactions in real-time, this SPR instrument was chosen for the development of an assay for angiotensinogen. Although there are reports in the literature of components of the RAS system being studied with SPR, most of the literature concerns the binding of (pro)renin to the (P)RR receptor, or the binding of inhibitors such as aliskiren to renin, immobilised primarily using a capture approach.[36, 103, 182, 183] Very little SPR work has been published involving angiotensinogen however, with only a single paper found after an extensive literature search. Cohen *et al.* used a Biacore™ instrument to measure the kinetic constants of the M235 and T235 variants of angiotensinogen to antibodies, as part of their work towards developing an immunoassay that allows the determination of the concentration of angiotensinogen, as well as the ratio of the two clinically relevant angiotensinogen variants in plasma.[25] Unfortunately, the authors only published the resulting kinetic constants of the analysis, and failed to present the measured data or the resulting fitted models, so it is difficult to glean much information from their SPR experiments.

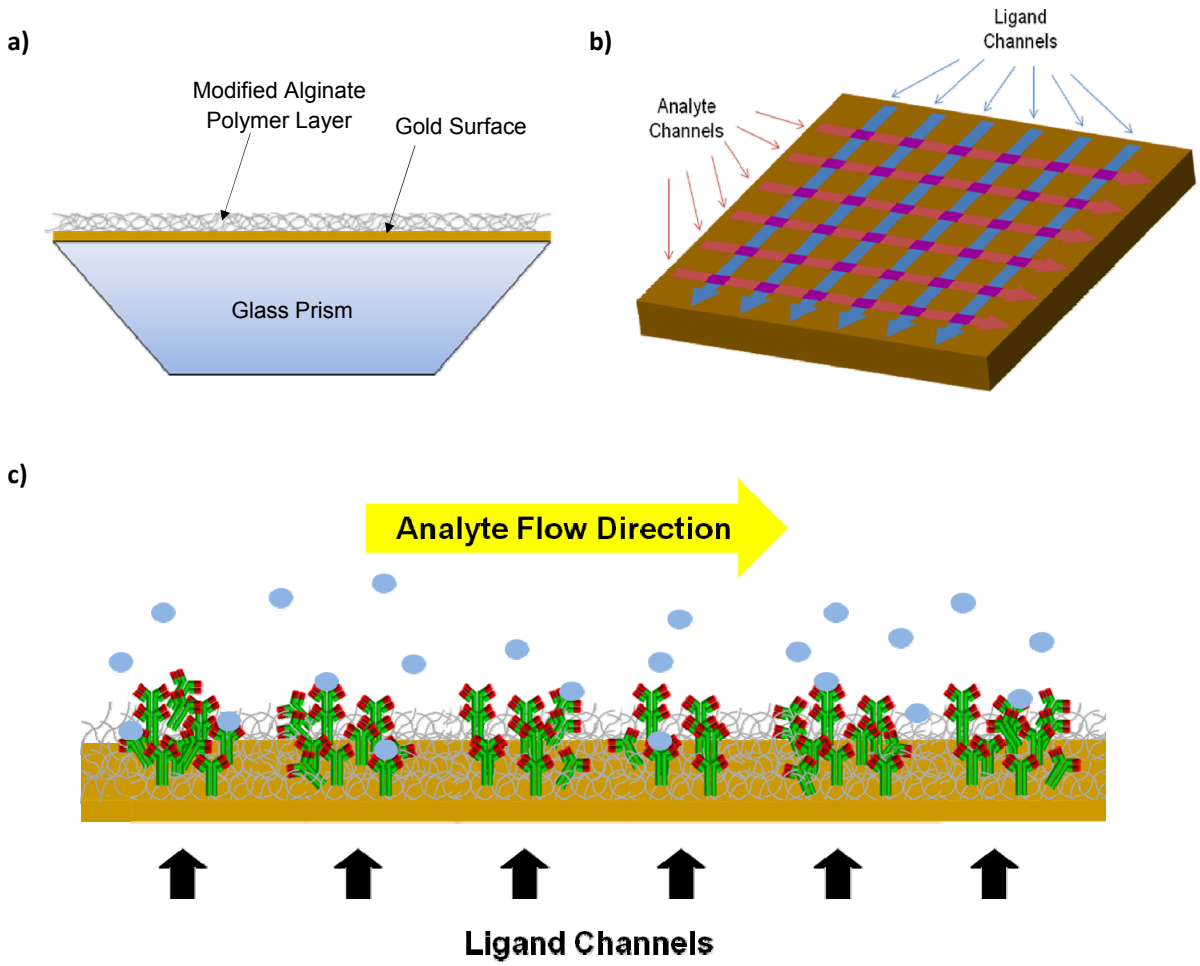


*Figure 4.2:*

*Schematic representation of a ProteOn™ XPR36 sensor chip (a) consisting of a glass prism coated with a thin layer of gold on the top surface of the chip. Above this is a layer of modified alginate polymer on which ligand is immobilised covalently. A 6 x 6 array (b) is formed on the chip due to the six vertical ligand channels (blue) and six horizontal analyte channels (pink) intersecting (purple) allowing up to 36 ligand-analyte interactions to be measured simultaneously in a single run. Due to the perpendicular nature of the array, analyte flowed through one channel is able to interact with all six ligand channels (c).*

In the work described in this chapter, several different approaches to detect angiotensinogen were used to develop a bioassay for this protein. The first approach employed the use of antibodies raised against angiotensinogen and is described in Section 4.2. As an alternative approach, Section 4.3 describes the immobilisation of renin directly onto the chip surface, providing yet another way to detect angiotensinogen using SPR technology.

## 4.2 SPR Bioassay for Angiotensinogen Using an Antibody

This bioassay development required the use of antibodies raised against human angiotensinogen. The 'human serpin A8/angiotensinogen antibody' (clone # 369439) produced by R&D Systems was primarily used in the following experiments, and will be referred to as 'anti-AGT mAb' from now on. This antibody is a monoclonal mouse $IgG_1$ antibody that was raised against full length recombinant human angiotensinogen (derived from a mouse myeloma cell line). Although this antibody has not been epitoped, it has been shown to have no cross-reactivity with other human serpins that may be present in plasma (see product datasheet). A second antibody produced by Santa Cruz Biotechnology, 'angiotensin (N-10)' (polyclonal goat antibody sc-7419) was also trialled initially, but due to inconsistencies in the antibody's response to angiotensinogen using SPR, the use of this antibody in a bioassay was not pursued further.

The first step in developing this SPR assay involved identifying the optimum conditions for immobilisation of the anti-AGT mAb onto the sensor chip surface. The level of ligand immobilisation, and hence the density of the ligand molecules on the sensor chip surface, is critical for obtaining good kinetic results—too high and the reaction can become limited by mass transport effects,[180, 181] too low and the response on analyte binding will be too low to be distinguished from instrument noise. Mass transport limitations occur when the rate of analyte diffusion from the aqueous solution to the chip surface (mass transport) is slower than the rate of the analyte binding to the immobilised ligand, resulting in mass transport being the rate-limiting step, and ultimately alteration of the apparent kinetics of analyte binding.[181] Fortunately, mass transport limitations can be minimised in most cases by lowering the ligand density and increasing the flow rate.[180, 181] Working with lower density surfaces tends to result in more random short-term noise in binding responses, but this is generally preferred to the artefacts such as complex binding events and mass transport limitations that can occur with higher density ligand surfaces.[142]

Amine coupling was chosen to immobilise the anti-AGT mAb antibody onto the surface of the sensor chip. This is by far the most straightforward and commonly used method for tethering ligands to sensor chip surfaces.[180, 184] For amine coupling, the chip surface is activated by using EDAC/NHS to activate the carboxyl groups of the carboxymethyl polymer layer to create reactive succinimide esters, leaving the carboxyl groups particularly poised to react directly with the primary amines present on the antibody's surface (primarily lysine residues), resulting in a covalent attachment or tethering of the antibody onto the chip surface[180, 181, 184] (Figure 4.3). The sensor chip surface is then deactivated with ethanolamine HCl to block any unreacted succinimide esters, preventing any further reaction with primary amines. This step also serves to help remove any non-specifically bound ligand molecules from the chip surface.[181]

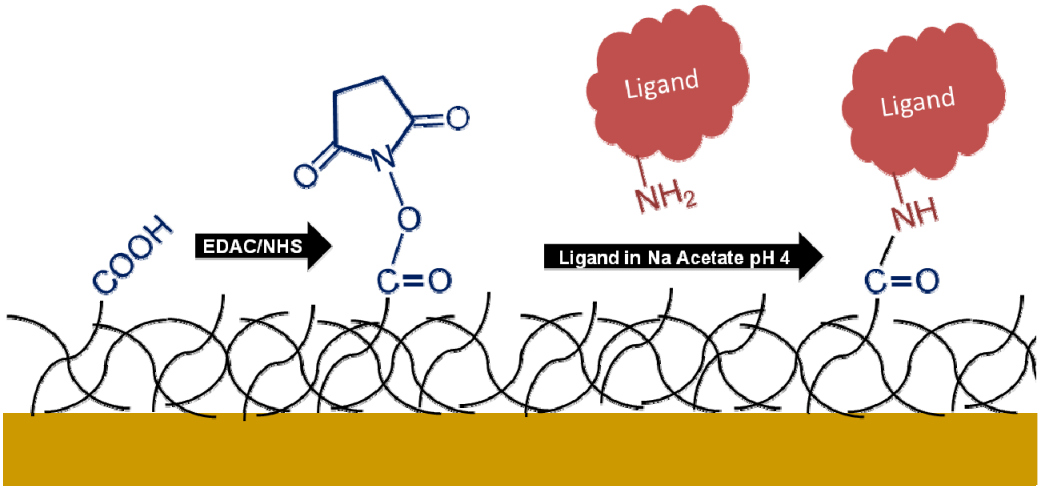


*Figure 4.3:*

*A schematic representation that depicts amine coupling immobilisation of a protein ligand to a sensor chip surface. The carboxyl groups on the polymer layer of the chip surface are activated with EDAC/NHS to create reactive succinimide esters which readily react with the primary amines present on lysine residues on the protein ligand to create a covalent irreversible bond to the chip surface.*

Activation and deactivation were carried out according to the default ProteOn™ XPR36 settings. Trials of the anti-AGT mAb in a sodium acetate buffer of varying pH revealed that sodium acetate pH 4 was the optimal coupling buffer, facilitating the highest levels of

immobilisation. Different levels of ligand immobilisation were trialled by varying the concentration of the anti-AGT mAb from 5 µg/mL to 0.75 µg/mL, which gave immobilisation levels from as high as 2000 RU down to approximately 250 RU. Subsequent optimisation and experiments were carried out with the lowest concentration of anti-AGT mAb trialled (0.75 µg/mL), as the resulting immobilised ligand density still gave adequate binding responses when tested with recombinant angiotensinogen, and was the surface least likely to be affected by any mass transport effects making it ideal for carrying out kinetic measurements. The sensorgram obtained from the activation, immobilisation, and deactivation of the surface using the optimised immobilisation conditions is shown in Figure 4.4.

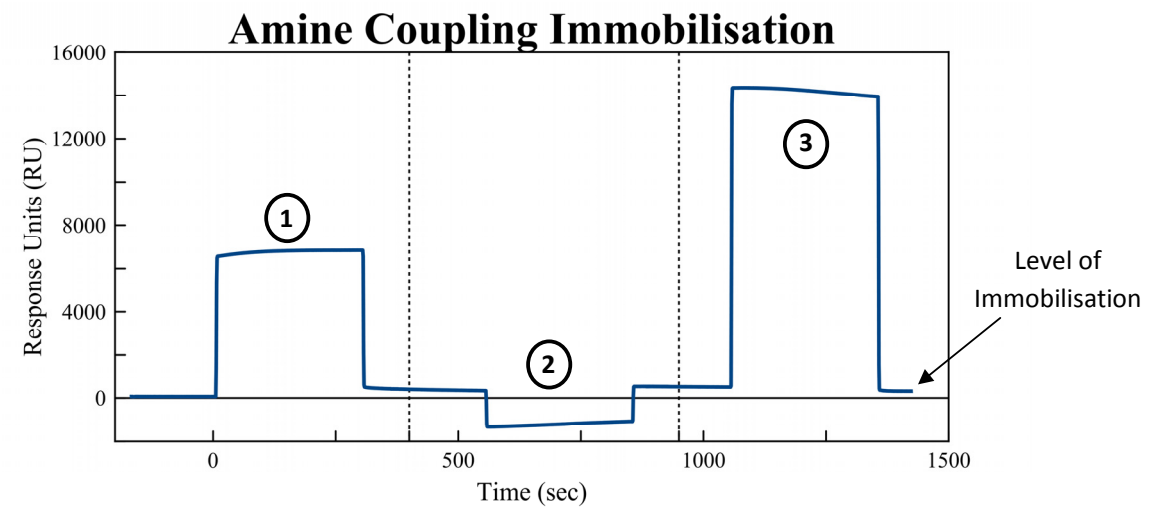


*Figure 4.4:*

*The sensorgram obtained when 0.75 µg/mL anti-AGT mAb antibody is immobilised via amine coupling to the sensor chip surface of a GLC chip. The surface is first ① activated with a 1:1 mixture of EDAC/NHS before the ligand is immobilised ② in a coupling buffer of sodium acetate pH 4. The surface is then deactivated ③ with ethanolamine HCl pH 8. The increase in RU following deactivation (from baseline prior to activation) is indicative of the level of ligand immobilised on the sensor chip surface.*

Because the association rate of the binding of angiotensinogen to the anti-AGT mAb was relatively slow, the contact time of analyte runs, and consequently the flow rate, needed to be

optimised to obtain maximal curvature and height of the binding response curves, allowing the concentration-dependent responses of angiotensinogen binding to be observed and more accurate kinetic analysis to be performed. The ProteOn™ XPR36 machine operates with a maximum set injection volume, meaning that the maximum association or contact time, is determined by the flow rate—the slower the flow rate, the longer the contact time. Flow rates from 100 µL/min to 25 µL/min were trialled and the slower flow rates were shown to have no effect on the slope of the association curve, indicating that slowing the flow rate down does not increase mass transport limitations in this case. Slower flow rates did allow the association phase to be substantially extended, and with the use of 2 mL deep well microplates rather than the standard 0.35 mL well microplates, a total contact time of 981 seconds (16 minutes and 21 seconds) could be achieved with a flow rate of 25 µL/min. Longer contact times were beyond the machine's capability because injection volumes of greater than 409 µL were not permitted. The ProteOn™ XPR36 does offer the co-inject function that allows a second injection of analyte, enabling the contact association time to be extended further, but when trialled, the second injection introduced anomalies in the sensorgram at the point of the second injection which would not allow accurate kinetic analysis to be carried out, and it was decided not to use the co-inject function in further experiments. A long dissociation time of 1800 seconds (30 minutes) was chosen following association, to allow sufficient dissociation to occur so that observable decay was visible.

Another parameter that needed to be optimised was the concentrations of angiotensinogen to be used in analyte interaction runs. The ability to run six different analyte concentrations simultaneously in parallel greatly streamlined this process as it meant that a whole dilution series of concentrations could be screened in a single run. Concentrations up to and including 3 µM of recombinant His-tagged or SUMO-tagged angiotensinogen were screened and gave binding responses of up to 50 RU. The major limiting factor in this process was the availability of recombinant angiotensinogen, as each run required a substantial amount of protein

due to the large injection volume. With replicates and all of the optimisation required prior to final data collection, this amounted to a considerable amount of angiotensinogen being consumed. Had more protein been readily available, data could have been collected at higher analyte concentrations, which may have allowed ligand saturation to be reached.

In order for this anti-AGT mAb surface be reused for multiple runs, regeneration optimisation had to be carried out to ensure that the surface adequately regenerated, so that the results of one analyte run could be accurately replicated. Demonstrating that an assay is repeatable and gives reproducible results over multiple runs is crucial for a robust assay and is one step towards showing that a given set of results is valid. If regeneration conditions are too harsh, the antibody surface will become damaged and a loss of activity will result in a decrease in binding response over subsequent regeneration cycles. Conversely, if the regeneration conditions are not harsh enough, some angiotensinogen will be left bound to the antibody surface following each analyte run, leading to a decrease in binding capacity through time. Regeneration for 18 seconds and 36 seconds using glycine HCl at pH 2.0, 2.5 and 3.0 was carried out over multiple cycles to determine the optimal conditions. A pulse of glycine HCl at pH 2.0 for 18 seconds was deemed sufficient to remove all remaining bound angiotensinogen without causing any significant loss of antibody activity, allowing the ligand surface to bind angiotensinogen reproducibly over many runs.

Finally, an appropriate surface had to be chosen as a reference to correct for any non-specific binding of the analyte to the surface as well as any differences in the refractive index between the sample buffer and running buffer. A blank channel, either unactivated, or activated and deactivated, could have been employed as the reference surface, but after careful consideration it was decided that anti-IgG mAb (a mouse IgG antibody) would instead be immobilised on a ligand channel at the same concentration as anti-AGT mAb and used as a reference channel, as this would most closely approximate the environment of the anti-AGT

mAb surface. Further systemic artefacts during a run could be corrected by double referencing the binding responses against an injection in the analyte direction containing only buffer.

With all optimisation complete, the assay was ready for use to measure the binding of recombinant angiotensinogen. The assay was primarily used to measure the binding of His-tagged angiotensinogen, which is described in the next chapter. The binding responses observed when SUMO-AGT was used as the analyte are shown in Figure 4.5. The analyte interaction run was carried out as optimised above, in a running buffer of PBST pH 7.4 at a flow rate of 25 µL/min for a total contact and dissociation time of 981 seconds and 600 seconds respectively. The reaction displays a concentration-dependent binding response to the SUMOylated

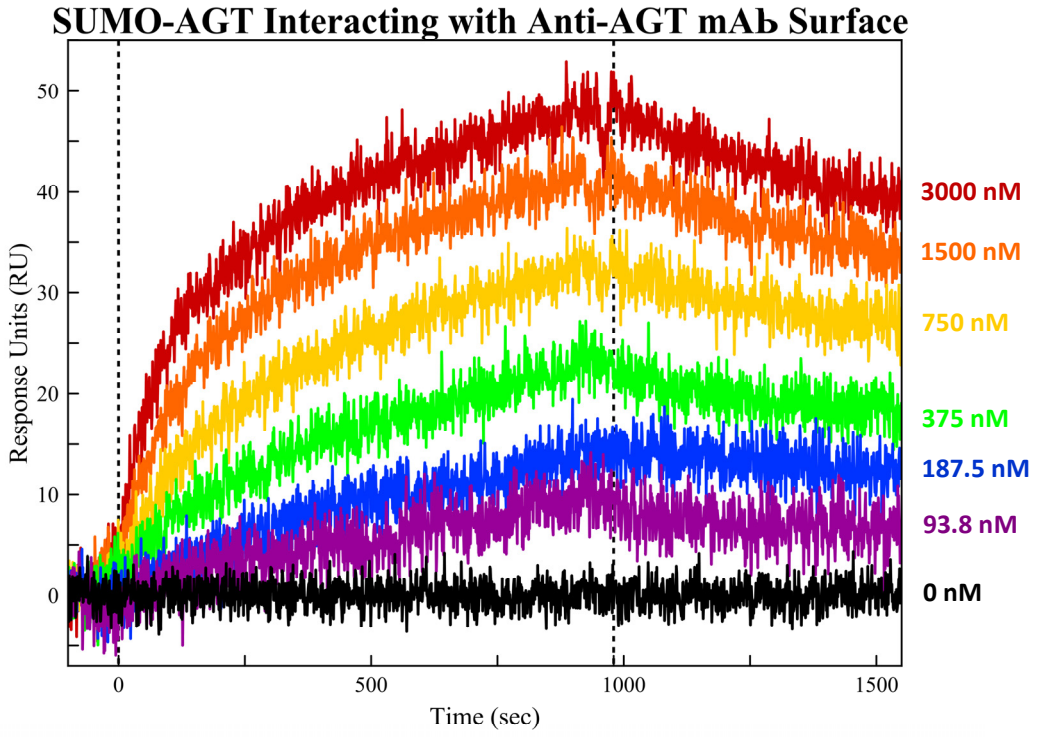


*Figure 4.5:*

*The sensorgram obtained when a dilution series of recombinant SUMOylated human angiotensinogen is flowed across an anti-AGT mAb antibody surface. SUMO-AGT was flowed across the surface at a flow rate of 25 µL/min for a total contact time of 981 seconds. Following association, running buffer was flowed across the surface for 10 minutes to allow dissociation to occur.*

angiotensinogen, giving a maximal response of approximately 50 RU. The binding did not reach ligand saturation, which may have been achieved with higher analyte concentrations, but there is sufficient curvature for kinetic analysis to be carried out.

Unlike responses with His-tagged angiotensinogen, which fit to a simple 1:1 interaction model, kinetic analysis of the responses obtained with SUMOylated angiotensinogen revealed that SUMO-AGT displayed more complex binding. A simple 1:1 Langmuir binding model describes the reaction that occurs between two molecules (analyte, A, and ligand, B) to form the complex AB (analyte-ligand complex) which can be written as the following equation:

$$A + B \underset{k_d}{\overset{k_a}{\rightleftharpoons}} AB \qquad (1)$$

where $k_a$ is the association rate constant and $k_d$ is the dissociation rate constant. This relationship gives rise to the kinetic rate equation:

$$\frac{d[AB]}{dt} = k_a[A][B] - k_d[AB] \qquad (2)$$

with [A] denoting the concentration of free analyte, [B] the concentration of immobilised ligand, and [AB] describes the concentration of analyte-ligand complex. This model assumes that the analyte and ligand are homogenous and that all binding events are independent,[180, 181] and would, in general, be the kinetic model expected when a monoclonal antibody binds an antigen, as it recognises a single epitope on the antigen's surface. Using ClampXP, fitting of this kinetic model to the SUMO-AGT responses resulted in a poor fit of the model when overlaid with the measured data, however, as shown in Figure 4.6. Several other kinetic models for more complex binding events were also tested to ascertain whether a better fit could be obtained (Figure 4.6). The conformational change model describes two conformations of the bound

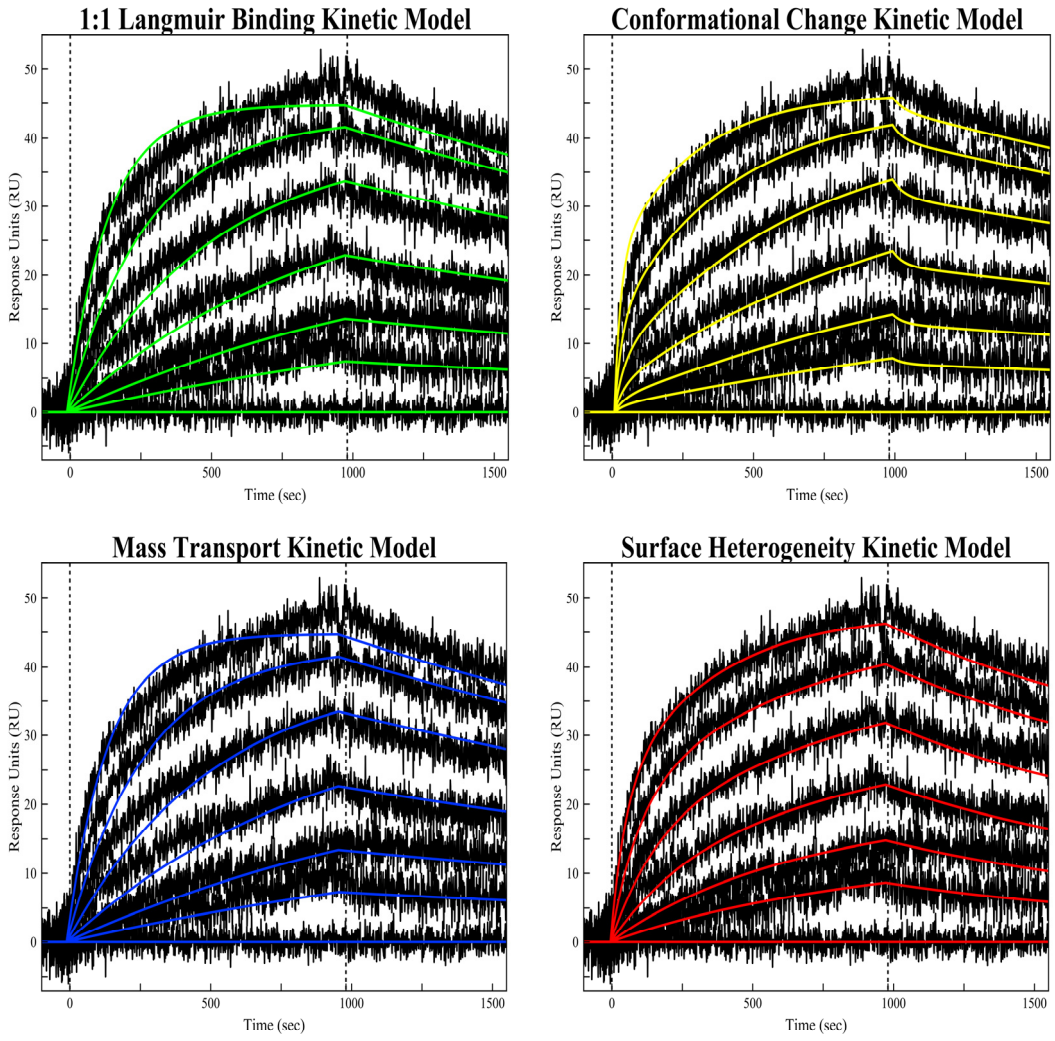


*Figure 4.6:*

*Kinetic fits of responses obtained when SUMO-AGT binds to the anti-AGT mAb surface. The data is shown in black, while the kinetic fits are overlaid in colour. The four kinetic models (simple 1:1 Langmuir binding, conformational change, mass transport, and surface heterogeneity) were fit to the same data displayed in Figure 4.5 using ClampXP software.*

complex, which could be the case if the binding of SUMO-AGT to the mAb triggered a conformational change (AB)* in the bound complex AB,[185] described by the following equation:

$$A + B \underset{k_{d1}}{\overset{k_{a1}}{\rightleftharpoons}} AB \underset{k_{d2}}{\overset{k_{a2}}{\rightleftharpoons}} (AB)^* \qquad (3)$$

The mass transport kinetic model incorporates a term $k_m$ that describes the initial rate of mass transport of the analyte to the ligand-bound surface,[186] and is described by Equation 4:

$$A_{bulk} \underset{k_m}{\overset{k_m}{\rightleftharpoons}} A_{surface} + B \underset{k_d}{\overset{k_a}{\rightleftharpoons}} AB \qquad (4)$$

The fourth and final model trialled was the surface heterogeneity model, which makes the assumption that there are two separate binding events occurring that contribute to the binding responses observed. This would be the case if a ligand has two sites capable of binding an analyte (denoted by B and B*),[186] or in the case of polyclonal antibodies which recognise more than one epitope on the antigen's surface. This type of binding can be described by Equations 5 and 6, and observed responses are a sum of both reactions occurring on the surface at the same time.

$$A + B \underset{k_{d1}}{\overset{k_{a1}}{\rightleftharpoons}} AB \qquad (5)$$

$$A + B^* \underset{k_{d2}}{\overset{k_{a2}}{\rightleftharpoons}} AB^* \qquad (6)$$

Of the four models trialled, only the surface heterogeneity model was shown to provide a good fit to the observed binding responses (Figures 4.6 and 4.7a). The residuals for this kinetic fit (Figure 4.7b) are low and randomly distributed, indicating a good fit to the data set. Interestingly, although each model returned vastly different association and dissociation rates, three of the four models (1:1 Langmuir binding, surface heterogeneity, and mass transport) gave $K_D$ values of approximately 150 nM, which is in good accordance with the $K_D$ values obtained for His-tagged angiotensinogen (discussed in Chapter Five). The obtained kinetic values

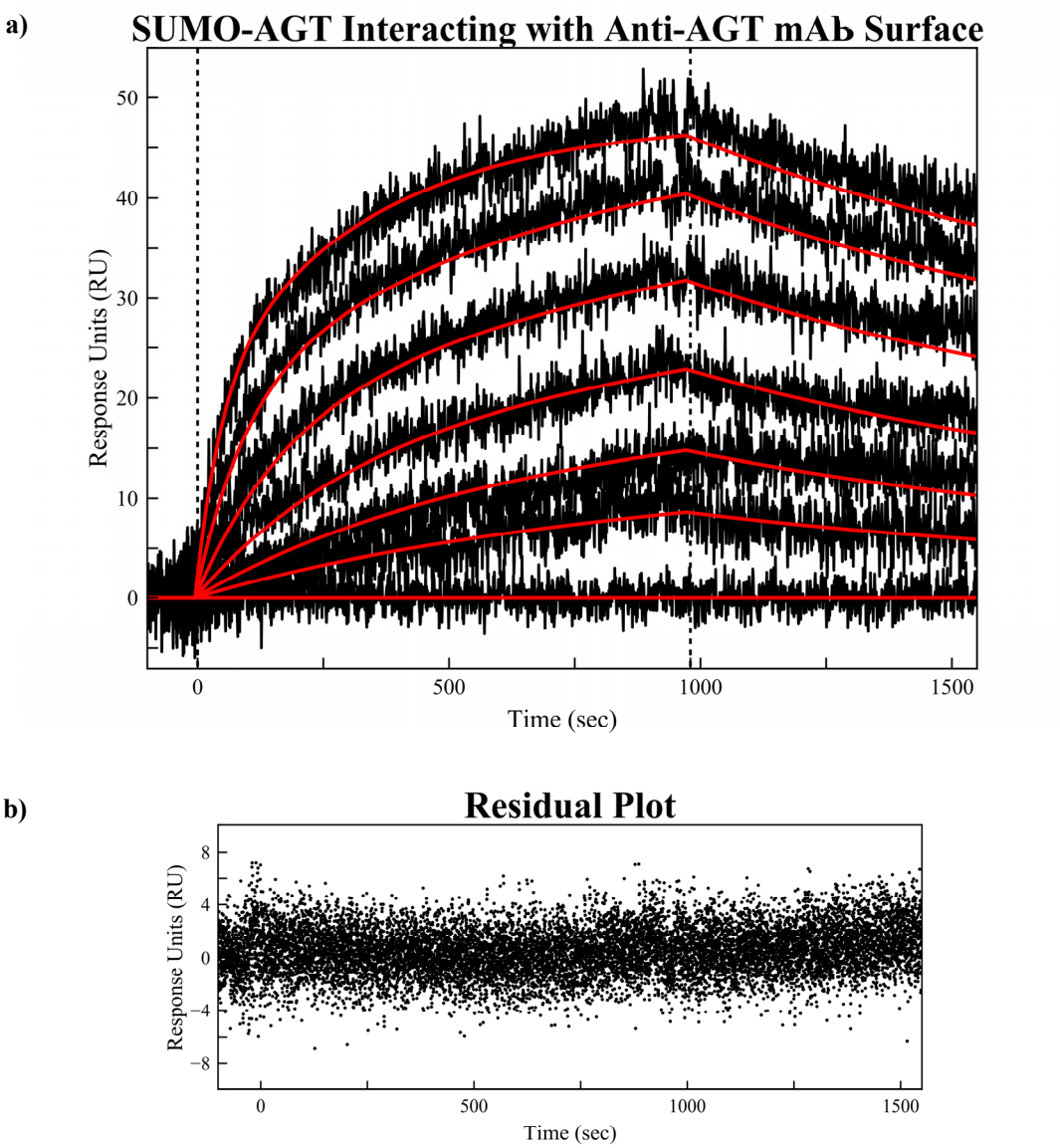


*Figure 4.7:*

*Results of the model fitting of the surface heterogeneity model to the binding responses of SUMOylated angiotensinogen to the anti-AGT mAb surface. The model (a) is shown in red overlaid on the measured data in black. The residual plot of the model fitting is shown in (b).*

including their associated errors are displayed in Table 4.1, along with the values obtained when the data were fit to the simple 1:1 binding model and the mass transport model (even though these two models do not provide a good fit to the data) for comparison.

Little information can be obtained from these kinetic analyses, however, and it is difficult to know which model is the correct one. While a good kinetic fit can, along with other experimental data, provide evidence in support of a proposed binding mechanism, it does not in itself validate a model. It is important to note that much care must be taken when evaluating different binding models to fit data as to whether the chosen model accurately describes the events physically taking place on the sensor chip surface, as several models could produce a similar fit to the same data. In fact, Rich *et al.* warn against 'model surfing' and stress that the simpler the binding model, the better, as it more likely approximates the binding events that are actually occurring.[142] Given that the kinetics of SUMO-AGT binding to the anti-AGT mAb show a complex binding mechanism, which deviates from the observed simple 1:1 binding of His-tagged angiotensinogen to the same antibody (described in Chapter Five), it seems likely that this

| Model and Equation | $k_a$ ($M^{-1}$ $s^{-1}$) | $k_d$ ($s^{-1}$) | $K_D$ (nM) |
|---|---|---|---|
| Simple 1:1 Langmuir binding model: A + B → AB | 2183 ± 7 | (3.10 ± 0.05) x $10^{-4}$ | 142 ± 2 |
| Mass Transport 1:1 binding model: A + B → AB | 2185 ± 10 | (2.98 ± 0.05) x $10^{-4}$ | 137 ± 2 |
| Surface heterogeneity model: | | | |
| A + B → AB | 7452 ± 214 | (1.12 ± 0.04) x $10^{-3}$ | 150 ± 6 |
| A + B* → AB* | 1300 ± 19 | (3.89 ± 0.01) x $10^{-7}$ | 30 ± 11 |

*Table 4.1:*

*Kinetic constants obtained from the model fitting of the simple 1:1 Langmuir binding model, the mass transport 1:1 binding model, and the surface heterogeneity model to the binding responses of SUMOylated angiotensinogen interacting with the anti-AGT mAb surface. Model fitting was carried out using the ClampXP program.*

alteration in kinetic behaviour may be due to the SUMO tag itself. As a negative control, SUMOylated CAT was flowed across the anti-AGT mAb surface as an analyte under the same conditions and no interactions were observed. Thus, it seems probable that while the SUMO tag itself does not bind to the antibody, the SUMO portion of the recombinant fusion protein may be altering the structure of the angiotensinogen molecule in such a way that non-simple 1:1 binding is displayed.

Overall, this assay set-up and optimisation has shown that it is possible to set up and assay recombinant angiotensinogen using SPR in a repeatable manner to give reproducible results, by utilising the anti-AGT monoclonal antibody supplied by R & D Systems. Although meaningful kinetic fits to the SUMOylated angiotensinogen binding responses could not be obtained, recombinant His-tagged angiotensinogen displays much simpler 1:1 Langmuir binding—a model that would be expected of such a system. This assay will be further explored in Chapter Five.

## 4.3 SPR Bioassay for Angiotensinogen Using Renin

As an alternative approach to detecting angiotensinogen using a monoclonal antibody (Section 4.2), renin immobilised to a sensor chip surface could be another, perhaps more specific, way in which an SPR-based assay for angiotensinogen could be developed. Studies involving renin on SPR instruments have already been reported in the literature.[36, 103, 182, 183] The binding of renin to inhibitors such as aliskiren and remikiren have been reported in the presence and absence of the (P)RR.[36, 182] The binding of renin and prorenin to the (P)RR[103, 182] or to antibodies,[183] has also been studied using SPR. The majority of these studies employed a capture approach for immobilisation whereby an antibody was directly coupled to the chip surface that was then used to capture and bind the (pro)renin or (P)RR in a non-covalent manner. Only a single study reported the use of a direct coupling method to immobilise renin.[36] None of these

studies investigated the interaction that occurs between renin and angiotensinogen using an SPR technique, however. To this end, direct coupling methods were used to immobilise renin to an SPR sensor chip surface to see if the reaction that takes place between renin and angiotensinogen can be measured using surface plasmon resonance.

Firstly, using amine coupling prorenin was immobilised either directly or on top of a spacer molecule, hexamethylenediamine, to the sensor chip surface. Prorenin is the inactive zymogen of renin, hence it was no surprise that no interactions were observed when angiotensinogen was allowed to flow across the prorenin surface. As prorenin can be cryoactivated non-proteolytically at approximately 4 °C, a cold analyte run was carried out in an attempt to activate the prorenin surface, whereby ice-cold angiotensinogen samples and running buffer were used. Unfortunately, no cryo-activation could be observed, as no responses were generated when angiotensinogen was flowed across the chip surface. An on-chip tryptic digest was performed to proteolytically activate the prorenin surface, and although a net decrease in refractive index (drop in the RU baseline) was observed, suggesting that the prosegment had been cleaved to activate renin, this surface again produced no responses with angiotensinogen.

Active renin (proteolytically activated by tryptic digest in solution and confirmed by SDS-PAGE (Figure 4.8)) was also immobilised using amine coupling directly or *via* the spacer hexamethylenediamine onto a sensor chip. Despite adequate levels of immobilisation, these renin surfaces also failed to interact and generate responses with angiotensinogen. These results thus begged the question as to whether the immobilisation process itself was somehow inactivating renin in such a way that it was no longer able to bind to angiotensinogen. Amine coupling, as described in Section 4.2, tethers ligand molecules to sensor chip surfaces using primary amines, which means that the ligand can be immobilised to the chip surface via any lysine residues present on the protein's surface. This facilitates immobilisation in essentially

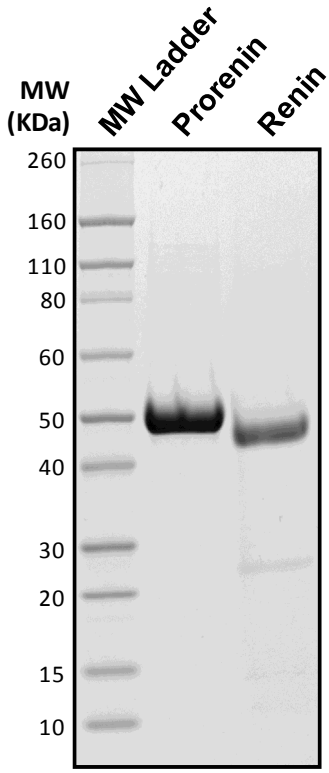


*Figure 4.8:*

*SDS-PAGE analysis of recombinant His-tagged glycosylated prorenin before (second lane) and after proteolytic cleavage of prorenin's prosegment with trypsin to give active renin (third lane). The MW ladder (Novex® Sharp Pre-stained Protein Standard) was loaded in the first lane.*

random orientations with the possibility of multiple couplings on the one ligand molecule, which could constrain the protein's conformation—reducing or even abolishing enzymatic activity.

Active renin contains 15 lysine residues and closer inspection of the crystal structure revealed that a large proportion of the lysine residues on renin are situated on the top face of renin in close proximity to the active site (Figure 4.9). Analysis of the renin amino acid sequence using Prop$K_a$ (Protein p$K_a$ Predictor version 3.1, developed by the Jensen Research Group, Department of Chemistry, University of Copenhagen)[187] uncovered that while 13 of renin's 15 lysine residues had a predicted p$K_a$ in the range of 10 to 11 (which is expected for this functionality), two residues, Lys 238 and Lys 239, stood out as having a substantially lower p$K_a$ of 9.26 and 9.36 respectively, indicated in yellow in Figure 4.9. These two lysines, having a lower p$K_a$, would be more likely charged at the pH in which immobilisation is carried

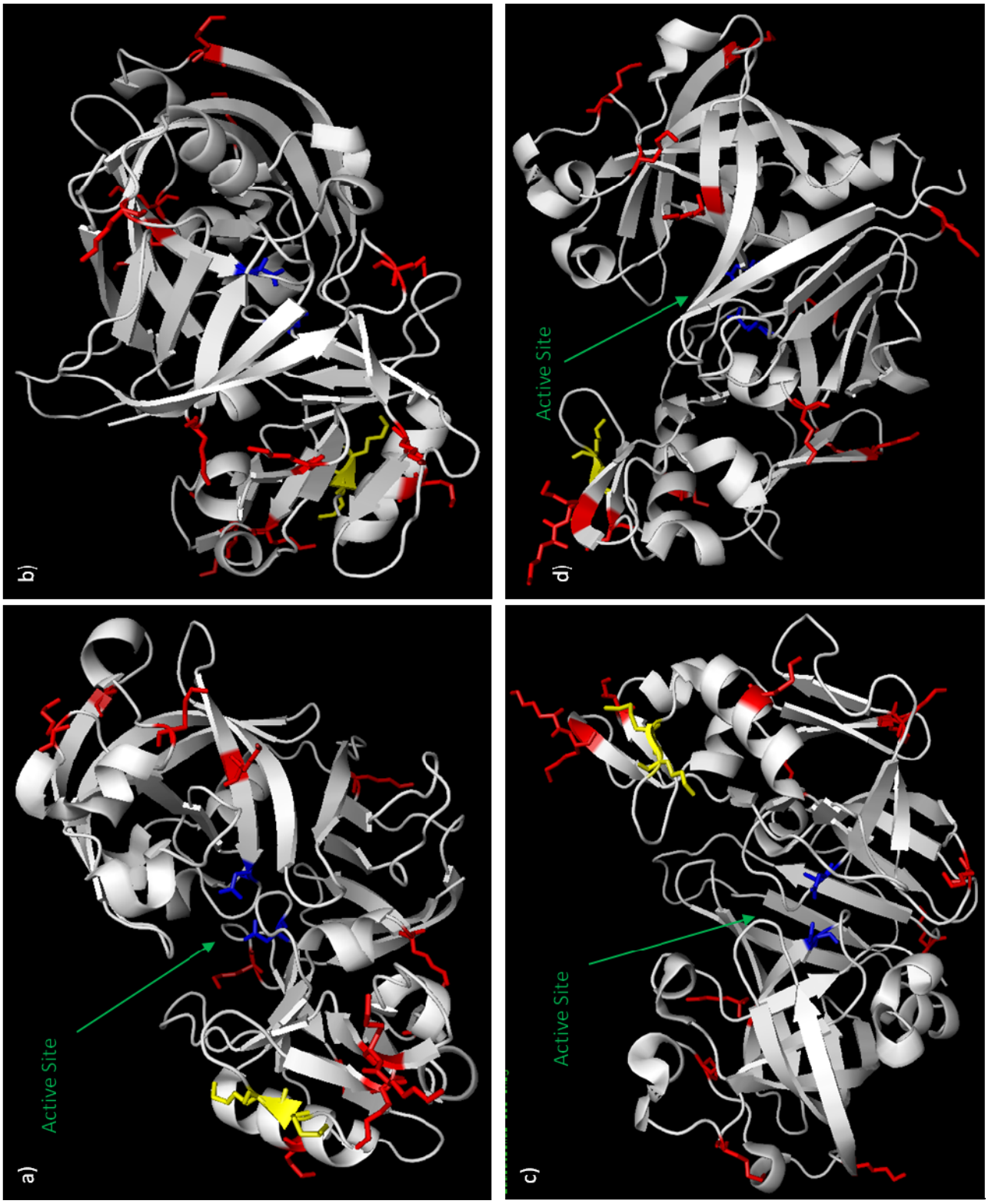


*Figure 4.9:*

*X-ray crystal structure of human renin (PDB 3VCM) showing the lysine residues available for amine coupling highlighted in red (Lys 238 and Lys 239 in yellow) and the catalytic aspartate residues in the active site shown in blue. The renin structure (white) is viewed from (a) above, looking down at the active site, (b) from below, and (c) and (d) from either side.*

out (pH 4), hinting that amine coupling may be directed to and far more likely to occur at these sites. Armed with this information, it was postulated that given the distribution of lysine residues and in particular Lys 238 and 239, the renin molecules were being tethered to the sensor chip surface either face down or on the side, in such an orientation that the active site is simply not accessible for angiotensinogen to bind for steric reasons, at least most of the time. Tethering of renin to the surface in close proximity to the active site could also have had an effect on the conformation/positioning of some of the residues present in renin's active site, potentially impacting on the enzyme's ability to carry out its catalytic function if angiotensinogen were to bind.

These observations point to a valid reason as to why direct immobilisation of renin to sensor chip surfaces *via* amine coupling has not been reported in the literature. This is not the first observation of renin having no activity on direct immobilisation either. In 2012, as this work was being carried out, Gossas *et al.* published work in which they attempted to measure the binding of small molecule inhibitors such as aliskiren and remikiren to renin by SPR, but they also found that the inhibitors failed to bind to the renin surface despite good levels of immobilisation. To address this, they utilised another direct immobilisation technique known as aldehyde coupling and found that the renin surface generated in this way was stable with a high analyte binding capacity, permitting the binding of the inhibitors to renin to be measured.[36] Aldehyde coupling facilitates the tethering of ligands (oxidised with sodium metaperiodate to generate reactive aldehyde groups on glycosyl residues such as sialic acid) to a sensor surface by their glycosylation residues.[184] Human renin has two glycosylation sites at Asn 5 and Asn 75,[188] both of which are located in positions distal to renin's active site (Figure 4.10). Covalent attachment of renin in this way may therefore provide a more specific orientation of immobilised renin molecules, while at the same time preventing any tethering in close proximity to the active

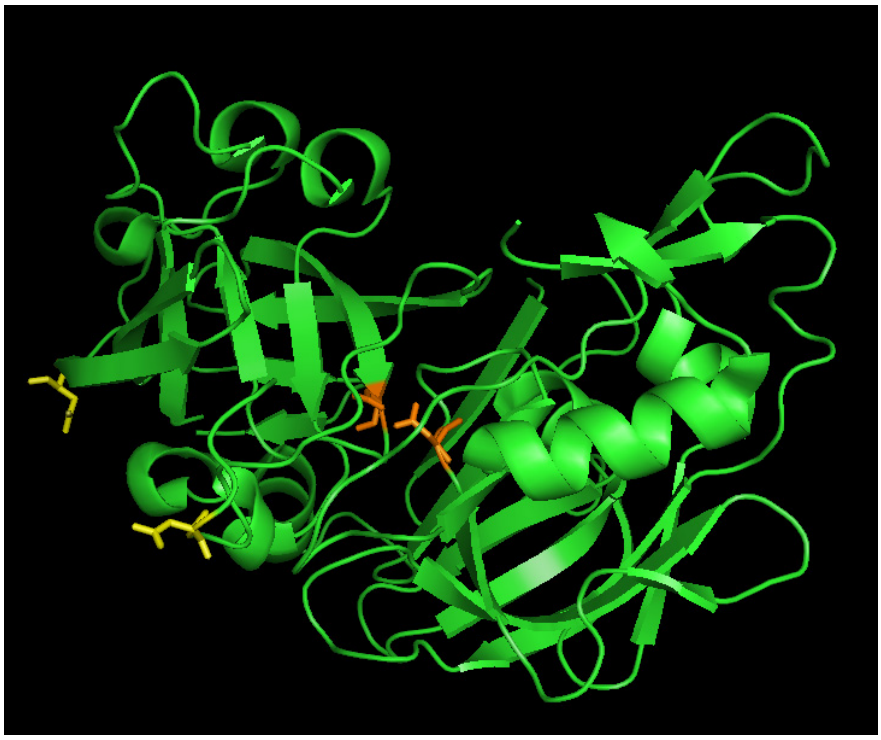

*Figure 4.10:*

*X-ray crystal structure of human renin (PDB 3VCM) showing residues Asn 5 and Asn 75 (yellow) which represent the two sites of glycosylation on renin. The catalytic aspartate residues are shown in orange to indicate the position of the active site.*

site. The chemistry involved for aldehyde coupling immobilisation to a surface is described in detail by O'Shannessy *et al.,*[189] and is summarised in Figure 4.11.

Due to the reported success of aldehyde coupling with renin, recombinant human glycosylated renin was immobilised using this technique to determine whether tethering via renin's glycosylation residues would facilitate interactions with angiotensinogen, a much larger analyte than the renin inhibitors. Aldehyde coupling was carried out following the protocol described in the Biacore Sensor Surface Handbook (GE Healthcare, downloadable from https://www.biacore.com/lifesciences/products/Consumables/guide/). Because this protocol is optimised for Biacore SPR biosensors that operate differently from the ProteOn™ XPR36, some changes to the protocol (outlined in Table 4.2) had to be made, primarily in terms of flow rates

| BIACORE RECOMMENDED PROTOCOL | | | NEW PROTOCOL FOR PROTEON™ XPR36 | | |
|---|---|---|---|---|---|
| **Injection** | **Flow Rate** | **Contact Time** | **Injection** | **Flow Rate** | **Contact Time** |
| 1) EDAC/NHS | 10 µL/min | 3 min | 1) EDAC/NHS | 25 µL/min | 3 min |
| 2) Hydrazine or Carbohydrazide | 10 µL/min | 7 min | 2) Carbohydrazide | 25 µL/min | 7 min |
| 3) Ethanolamine HCl pH 8 | 10 µL/min | 7 min | 3) Ethanolamine HCl pH 8 | 25 µL/min | 7 min |
| 4) Ligand | 10 µL/min | 7 min | 4) Ligand | 30 µL/min | 7 min |
| 5) Sodium Cyanoborohydride | 2 µL/min | 20 min | 5) Sodium Triacetoxyborohydride (double injection) | 25 µL/min | 10 min x 2 |

*Table 4.2:*

*Table summarises the protocol conditions for ligand immobilisation via aldehyde coupling to an SPR sensor chip surface. The left-hand half of the table outlines the protocol recommended by the Biacore Sensor Surface Handbook (GE Healthcare, Uppsala, Sweden) for aldehyde coupling on Biacore SPR biosensors. The right half of the table describes the adapted protocol for aldehyde coupling that was developed here for use on the ProteOn™ XPR36.*

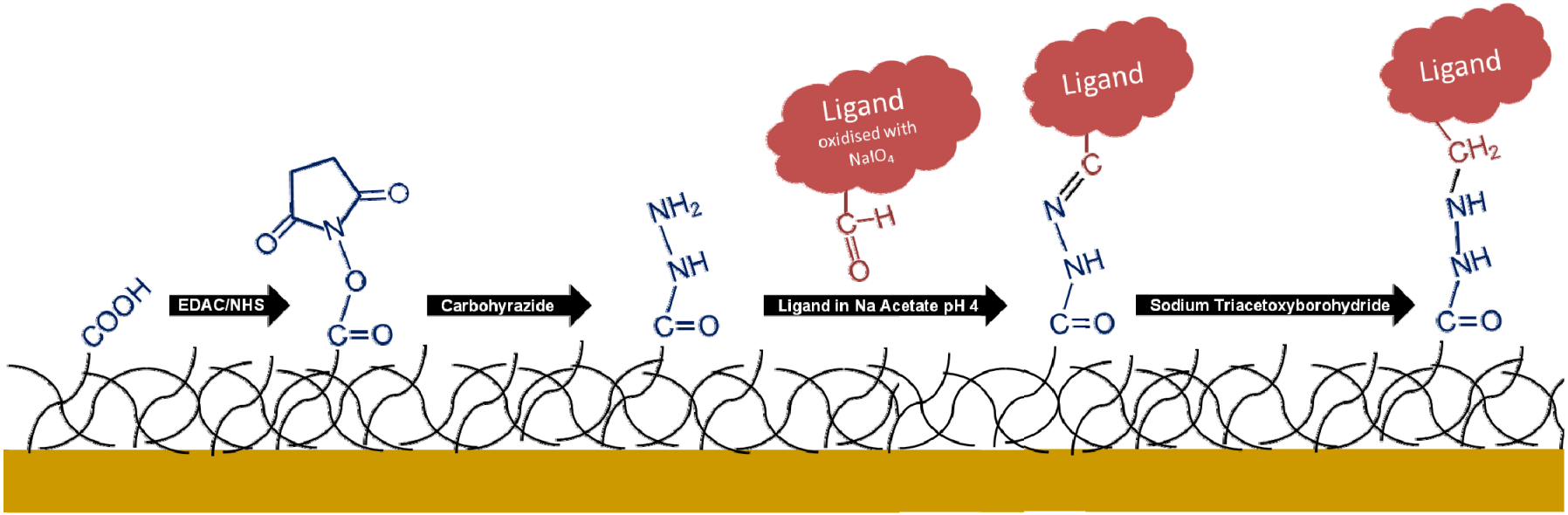


*Figure 4.11:*

*A schematic representation that depicts aldehyde coupling immobilisation of a protein ligand to a sensor chip surface. The carboxyl groups on the polymer layer of the chip surface are activated with EDAC/NHS to create reactive succinimide esters, which readily react with carbohydrazide to introduce hydrazide groups to the chip surface. The protein ligand is then immobilised via the reactive aldehyde groups (generated on glycosyl residues through oxidation with sodium metaperiodate) to create a covalent irreversible bond to the chip surface. The covalent bond created between the ligand and surface is further stabilised by reducing the bond with a reducing agent.*

and contact times. Due to the inherent toxicity of hydrazine and sodium cyanoborohydride, these compounds were substituted for the less toxic alternatives carbohydrazide and sodium triactetoxyborohydride, respectively. Further experimental details are described in Chapter Two.

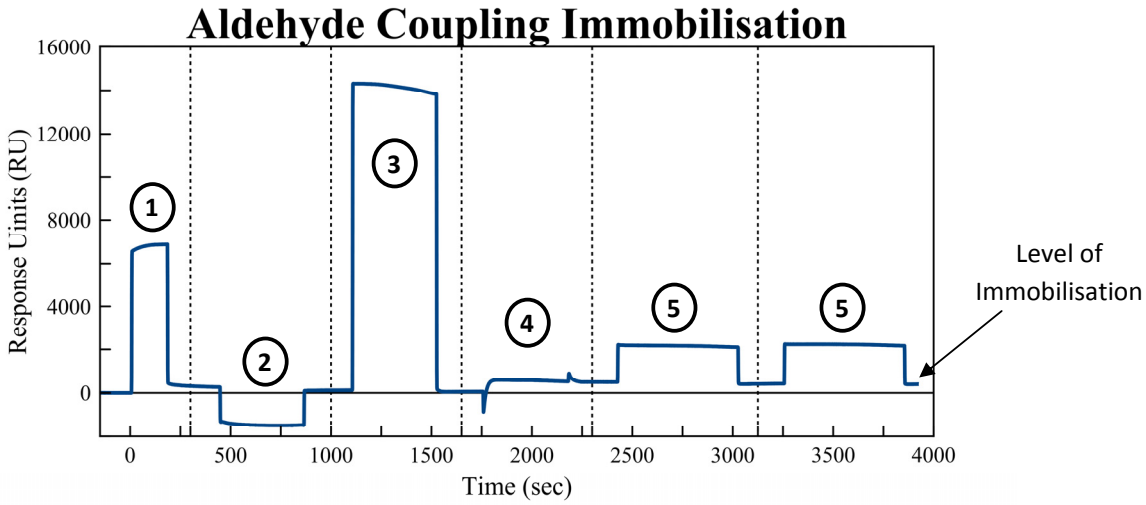


*Figure 4.12:*

*The sensorgram obtained when 0.01 mg/mL recombinant human renin is immobilised via aldehyde coupling to the sensor chip surface of a GLC chip. The surface is first ① activated with a 1:1 mixture of EDAC/NHS, before hydrazide groups are introduced to the surface with carbohydrazide ②. The surface is then deactivated ③ with ethanolamine HCl pH 8 to deactivate any remaining reactive succinimide esters. Then renin (oxidised with sodium metaperiodate) is immobilised ④ onto the chip surface in a coupling buffer of sodium acetate pH 4 or 5. As a final step, the covalent bond formed between the ligand and the chip surface is stabilised by flowing across a double injection ⑤ of the reducing agent sodium triacetoxyborohydride. The increase in RU from baseline following reduction is indicative of the level of ligand immobilised on the sensor chip surface.*

Immobilisation of renin mediated by aldehyde coupling worked well and led to good levels of immobilisation, with immobilisation at pH 4 giving higher levels of ligand density than immobilisation at pH 5 (530 RU vs 350 RU, respectively) and the sensorgram obtained is shown

above in Figure 4.12. Ligand immobilisation at both pH 4 and 5 was trialled, as it has been demonstrated that the pH that yields the highest levels of immobilisation may not always be the optimal conditions for immobilisation in terms of the ligand's activity.[179] An unactivated blank channel was used as a reference channel, while SUMO-CAT was used as a negative analyte control. With bated breath, angiotensinogen was flowed across the renin surface and excitingly angiotensinogen (SUMO-AGT) was found to interact with the renin surface to produce binding responses in a concentration dependent manner, with the pH 4 immobilised surface giving larger binding responses (Figure 4.13a)—finally, success after much trial and error!

Subsequent analyte runs using the same concentrations of angiotensinogen revealed that although binding responses were still obtained in a concentration-dependent manner, the binding capacity of the surface had greatly decreased, as the responses were of a much smaller magnitude (Figure 4.13b). This could either be a result of the regeneration conditions being too harsh and causing a loss of enzymatic activity through time, or conversely due to poor regeneration leading to a build up of bound angiotensinogen on the chip surface. An 18 second pulse of glycine HCl pH 2.0 was used as a regeneration solution for these experiments, and although quite harsh, was not thought to be too damaging to the renin surface. Gossas *et al.* had carried out extensive regeneration scouts and found the aldehyde-coupled renin surface to be stable for several days without a significant loss of binding capacity even when subjected to 30 second pulses of low and high pH solutions, as well as solutions containing high ionic strength, complexing agents, detergents, organic solvents, or chaotropic substances.[36] It is therefore likely that the observed decrease in binding capacity with subsequent analyte runs is simply due to incomplete removal of the bound angiotensinogen molecules following dissociation.

Due to time constraints, further optimisation of this assay to permit final data collection was not possible, and for this reason no further kinetic analysis was performed on the collected data. This assay is thus presented here as a proof of concept that the binding of angiotensinogen

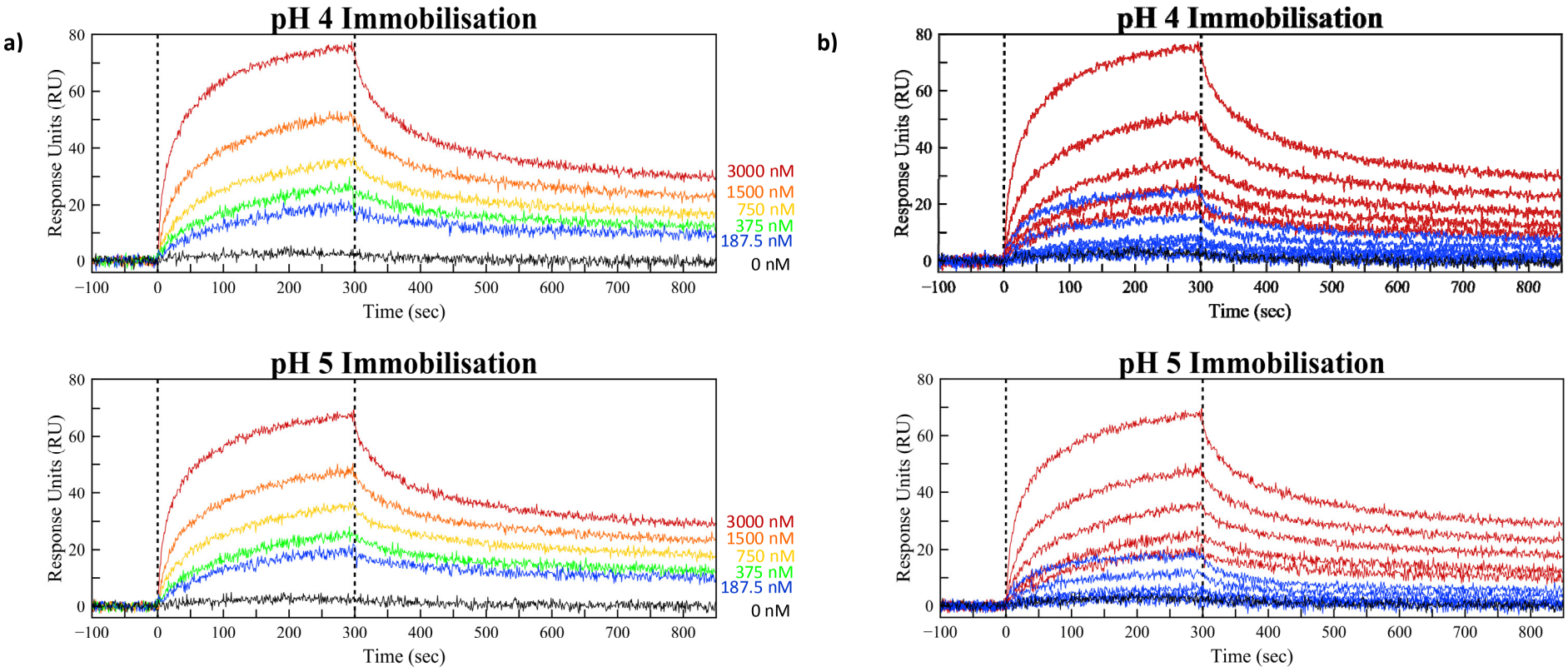


*Figure 4.13:*

*(a) The sensorgram obtained when a dilution series of recombinant SUMOylated human angiotensinogen is flowed across a sensor chip surface containing renin immobilised via aldehyde coupling. SUMO-AGT was flowed across the surface at a flow rate of 50 µL/min for a total contact time of 300 seconds. Following association, running buffer was flowed across the surface for 10 minutes to allow dissociation to occur. The surface was shown to display a decrease in binding capacity over several runs as shown in (b). The first analyte run is in red and a subsequent run at the same concentrations of SUMO-AGT is shown in blue.*

to renin can be measured and studied by directly immobilising renin to a sensor chip surface using aldehyde coupling, and is likely to constitute the first report of the interaction between renin and angiotensinogen being studied using surface plasmon resonance. With more time and resources, this assay could be further optimised into a functional assay used to detect and study the interactions taking place between renin and angiotensinogen.

## 4.4 SUMMARY

This chapter presents the development of two SPR-based bioassays for the detection and quantification of human angiotensinogen. The first assay makes use of monoclonal antibodies to produce a stable ligand surface capable of detecting angiotensinogen and giving reproducible results over several injection cycles. The second assay involves the immobilisation of human renin to a sensor chip surface by tethering renin's glycosylation residues to the surface via aldehyde coupling, producing a renin surface that demonstrates clear concentration-dependent binding responses in the presence of angiotensinogen. Despite the second assay requiring further fine-tuning, both assays clearly exemplify that human angiotensinogen can be assayed using surface plasmon resonance and they provide a useful tool at researchers' disposal for further research into angiotensinogen and its medical relevance.

*Chapter Five*

# REDUCED AND OXIDISED ANGIOTENSINOGEN: IS THERE REALLY A DIFFERENCE?

## 5.1 INTRODUCTION

With the foundations now laid by the work described in Chapters Three and Four, it was time to address the big questions and ultimate goal of this thesis: 1) is it possible to experimentally make a distinction between the reduced and oxidised forms of angiotensinogen? 2) What really is the difference between the two redox states of the protein that results in the differential reactivity of renin to these two forms? And 3) can these differences be used to develop a diagnostic bioassay for pre-eclampsia? The results of this chapter are thus presented in order to probe the redox switch of this medically important protein in an attempt to gain a better understanding of angiotensinogen's two redox states and ultimately test whether these two forms can be distinguished experimentally in an SPR-based bioassay.

Firstly, making use of sulfydryl chemistry, angiotensinogen was reacted with polyethylene glycol that contained a maleimide functionality to quantify the redox state of the protein under reducing and non-reducing conditions (Section 5.2). Secondly, the antibody-based SPR assay for angiotensinogen described in Chapter Four was used to test whether reduced and oxidised angiotensinogen can be discriminated experimentally (Section 5.3), in a step towards a diagnostic bioassay being developed. Finally, by undertaking molecular dynamic simulations (Section 5.4), the reduced and oxidised forms of angiotensinogen were further probed at a molecular level in an attempt to unravel the differences between the two forms, underpinning their differential reactivity.

## 5.2 Quantification of the Free Cysteines in Reduced and Oxidised Angiotensinogen

Angiotensinogen contains four cysteine residues, but only two of these residues, namely Cys 18 and Cys 138, are evolutionarily conserved across species and are involved in the formation of an intramolecular disulfide bond. Zhou *et al.* described this disulfide bridge as labile, having a reduction potential of –230 mV at pH 7 and 25 °C.[1] Following expression, angiotensinogen is secreted from the endoplasmic reticulum in the oxidised form, in a predictable fashion, and is subsequently reduced to the free cysteine reduced state in the circulation.[1] These researchers went on further to show that, in the plasma pool, angiotensinogen exists as a stable ratio of 40:60 of the reduced to oxidised forms, regardless of age or gender in healthy individuals, while women in their third trimester who were suffering from pre-eclampsia had altered proportions of angiotensinogen in their plasma pool, displaying far greater levels of the oxidised form.[1] In order to determine these plasma ratios, researchers performed SDS-PAGE and western blotting on plasma samples that had been reacted with polyethylene glycol 5000 containing a maleimide functionality (mPEG 5000). Because oxidised angiotensinogen contains only two free cysteine residues to react with the mPEG molecules, while reduced angiotensinogen contains a total of four cysteines, the two redox forms were visually distinguishable due to the difference in mass following conjugation to mPEG 5000 (depicted in Figure 5.1).

Undertaking a similar approach, recombinant angiotensinogen (expressed in *E. coli*) was reacted with mPEG 5000 in the presence or absence of the reducing agent TCEP to quantify the redox state of the recombinantly produced protein. Because bacterial cell protein expression does not always lead to disulfide bond formation due to the reducing environment

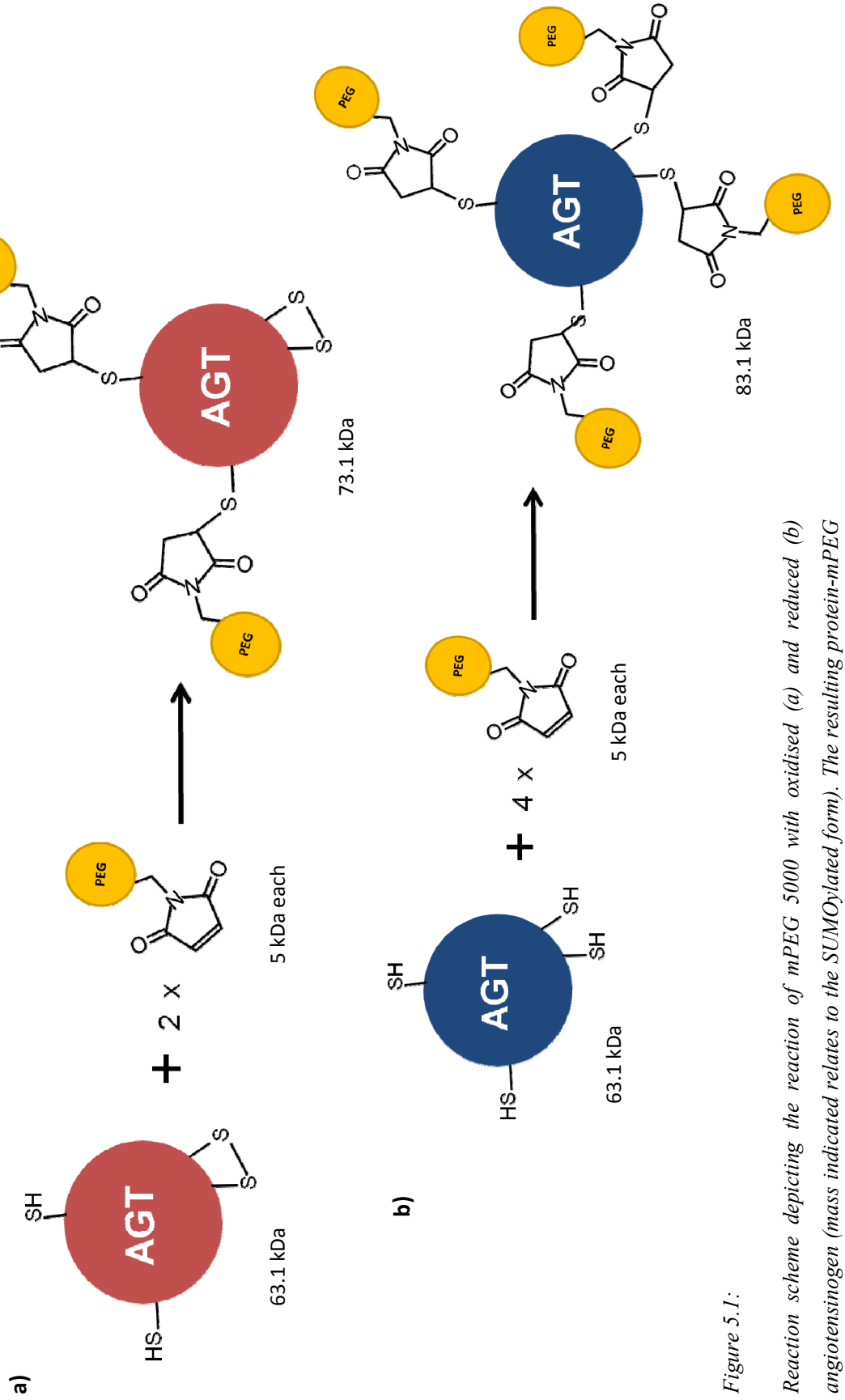


*Figure 5.1:*

*Reaction scheme depicting the reaction of mPEG 5000 with oxidised (a) and reduced (b) angiotensinogen (mass indicated relates to the SUMOylated form). The resulting protein-mPEG conjugates contain two or four mPEG adducts respectively—a mass difference that is visible by SDS-PAGE analysis.*

within the cell's cytoplasm,[190, 191] it was necessary to determine whether both redox states could be generated for further experiments. SUMOylated angiotensinogen was used for these reactions and, since the SUMO fusion tag does not contain any cysteine residues, it should not have an effect on the reaction of mPEG with angiotensinogen's four cysteine residues. The reactions were incubated overnight in a shaking incubator at 25 °C and samples were taken at the time points of 1.5 hours, 4 hours, and 18 hours (overnight) following the addition of mPEG to the protein solution. Samples of protein, in the presence or absence of reducing agent, were taken prior to, and immediately following, the addition of mPEG as controls. The reactions were carried out in PBS at pH 7.2 so that side reactions of mPEG with lysine residues, which occur at higher pH's,[192] were minimised. The results of these reactions were revealed by SDS-PAGE analysis, and are shown in Figure 5.2.

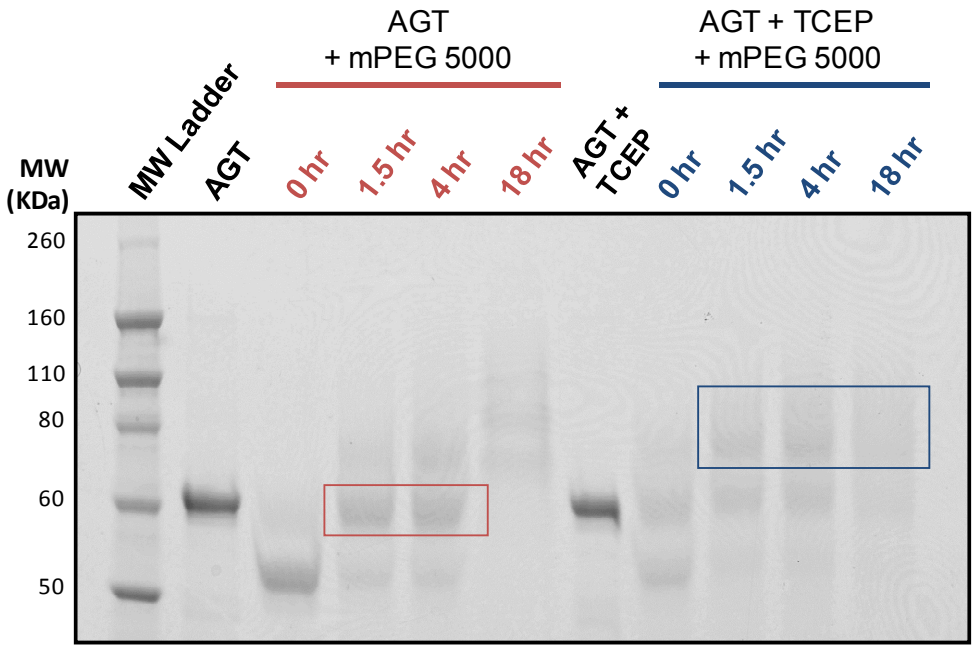


*Figure 5.2:*

*SDS-PAGE analysis of the time course of the reaction between recombinant SUMOylated angiotensinogen with mPEG 5000 in the presence or absence of reducing agent. The molecular weight marker (Novex® Sharp Pre-stained Protein Standard) was loaded in the first lane. The oxidised protein species are indicated in the red box while the reduced species are shown in the blue box.*

On first glance, the effect that the addition of mPEG had was strikingly obvious, and unexpectedly so. The samples of angiotensinogen taken immediately following mPEG addition resulted, in both cases, in angiotensinogen displaying an apparent decrease in molecular weight of approximately 10 kDa. Thus, the mPEG molecules seem to be altering the electrophoretic mobility of the protein in the gel, even in the samples taken immediately following mPEG addition, prior to any conjugation having taken place. The addition of mPEG also caused smearing of the proteins on the gel. PEG has been reported to bind to SDS micelles, causing an alteration in the electrophoretic mobility of proteins—the magnitude of which is largely determined by the size of the protein of interest and its proximity to the PEG front during electrophoresis.[193] As a consequence, this unfortunately meant it was difficult to obtain accurate protein sizes using electrophoresis, but it was nonetheless clear that adding mPEG had increased the protein size. SUMOylated angiotensinogen has a molecular weight of 63.1 kDa, and on conjugation with mPEG 5000, oxidised angiotensinogen is expected to have a molecular weight of 73.1 kDa, while reduced angiotensinogen is predicted to have a molecular weight of 83.1 kDa. Incubation with mPEG for 1.5 or 4 hours in the absence of reducing agent led to angiotensinogen-mPEG conjugates that were, predominately, of a smaller molecular weight when compared to the same time points in the presence of reducing agent, indicative that Cys 18 and Cys 138 are disulfide bonded prior to reduction. Although the separation of the protein into the oxidised and reduced forms is not clear cut with multiple species present, there is a distinct difference in the weight of the species generated when reacted with mPEG in the presence or absence of reducing agent, allowing the possibility of angiotensinogen to be derivatised in either the reduced or oxidised form. Repeating the experiment with mPEG 10000 instead of mPEG 5000 gave identical results except that the protein bands on the gel were even more smeared and the mPEG adducts were a larger molecular weight, as expected (each mPEG is 10 kDa compared to 5 kDa for mPEG 5000).

Interestingly, following overnight incubation with mPEG, angiotensinogen, in the absence of reducing agent, unexpectedly increased in molecular weight, generating species that were of a similar size to the reduced conjugate species. This suggests that during longer incubations, the reaction of mPEG with free thiols was driving the reversible labile disulfide bond formation/breakage reaction in the forward direction toward disulfide breakage, essentially by scavenging free cysteines as they became available, resulting in a subsequent loss of the disulfide-bonded oxidised species over time, and a gradual increase in the reduced angiotensinogen species. Because of this, any derivatisation of angiotensinogen into the reduced and oxidised forms by capping the cysteine thiols with maleimide and its derivatives must be done on as short a time-scale as possible to prevent conversion of the oxidised form into the reduced form.

Overall, this demonstrates that angiotensinogen, expressed recombinantly in bacterial cells, is predominately, although not 100%, present in the oxidised disulfide bonded form of the protein. Subsequent reduction and breakage of the disulfide bridge between Cys 18 and Cys 138 with a reducing agent results in all four cysteines being available for conjugation with a maleimide compound, preventing reformation of the disulfide bond between these two residues.

## 5.3 SPR Assay for Reduced and Oxidised Angiotensinogen

Having developed an SPR-based assay capable of detecting human angiotensinogen using monoclonal antibodies (Chapter Four), it was now possible to see if reduced and oxidised angiotensinogen could be distinguished experimentally using this technique. A multiplexing approach was undertaken for data collection, which, in addition to repeat analyte injections, was able to show that the results obtained were not only accurate, but also reproducible. The anti-AGT mAb antibody was immobilised at the same concentration on four activated ligand channels to generate four anti-AGT mAb surfaces of the same ligand density. The resulting

levels of immobilised antibody following deactivation are shown in Table 5.1, and demonstrate that the ligand density on all channels was very similar. A further channel was immobilised with the anti-IgG mAb at the same concentration of antibody to serve as a reference surface.

| ANTI-AGT MAB SURFACE | LEVEL OF IMMOBILISATION (RU) |
|---|---|
| Surface 1 | 235 |
| Surface 2 | 248 |
| Surface 3 | 247 |
| Surface 4 | 268 |

*Table 5.1:*

*Levels of anti-AGT mAb antibody immobilisation following deactivation on each of the ligand channels used for reduced and oxidised angiotensinogen data collection.*

Recombinant reduced and oxidised His-tagged human angiotensinogen expressed in *E. coli* cells was used in these experiments, and was a kind gift from Tim Yandle and Darrell Wang (Endolab, Canterbury Health Laboratories). Prior to receiving this protein, the angiotensinogen had been derivatised at Endolab as either reduced or oxidised angiotensinogen in the presence of *N*-ethylmaleimide (NEM) and dithiothreitol (DTT), or NEM alone, respectively, and mass spectrometry studies of these two forms confirmed that the proteins existed in the correct disulfide bonded (oxidised) or free cysteine (reduced) redox states (unpublished data, personal communication with Stephen Brennan, University of Otago, Christchurch). The reduced and oxidised angiotensinogen samples were run as analytes on the SPR as a concentration series with a starting concentration of 2 μM and a dilution factor of two, such that concentrations of 2 μM, 1 μM, 500 nM, 250 nM, 125 nM, and 62.5 nM of both reduced and oxidised angiotensinogen were measured. Each concentration set of angiotensinogen was injected multiple times to obtain

replicate measurements. Oxidised angiotensinogen samples were injected firstly in an ordered fashion, and then in a randomised order, and the same approach was carried out with reduced angiotensinogen, to show that the binding responses measured were independent of the analyte channel used. Finally, the binding responses of the three highest concentrations of reduced/oxidised angiotensinogen were measured in the same analyte run, firstly in ordered fashion, and as a repeat in a randomised order. Thus, all the binding data for each channel was composed of at least two replicates for each concentration of reduced and oxidised angiotensinogen.

Because SPR is such a sensitive technique, any differences in protein concentration could have had an effect on the results so it was critical that accurate concentration of each of the proteins was obtained. Although the Nanodrop spectrophotometer was used to determine protein concentrations during the initial assay development and optimisation, it was deemed that this method was inaccurate for determining precise concentrations of the reduced and oxidised angiotensinogen samples as both NEM and DTT, present in the protein samples, have an absorbance at 280 nm, resulting in differences in the apparent protein concentrations measured. To circumvent this, another method was employed instead to determine accurate protein concentrations, namely the *o*-phthalaldehyde (OPA) fluorescent protein assay. In the presence of mercaptoethanol, *o*-phthalaldehyde reacts with primary amine groups in proteins (i.e. terminal amino acids of proteins and the ε-amino group of lysine residues) to produce a blue fluorescent product which has maximum excitation at 340 nm and maximum emission at 455 nm.[143, 144] This fluorescent protein assay is advantageous, not only due to its sensitivity, but also because it is compatible with a wide range of buffer additives including detergents and reducing agents. In addition, both reduced and oxidised angiotensinogen contain identical primary amine content, so there should be no bias due to differing amine content. To ensure that the sensitivity of this assay is unaffected by DTT and NEM, standard curves were generated using BSA at a range of

concentrations in the presence and absence of these compounds (Figure 5.3). NEM and DTT, either alone or combined were shown to have no effect on the assay with a linear calibration curve produced that was not affected by the addition of these compounds.

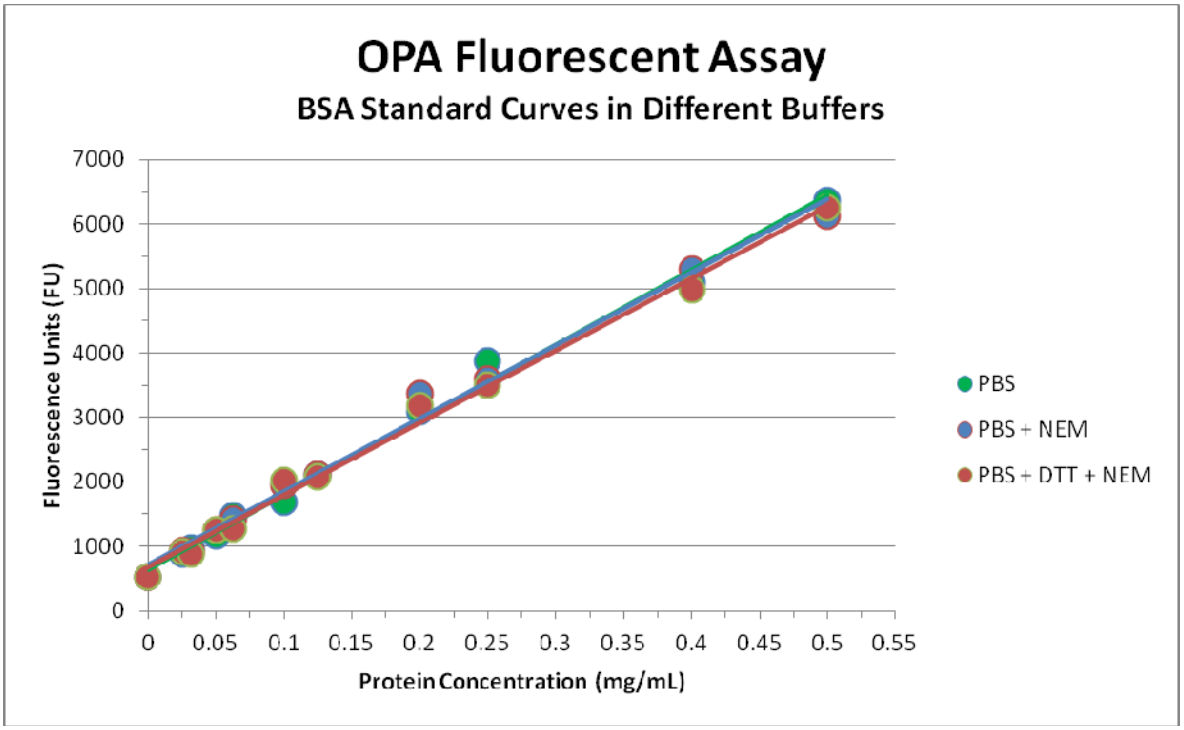


*Figure 5.3:*

*BSA standard curves generated using the o-phthalaldehyde fluorescent protein assay. The BSA samples were prepared either in PBS pH 7.4 alone, or with the addition of NEM, or DTT and NEM at concentrations equivalent to those present in the angiotensinogen protein samples.*

The reduced and oxidised angiotensinogen analyte runs were performed as per the protocol developed in Section 4.2. Briefly, samples were injected at a flow rate of 25 µL/min for a total contact time of 981 seconds, followed by a dissociation time of 1800 seconds. PBST pH 7.4 was used as the running buffer for all experiments and also to prepare the dilutions of angiotensinogen samples. All experiments were performed at 25 °C, and a single regeneration step (18 second pulse of glycine HCl pH 2) followed by four blank buffer runs were performed

between each analyte runs. All data sets were double referenced against both the anti-IgG mAb reference surface, and against buffer injections containing no protein. The binding responses (including replicates) obtained as a result of oxidised or reduced angiotensinogen interacting with the anti-AGT mAb surfaces can be seen in Figures 5.4 and 5.5, respectively.

The binding responses, although noisy, clearly show concentration-dependent responses as a result of the reduced and oxidised angiotensinogen binding the anti-AGT mAb surfaces. Replicates of each analyte concentration overlay well, and there are only subtle differences in the magnitude of responses between ligand channels that correlate with the small differences in immobilised ligand density on these surfaces (Table 5.1), demonstrating that these results are reproducible. Although ligand saturation was not reached, each set of sensorgrams shows visible curvature in the association phase and decay in the dissociation phase, which is ideal for kinetic analysis. Even prior to kinetic analysis, the differences between reduced and oxidised angiotensinogen binding to the ligand surfaces at the same analyte concentrations are clearly visible when overlaid, as can be seen in Figure 5.6.

Kinetic analysis of these responses was able to unravel these differences further. All kinetic analysis was carried out using ClampXP, a data analysis program that uses numerical integration and non-linear global curve fitting algorithms to fit measured data to kinetic binding models.[145] To demonstrate that the assay was able to generate reproducible results, the data set from each anti-AGT mAb ligand channel was analysed and fit to a kinetic model separately and independently of the other ligand channels. The binding data from reduced and oxidised angiotensinogen were fit to a simple 1:1 Langmuir binding model (described in Section 4.2).

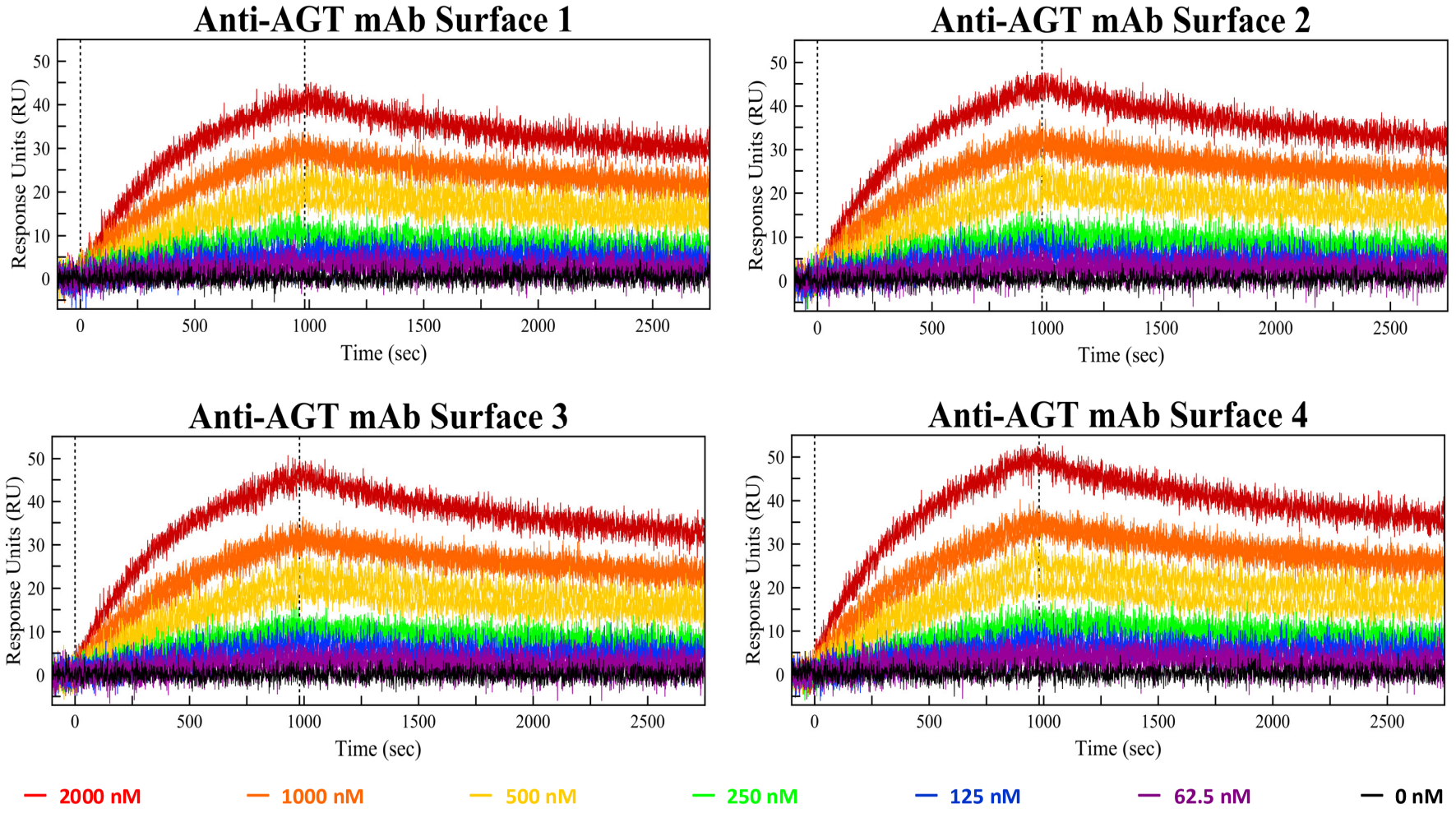


*Figure 5.4:*

*Sensorgrams of the binding responses obtained when a dilution series of recombinant oxidised human angiotensinogen was flowed across the four anti-AGT mAb antibody surfaces. Angiotensinogen was flowed across the surface at a flow rate of 25 µL/min for a total contact time of 981 seconds. Following association, running buffer was flowed across the surface for 30 minutes to allow dissociation to occur. Replicate injections of each concentration are shown overlaid.*

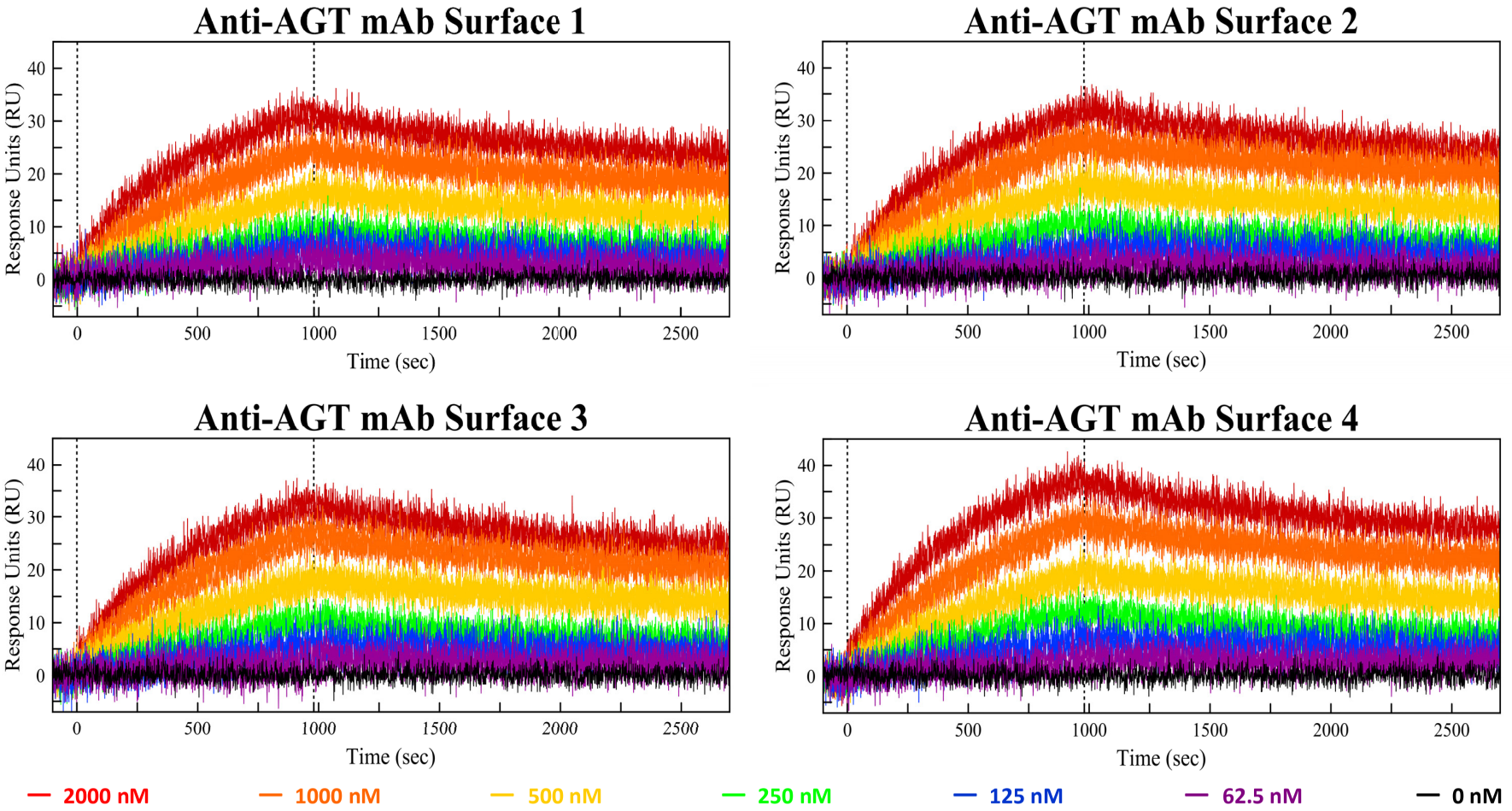


*Figure 5.5:*

*Sensorgrams of the binding responses obtained when a dilution series of recombinant reduced human angiotensinogen was flowed across the four anti-AGT mAb antibody surfaces. Angiotensinogen was flowed across the surface at a flow rate of 25 µL/min for a total contact time of 981 seconds. Following association, running buffer was flowed across the surface for 30 minutes to allow dissociation to occur. Replicate injections of each concentration are shown overlaid.*

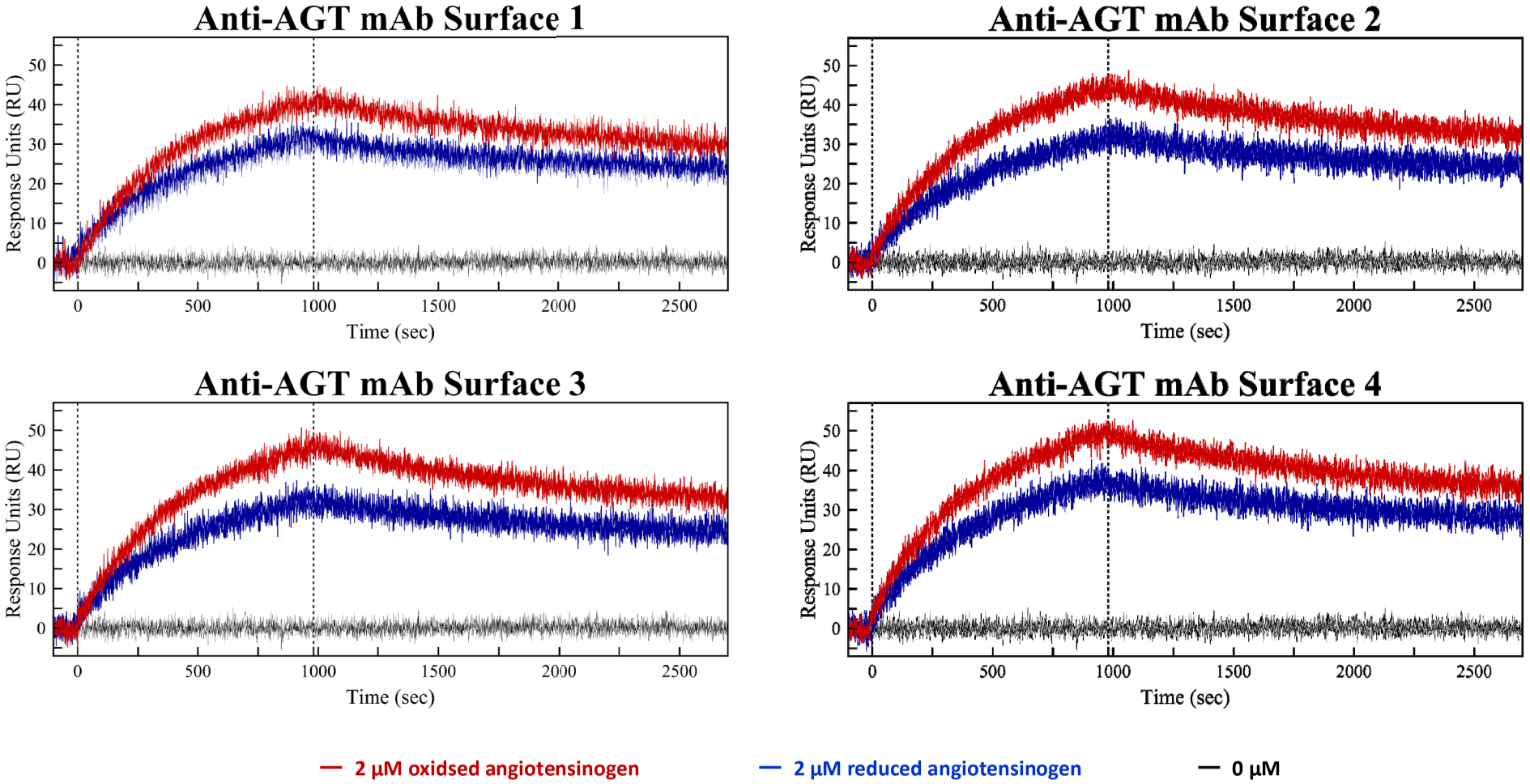


*Figure 5.6:*

*Comparison of the sensorgrams of the binding responses obtained when recombinant oxidised and reduced human angiotensinogen at a concentration of 2 µM were flowed across the four anti-AGT mAb antibody surfaces. Angiotensinogen was flowed across the surface at a flow rate of 25 µL/min for a total contact time of 981 seconds. Following association, running buffer was flowed across the surface for 30 minutes to allow dissociation to occur. Replicate injections of each analyte are shown overlaid.*

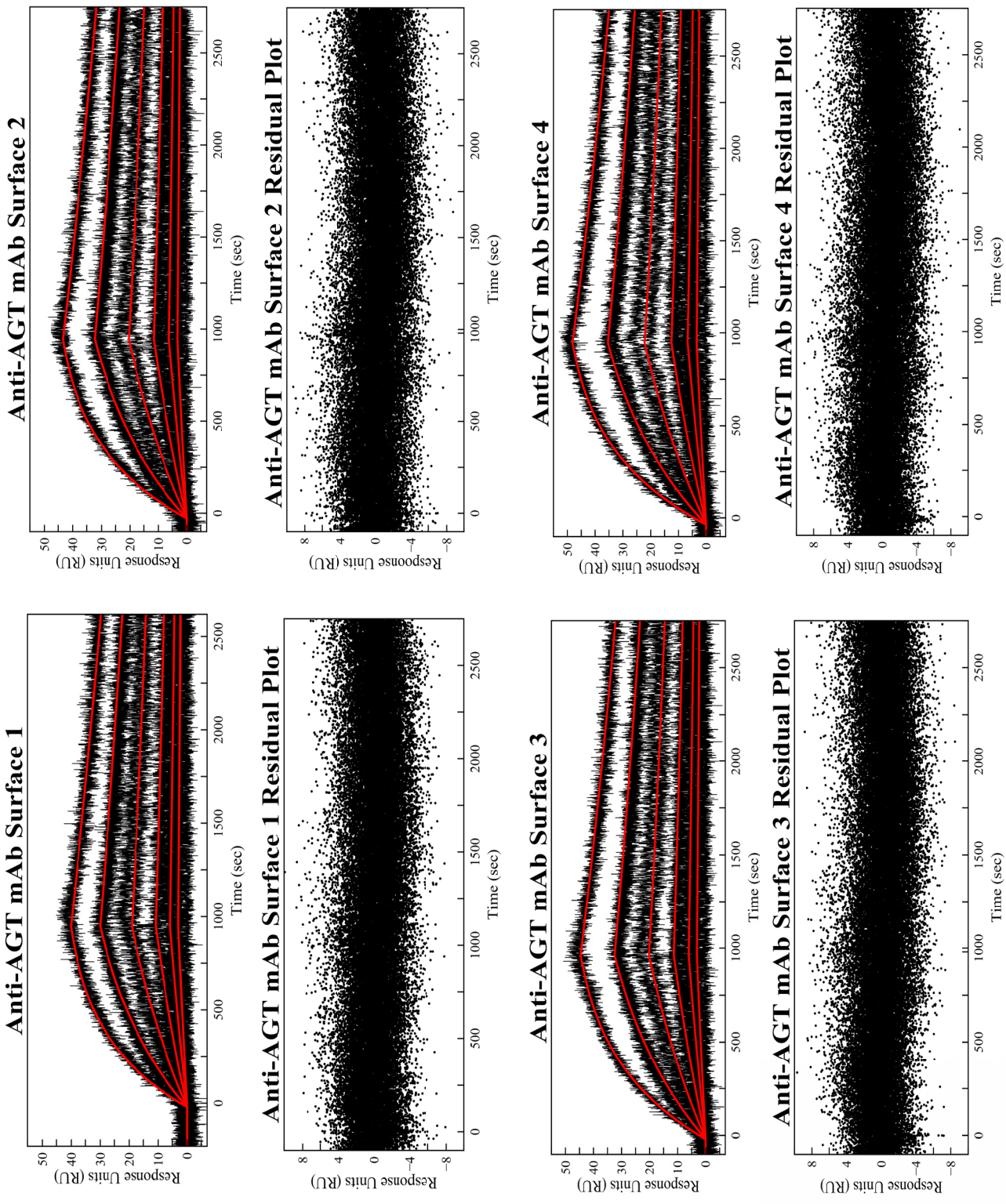


*Figure 5.7:*

*Oxidised angiotensinogen binding responses from each anti-AGT mAb surface (data shown in Figure 5.4) were fit to a 1:1 Langmuir binding model using ClampXP. The data is shown in black while the kinetic model fits are overlaid in red. The residual plot of the model fitting is also shown beneath each sensorgram.*

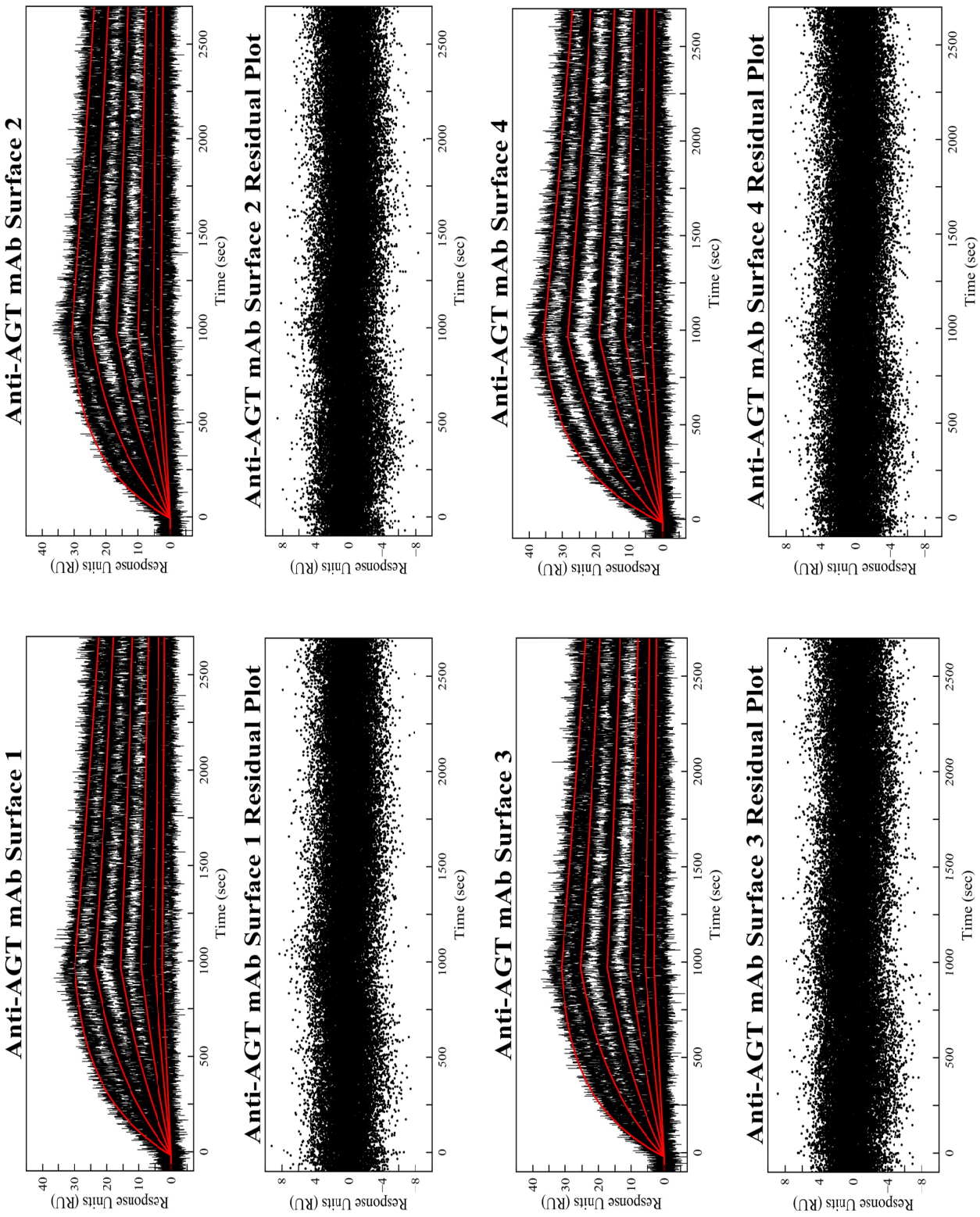


*Figure 5.8:*

*Reduced angiotensinogen binding responses from each anti-AGT mAb surface (data shown in Figure 5.5) were fit to a 1:1 Langmuir binding model using ClampXP. The data is shown in black while the kinetic model fits are overlaid in red. The residual plot of the model fitting is also shown beneath each sensorgram.*

The models overlaid nicely on the measured data from each anti-AGT mAb surface, and the residual plots also indicated that the kinetic fits are an excellent description of the data. The plots show that the residuals are randomly scattered about the baseline with an amplitude of ± 4 RU, which would be expected given the noise shown on the sensorgrams (Figures 5.7 and 5.8). The kinetic constants and standard deviations resulting from the best fit data for each surface, for both reduced and oxidised angiotensinogen, are summarised in Table 5.2. The standard deviations from the fitting of the kinetic parameters are small, indicating that the rate constants for each data set are well defined. Both the kinetic association ($k_a$) and dissociation ($k_d$) rate constants were different for the two redox forms, with oxidised angiotensinogen displaying a slower association rate and faster dissociation rate than reduced angiotensinogen ($k_a$: 1121 $M^{-1}$ $s^{-1}$ vs. 1510 $M^{-1}$ $s^{-1}$ and $k_d$: 1.78 x $10^{-4}$ $s^{-1}$vs. 1.55 x $10^{-4}$ $s^{-1}$, respectively). Figure 5.9 shows that the kinetic rate constants for the two redox forms of angiotensinogen are distinctly different.

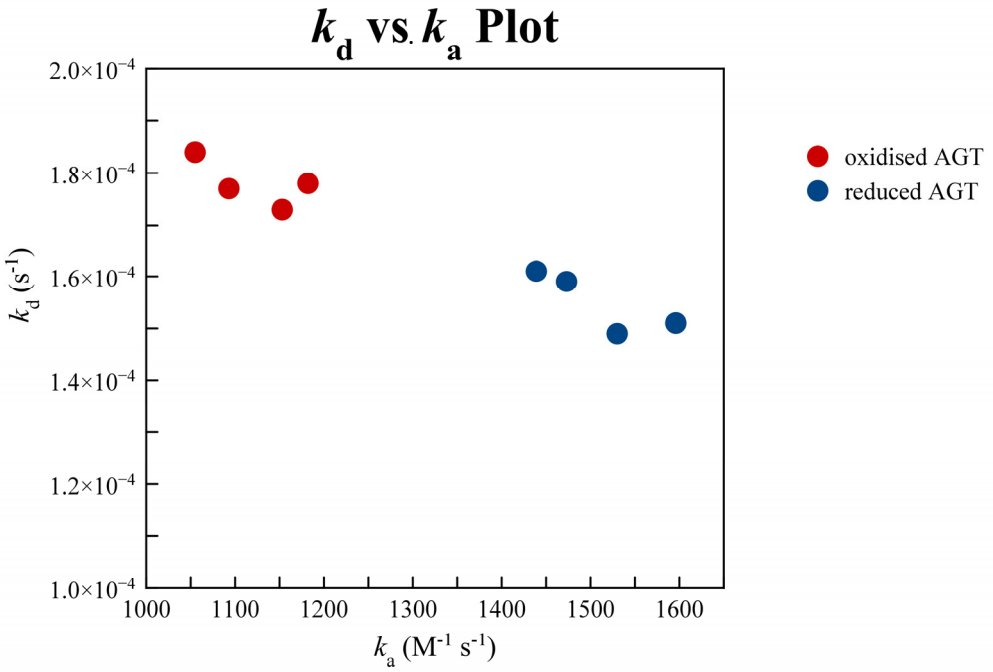


*Figure 5.9:*

*$k_a$ versus $k_d$ plot of the kinetic parameters determined for reduced (blue) and oxidised (red) angiotensinogen binding to each anti-mAb ligand surface by fitting the simple 1:1 Langmuir binding model to each data set (each data point represents one anti-mAb antibody surface).*

| **OXIDISED ANGIOTENSINOGEN** | | | |
|---|---|---|---|
| **Anti-AGT mAb Surface** | $k_a$ ($M^{-1}$ $s^{-1}$) | $k_d$ ($s^{-1}$) | $K_D$ (nM) |
| Surface 1 | 1182 ± 4 | (1.78 ± 0.01) x $10^{-4}$ | 150 ± 1 |
| Surface 2 | 1153 ± 4 | (1.73 ± 0.01) x $10^{-4}$ | 150 ± 1 |
| Surface 3 | 1055 ± 4 | (1.84 ± 0.01) x $10^{-4}$ | 174 ± 1 |
| Surface 4 | 1093 ± 3 | (1.77 ± 0.01) x $10^{-4}$ | 162 ± 1 |
| **REDUCED ANGIOTENSINOGEN** | | | |
| **Anti-AGT mAb Surface** | $k_a$ ($M^{-1}$ $s^{-1}$) | $k_d$ ($s^{-1}$) | $K_D$ (nM) |
| Surface 1 | 1439 ± 6 | (1.61 ± 1) x $10^{-4}$ | 112 ± 1 |
| Surface 2 | 1534 ± 6 | (1.49 ± 1) x $10^{-4}$ | 97.3 ± 0.9 |
| Surface 3 | 1596 ± 6 | (1.51 ± 1) x $10^{-4}$ | 94.8 ± 0.9 |
| Surface 4 | 1473 ± 5 | (1.59 ± 1) x $10^{-4}$ | 108.1 ± 0.8 |
| **AVERAGES** | | | |
| | $k_a$ ($M^{-1}$ $s^{-1}$) | $k_d$ ($s^{-1}$) | $K_D$ (nM) |
| Oxidised Angiotensinogen | 1121 ± 4 | (1.78 ± 0.01) x $10^{-4}$ | 159 ± 1 |
| Reduced Angiotensinogen | 1510 ± 6 | (1.55 ± 0.01) x $10^{-4}$ | 103.1 ± 0.9 |
| Independent Samples *t*-Test (p-value) | <0.0001 | <0.0001 | <0.0001 |
| *t*-value | -107.89 | 32.53 | 83.10 |
| degrees of freedom | 5 | 5 | 5 |

*Table 5.2:*

*Kinetic values obtained from the fitting of the simple 1:1 Langmuir binding model to the binding responses of reduced and oxidised recombinant angiotensinogen on each anti-AGT mAb surface (data and model fits shown in Figures 5.7 and 5.8) Model fitting was carried out using ClampXP. Independent samples t-tests were performed on the mean anti-AGT mAb surface $k_a$, $k_d$, and $K_D$ values for oxidised and reduced angiotensinogen to test the statistical significance of the differences between the two redox forms.*

The differences in the association and dissociation rate constants led to different dissociation constants ($K_D = k_d/k_a$) for the angiotensinogen-antibody complex, depending on the redox state of the protein. Oxidised angiotensinogen was determined to have a mean $K_D$ value of 159 nM while reduced angiotensinogen had a mean $K_D$ value of only 103.1 nM. The dissociation constant is a measure of the affinity of the anti-AGT mAb antibody for the angiotensinogen protein, and thus, gives an idea of how tightly angiotensinogen binds to the ligand surface. Therefore, reduced angiotensinogen, having a lower $K_D$ value, binds to the anti-AGT mAb more tightly than oxidised angiotensinogen. Furthermore, statistical analysis revealed that the differences in the $k_a$, $k_d$, and $K_D$ values between reduced and oxidised angiotensinogen were statistically significant, having p-values of $< 0.0001$ (Table 5.2). Despite the small sample size ($n = 4$ for both reduced and oxidised angiotensinogen), each set of kinetic rate constants was derived from the kinetic fit of the model to multiple replicates, thus the statistical significance should accurately represent the differences observed, especially given the small standard deviations that were defined for each of the rate constants.

To validate that the kinetic models for the 1:1 Langmuir binding of reduced and oxidised angiotensinogen to the anti-AGT mAb surface were fitted correctly, each data set was subjected to Monte Carlo analysis, a feature of the ClampXP program. Monte Carlo tests are carried out to determine whether the obtained set of kinetic rate constants for a particular fit can be consistently generated using vastly different starting parameter values.[194] Despite starting the fitting process of each data set from kinetic parameters that varied from the initial value by as much as 1000%, the 50 cycles of Monte Carlo fits demonstrated that, even with the addition of random short-term noise, all results converged on the same set of $k_a$ and $k_d$ values, strongly supporting the validity of the kinetic model fitting to each data set. In addition, each data set was independently fitted to a simple 1:1 Langmuir binding model using the Scrubber program and the same results were obtained. Finally, as each of the anti-AGT mAb surfaces are independent from each other, the

kinetic rate constants obtained from model fitting of the data collected from each ligand surface serve to both validate the model fits obtained, and demonstrate that the results are reproducible.

Overall, these results clearly demonstrate that by using the antibody-based SPR assay that was developed in Section 4.2, recombinant non-glycosylated reduced and oxidised angiotensinogen can be experimentally distinguished in a reliable and reproducible fashion. The anti-AGT mAb antibody surface has a statistically significant higher affinity for the reduced form of angiotensinogen when compared with the oxidised form, due to differences in both the association and dissociation rates of the two redox states of angiotensinogen protein when interacting with the immobilised antibody. These differences are especially significant in light of the intrinsic similarity of the two redox states of angiotensinogen, which differ only in the presence or absence of a disulfide bond, and the results certainly give credit to the sensitivity of the SPR technique to be able to facilitate the detection of these minute structural differences.

## 5.4 MOLECULAR DYNAMIC SIMULATIONS

The idea that the entire angiotensinogen protein, rather than just the N-terminal portion, may play a role in the reaction with renin is not a new one. Streatfeild-James *et al.* elegantly showed that angiotensinogen's tertiary structure plays a pivotal role in the reaction with renin, in terms of the reaction rate, and also with regard to the affinity that renin displays for angiotensinogen.[126] Zhou *et al.* went on further to show that binding of angiotensinogen to renin is accompanied by a 10 Å displacement of the CD loop containing Cys 138 that simultaneously presents the N-terminal peptide to renin's active site cleft, movements carried out in a concerted manner mediated by angiotensinogen's disulfide bond.[1] The solving of the x-ray crystal structures of angiotensinogen, alone, and bound to renin, revealed that the interactions that occur in the renin-angiotensinogen complex are not limited to angiotensinogen's N-terminal substrate and renin's active site cleft, but rather encompass a considerable 670 Å of predominantly

hydrophobic contact surface area between the bodies of the two proteins.[1] These studies provide strong evidence in opposition of the once widely held hypothesis that angiotensinogen was simply a passive carrier of the angiotensin peptide,[126] and hint towards the critical role that the Cys 18 and Cys 138 residues may play in facilitating these structural changes.

To delve deeper into the mechanisms by which the two redox states of angiotensinogen interact differentially with renin, and also with the anti-AGT mAb antibody, human angiotensinogen was subjected to molecular dynamics (MD) simulations. These simulations were performed to ascertain whether the experimentally observed differences between the reduced and oxidised forms can be explained by the protein's molecular motions, mediated or perhaps prevented by the Cys 18 and Cys 138 disulfide bond. Molecular dynamic simulations are able to 'breathe life' into the static images of a protein structure captured by x-ray crystallography, and allow us a glimpse into the energy landscape and structural conformations a protein may explore over a small time-scale that are otherwise unable to be visualised by the naked eye.[195, 196] Modelling of a given protein at the molecular level is achieved by computational simulation of atomic trajectories by the numerical solving of Newton's equations of motion in a system of *N* interacting atoms,[196, 197] ultimately generating a trajectory of molecular movements over a given time-scale (typically in the ns range, although μs simulations have been reported[195, 196, 198]).

To this end, MD simulations were carried out on human angiotensinogen (PDB structure 2WXW) in the presence or absence of the disulfide bond between Cys 18 and Cys 138 at 300 K (approximately 25 °C) in triplicate for simulation trajectories of 500 ns. Initial analysis was carried out by calculating the root mean square deviations (RMSD) and root mean square fluctuations (RMSF) across the triplicate trajectories for both reduced and oxidised angiotensinogen. The RMSD plot shows the deviations of the Cα atoms from the initial energy minimised structure, and revealed that for the first 350 ns the reduced angiotensinogen presents

with a higher RMSD than the oxidised form (Figure 5.10), but in the final 150 ns, the oxidised protein deviates further away from the starting coordinates yielding mean RMSD values of 4.18 Å for oxidised and 4.32 Å for reduced angiotensinogen—a difference of only 0.14 Å that is not highly significant given that the RMSD values are an average metric, suggesting that the two forms of angiotensinogen display similar overall dynamics.

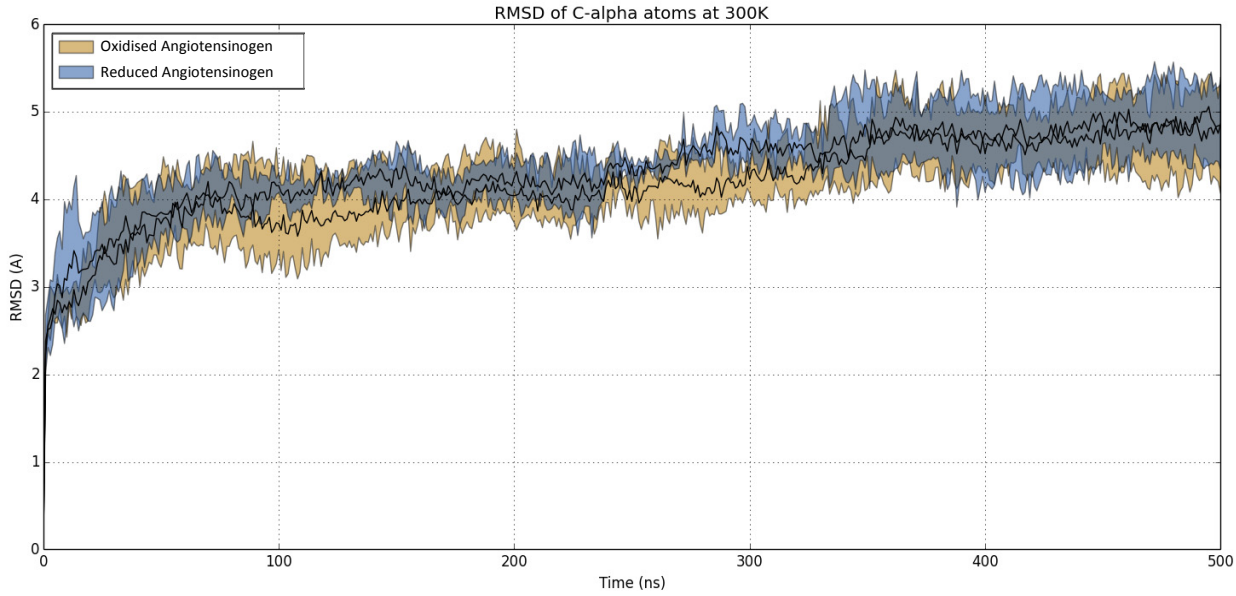


*Figure 5.10:*

*RMSD plot of the Cα atoms from oxidised (brown) and reduced (blue) human angiotensinogen over 500 ns. Each plot shows the mean RMSD over the three replicates as well as the minimum/maximum deviation.*

It is difficult to make any solid conclusions about the specific dynamics of the two redox states from the RMSD plots alone, and closer inspection of the RMSF plot, which highlights the deviation differences for each residue, revealed that there are in fact quite distinct differences between the dynamics of reduced and oxidised angiotensinogen. As can be seen in Figure 5.11, there are large differences in the fluctuations of the N-terminus of reduced angiotensinogen, with

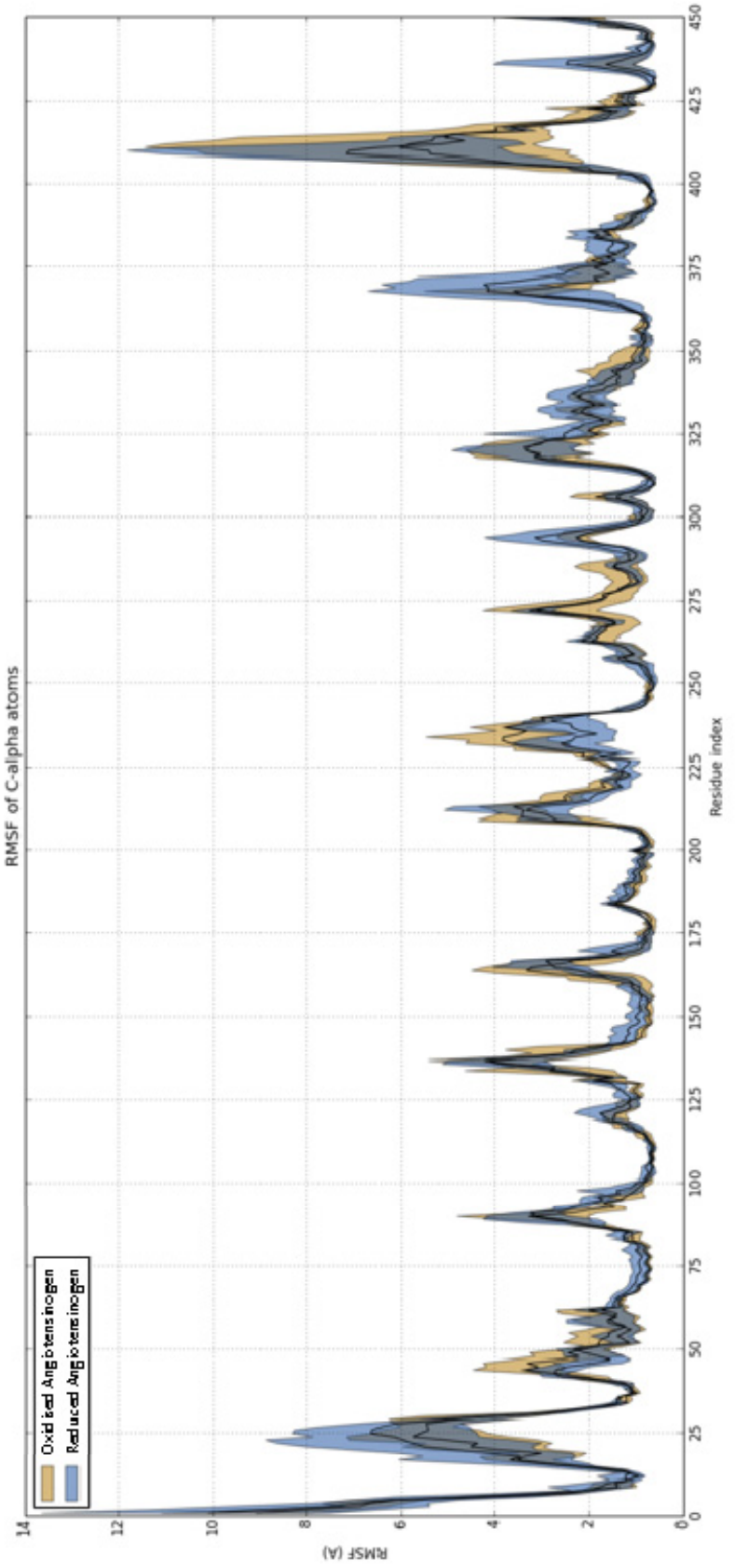


*Figure 5.11:*

*RMSF plot of the Cα atoms from oxidised (brown) and reduced (blue) human angiotensinogen over 500 ns. Each plot shows the mean RMSF over the three replicates as well as the minimum/maximum deviation.*

a maximum deviation of 10 Å, compared to the maximum deviation of 8 Å for oxidised angiotensinogen. Furthermore, reduced angiotensinogen presents much greater deviations in the region between residues 5 and 30, which includes the angiotensin-I peptide and renin cleavage site, as well as Cys 18. It appears that reduction of the disulfide bond between Cys 18 and Cys 138 increases the dynamics surrounding helix A2 of angiotensinogen. Interestingly, this increase in dynamics around Cys 18 in reduced angiotensinogen appears to come hand in hand with a decrease in the dynamics in the region encompassing residues 45 to 65 (helix A1). Increases in the dynamics of the reduced form were also observed around residues 80 – 90, 130 – 140, 360 – 375, and 405 – 415 (reactive centre loop) when compared to the oxidised form (Figure 5.12).

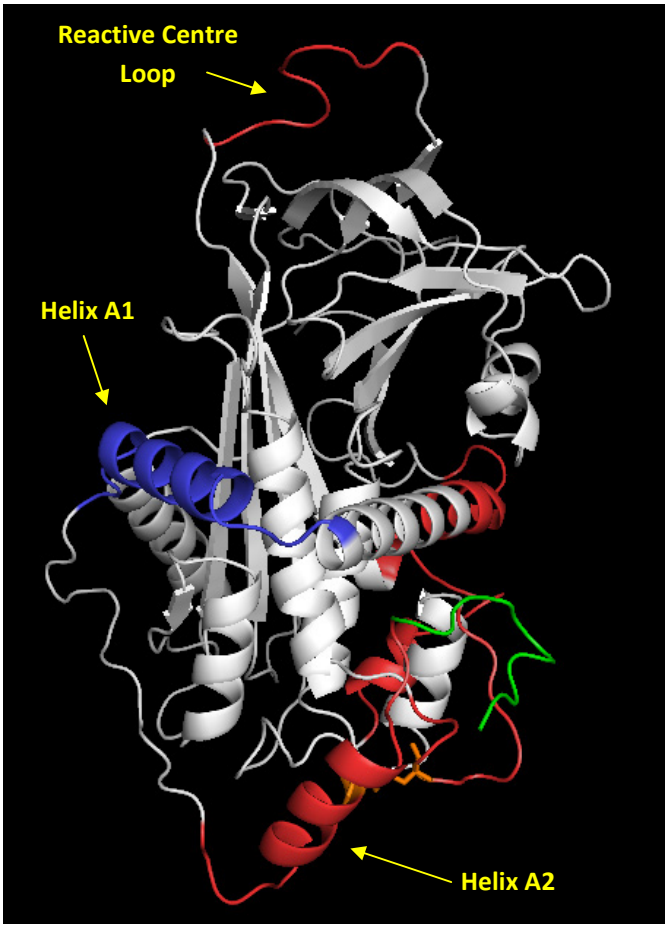


*Figure 5.12:*

*The complete structure of human angiotensinogen (PDB file 2WXW) used for MD simulations is shown, with the missing loops and side chain residues modelled using MODELLER. The angiotensinogen protein is shown in white with the N-terminal angiotensin-I peptide in green and the Cys 18 and Cys 138 residues involved in the disulfide bond highlighted in orange.*

*Regions identified by MD simulation as being more dynamic in the reduced form are shown in red, while less dynamic regions are in blue.*

Movies generated from the simulated trajectories of reduced and oxidised angiotensinogen quite strikingly reveal that the loss of the disulfide bridge between Cys 18 and Cys 138 results in a large increase in the dynamics of the surface alpha helices surrounding helix A2—a phenomenon not observed in the oxidised form of angiotensinogen, suggesting that there may be an energetic acceptance for solvation in the N-terminal region of angiotensinogen on breakage of the disulfide bond. Also noteworthy is the loss of the secondary structure of helix A2 that was observed in the simulation trajectory of reduced angiotensinogen only. The 50 most common conformations adopted by the reduced and oxidised forms of angiotensinogen during the trajectory are shown in Figure 5.13, while Figure 5.14 illustrates snapshots of the trajectories for each of the redox forms every 50 ns. These clearly show the differences between the two structures, as well as the distinct disruption to secondary structure that occurs particularly in the areas encompassing helix A2 and as well as helix C (residues surrounding 120 – 146).

It is clear from these MD simulations that the loss of the disulfide bridge between Cys 18 and Cys 138 results in angiotensinogen being far more dynamic in the regions surrounding the two cysteine residues, with distinct disruptions to secondary structure taking place. These results were to a certain extent expected, as on disulfide bond breakage there would no longer be any physical constraint holding the N-terminal region in place. Thus, the extra mobility of these regions in the reduced form of angiotensinogen is potentially frustrating or occluding the binding of renin to angiotensinogen as compared with the oxidised form. This is in line with the experimental data presented by Zhou *et al.* that showed renin had differential binding affinities for the two forms, with a fourfold increase in renin-binding affinity in the presence of the (P)RR with oxidised angiotensinogen only.[1] The differential binding affinity of anti-AGT mAb for the two redox forms of angiotensinogen could also be explained in part by these increased dynamics. The anti-AGT mAb displayed a higher affinity for the reduced form compared with the oxidised

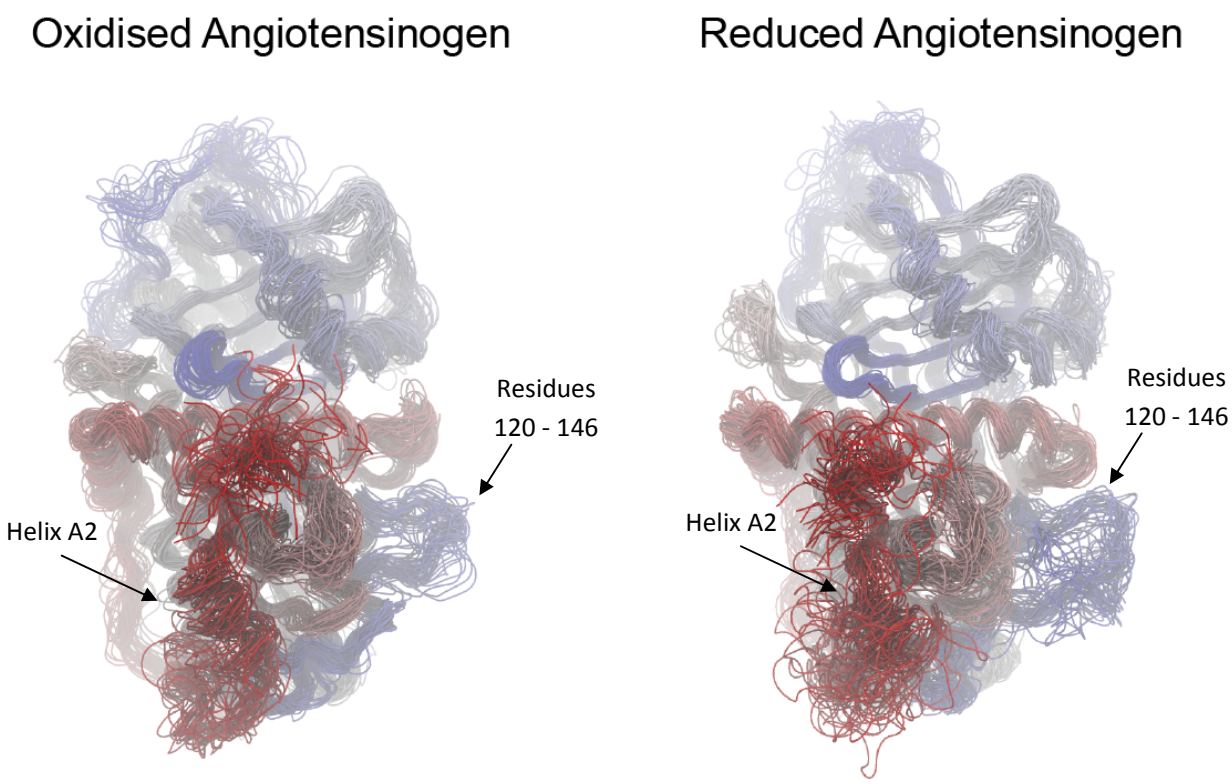


*Figure 5.13:*

*The top 50 clustered conformations of reduced and oxidised human angiotensinogen over MD simulation trajectories of 500 ns. The structures are coloured by residue index from red to blue.*

form, and this may be due to the more dynamic reduced form being more readily able to present the antibody with its epitope in a favourable conformation for binding, compared with the oxidised form in its constrained conformation.

Furthermore, Zhou *et al.* identified that helix C and the CD-loop of angiotensinogen make contact with the N-terminal lobe of renin in the renin-angiotensinogen bound complex,[1] and since both of these regions were found to be more dynamic in the reduced state, it seems likely that these dynamic areas may disrupt binding of reduced angiotensinogen to renin. As these simulations were being carried out, Brás *et al.* published work in which they performed computational alanine scanning mutagenesis on the structure of bound renin and angiotensinogen

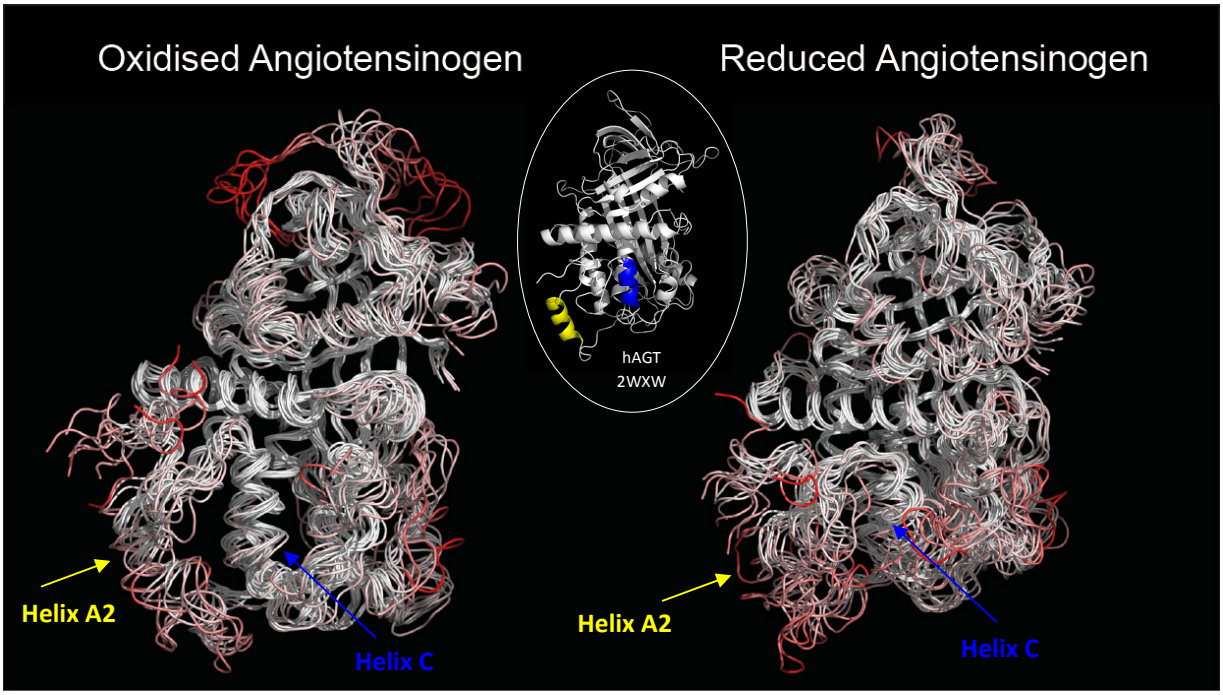


*Figure 5.14:*

*Simulation snapshots taken every 50 ns for reduced and oxidised human angiotensinogen over a MD simulation trajectory of 500 ns. The structures are coloured by RMSD from the average residue position, from white being 0 Å to red being ≥ 6 Å. The starting angiotensinogen structure is shown inset for comparison with helix A2 in yellow and helix C in blue.*

(PDB 2X0B) on all residues that are found at the interface between the two proteins when bound.[199] This approach enabled them to quickly identify residues (termed hot and warm spots) that were important for binding interactions, as mutation to alanine resulted in significant increases in the binding free energies.[199] Interestingly, of the eight hot spot residues on angiotensinogen that they identified, six of these were also found to be more dynamic in the reduced form of angiotensinogen in the MD simulations presented here. In addition, five of the ten warm spot residues were found to be more dynamic in reduced angiotensinogen, while a further three of these ten warm spots were less dynamic in the reduced form compared with oxidised. Thus, loss of angiotensinogen's disulfide bridge results in increased dynamics in

reduced angiotensinogen in regions containing many interfacial residues that are critical for forming binding interactions with renin.

The MD simulations presented here for reduced and oxidised angiotensinogen clearly demonstrate that breakage of the disulfide bond which exists between Cys 18 and Cys 138 in angiotensinogen results in more dynamic regions within the protein structure, as well as disruption of secondary structure in regions that are critical for forming binding interactions on complex with renin. Although the overall dynamics of each redox state are similar, a closer look at the residues in the trajectories reveals quite distinct differences in the dynamics between the two forms. Thus, these trajectories provide a tentative explanation as to the reported differential binding affinity of renin for the reduced and oxidised forms of angiotensinogen, and also suggest that the increased dynamics of the reduced protein's structure may free up and present the anti-AGT mAb's binding epitope more readily than the oxidised form of angiotensinogen is capable, resulting in the antibody having a higher affinity for reduced angiotensinogen when tested using the SPR bioassay.

## 5.5 SUMMARY

In summary, this chapter presents an investigation into the reduced and oxidised forms of angiotensinogen, and the differences that exist between these two forms. Angiotensinogen was shown to be predominantly expressed in the disulfide bonded oxidised form when produced recombinantly in *E. coli*. These two forms can also be reliably and reproducibly differentiated using an antibody-based SPR assay for angiotensinogen. This assay demonstrated that the two redox states were shown to differ significantly in both their association and dissociation rates to the anti-AGT mAb antibody, and thus the antibody displays differential binding affinity for the two forms—a significant step toward the development of a diagnostic bioassay. To elucidate the mechanisms underlying the observed differences between the reduced and oxidised forms,

molecular dynamic simulations were carried out and strikingly revealed that reduced angiotensinogen is more dynamic in regions critical for renin binding, as a result of the loss of the crucial disulfide bond between Cys 18 and Cys 138.

# *Chapter Six*

# DISCUSSION

## 6.1 PRODUCTION OF RECOMBINANT HUMAN ANGIOTENSINOGEN

Successful expression and purification of recombinant angiotensinogen was achieved from a bacterial expression system after much trial and error using the SUMO fusion tag; an approach that had been undertaken before by others.[1] Although this approach allowed the isolation of native recombinant angiotensinogen following tag cleavage using SUMO Protease, the cleavage reaction also unintentionally resulted in the loss of the disulfide bond between Cys 18 and Cys 138 due to the DTT present in the protease buffer that was required for the activity of the protease. This, coupled with the cost of the SUMO protease, led to the decision to leave the tag intact on the angiotensinogen protein so that the angiotensinogen would be in the desired oxidised form. This could have perhaps perturbed the tertiary structure of the angiotensinogen protein, particularly as the tag was attached to the N-terminus of angiotensinogen—the business end of the protein molecule.

Evidence of potential perturbation to protein structure was seen in the deviation of the SUMO-AGT binding kinetics compared with the simple 1:1 Langmuir binding observed for His-tagged angiotensinogen in the antibody-based SPR assay. Although the SUMO tag itself does not appear to interact with the anti-AGT mAb surface (no interactions were observed with SUMO-CAT), this does not rule out the impact that the SUMO tag may be having on the tertiary structure of the angiotensinogen protein. The SUMO fusion tag is relatively large (11 kDa) when compared to the size of angiotensinogen (50 kDa) and it is unknown how these two proteins may be interacting, as it is possible that the SUMO protein could be packing against the angiotensinogen protein surface. Further structural characterisation will need to be undertaken to

further elucidate whether the SUMO protein is altering the angiotensinogen protein in any way, and thus whether the SUMO-tagged angiotensinogen protein is an appropriate substitute to be working with in terms of the protein being representative of native angiotensinogen. X-ray crystallography, small angle x-ray scattering, and dynamic light scattering studies on SUMOylated angiotensinogen may shed more light in this regard.

One solution to this, of course, would be to express angiotensinogen either untagged or with a smaller tag, such as a His-tag, that would be far less likely to have an impact in terms of altering angiotensinogen's reactivity or perturbing the tertiary structure of angiotensinogen. The expression trials carried out during this work found the His-tagged version of angiotensinogen (from pET_16b_AGT construct) to be completely insoluble, while the untagged version was not found to overexpress from the pETDuet plasmid. These expression trials were not exhaustive however and several more approaches could have been trialled if more time had been permitted. The addition of 1% glucose was found to greatly increase the solubility of SUMOylated angiotensinogen, but was not trialled for the expression of angiotensinogen from the pET_16b_AGT and pETDuet_DsbC_AGT constructs, and is an approach that may have been helpful in these cases as well. Another approach not trialled was expression at lower temperatures, which results in slower expression, facilitating more time for correct protein folding. Expression of the protein from other DNA constructs may also have been another way to achieve soluble angiotensinogen, and many different plasmids are now commercially available, including plasmids that facilitate co-expression of the protein of interest with chaperone proteins that greatly aid in the production of correctly folded protein. In addition, only the *E. coli* bacterial expression system was tried, but more success may have been achieved with a eukaryotic expression system.

Overall, despite the difficulties, this work demonstrates that pure recombinant non-glycosylated human angiotensinogen (predominantly in the oxidised form) can be successfully

expressed and purified from bacterial cells using the SUMO fusion tag. Cleavage of the SUMO tag can be carried out if downstream applications requires native untagged angiotensinogen, but this tag removal does also result in the loss of the critical disulfide bond between Cys 18 and Cys 138, which was undesirable and thus was avoided in this work by leaving the tag intact.

## 6.2 Assay Development and Validation of Results

Working with a mouse monoclonal antibody raised against human angiotensinogen, it was possible to develop a sensitive and reproducible SPR assay for angiotensinogen that displayed nanomolar affinity for recombinant non-glycosylated human angiotensinogen. Although this is not a particularly high affinity for a monoclonal antibody (picomolar and even femtomolar affinities for antibodies have been reported),[200] this affinity is within the ideal range for measurement using SPR.[201] Binding of the antibody surface to His-tagged angiotensinogen resulted in a simple 1:1 Langmuir binding mechanism being observed, allowing facile kinetic fitting of a binding model to the measured data. The binding of an antigen to a monoclonal antibody would be expected to display simple 1:1 binding due to the antibody recognizing a single epitope on the antigen's surface. Thus, it was interesting that the binding responses measured when SUMOylated angiotensinogen bound the antibody surface deviated from the simple 1:1 binding model. Rather, the binding responses fit well to a surface heterogeneity model, but as discussed in Chapter Four it is difficult to know if this binding model accurately represents the binding events occurring at the sensor chip surface. It is highly possible that the SUMO tag is altering the tertiary structure of angiotensinogen, or perhaps associating with angiotensinogen in such a way that the epitope is being shielded, altering the binding kinetics or partially preventing binding altogether. Interestingly enough, the 1:1 Langmuir binding model, and the 1:1 mass transport binding model, despite not describing the measured binding data well, returned $K_D$ values of approximately 140 nM—very similar to the $K_D$ value of 150 nM obtained

for the same binding responses when fit to the surface heterogeneity model. These values are all in good accordance with those obtained for oxidised angiotensinogen, further evidence in support of the recombinant angiotensinogen existing in the disulfide bridged oxidised form prior to exposure to a reducing agent.

One limitation that slowed assay development was the availability of large amounts of recombinant angiotensinogen, particularly in the optimisation steps of the SPR assay that consumed a considerable amount of protein. If more protein had been readily available (being plagued with protein insolubility meant that in-house expression of SUMO-AGT was only achieved in the final months of this project), ligand saturation by using higher concentrations of analyte could have been obtained. Ligand saturation means that the ligand surface has reached its maximum binding capacity, which would allow more accurate fitting of kinetic models and also provides an additional means for obtaining $K_D$ values by equilibrium analysis for the interaction between the antibody and angiotensinogen. This would provide a further validation of the kinetic results if equilibrium and kinetic analysis yield the same $K_D$ values.

Careful experimental design was undertaken to ensure that the SPR results obtained were reliable and could be readily reproduced when measuring the binding responses of reduced and oxidised angiotensinogen to the antibody surface. The analyte binding responses were measured on four independent ligand surfaces that had very similar levels of immobilised antibody, which served as separate replicates. Each channel generated very similar results indicating that this assay is highly reproducible. In addition, each concentration of analyte was injected at least twice across each ligand surface, with each replicate injection taking place in a different analyte channel. The replicates overlaid well for each concentration despite the noisiness of the curves, again providing strong evidence that this assay is able to generate reliable data over several injection cycles. Each dataset was analysed independently using two different software programs; the two programs generated the same kinetic results and the results were very

concordant between the four antibody surfaces, suggesting that the results for reduced angiotensinogen and oxidised angiotensinogen are accurate. The correct fitting of the kinetic models were further verified by carrying out Monte Carlo analysis on each dataset, which revealed that the kinetic rate constants could be reliably fitted to the measured data irrespective of the starting parameter values and random short term noise.

Switching the analyte and ligand is another good check to validate the kinetic results obtained, but unfortunately the timeframe of this project did not permit further validation of the results in this manner. In this approach, angiotensinogen would be immobilised to the sensor chip surface and anti-AGT mAb antibody would be used as the analyte. If the binding responses observed during this set up were in good accordance with the results presented here, this would provide very good evidence that these results are an accurate representation of the interactions taking place between the antibody and angiotensinogen in its respective redox forms. Care would need to be taken though when carrying out such a swap of binding partners, if this was an approach pursued in the future to validate the present results. The antibody, being a far larger protein, could quite possibly be subject to mass transport effects so careful experimental design would be needed to minimise these effects. In addition, the MD simulation results presented in Chapter Five demonstrate that there are clear differences in the dynamics between the two forms of angiotensinogen. Whether these dynamic differences would be permitted to occur when immobilised to a sensor chip surface is unknown, and it may be that a capture approach or an alternative method to amine coupling may need to be used for immobilisation, as was found to be the case with renin.

## 6.3 Differences between Reduced and Oxidised Angiotensinogen

Reaction with mPEG clearly demonstrated that, similar to eukaryotic expression, angiotensinogen produced recombinantly in a bacterial expression system (SUMO-AGT) is

expressed predominantly in the oxidised form with the disulfide bond intact, which is supported by the SPR data obtained. Exposure to reducing agent was also shown to be capable of breaking this disulfide bond, allowing all four cysteine residues to be free to conjugate with mPEG. Binding of PEG to the SDS micelles during SDS-PAGE electrophoresis did unfortunately mean that accurate determination of the size of each of the mPEG-angiotensinogen conjugates was not possible, other than a clear increase in protein molecular weight on conjugation with mPEG being visible, an observation that has been reported previously in the literature.[193, 202] If more time had been permissible, the experiment could have been repeated, and the gels run with a much lower concentration of SDS in the running buffer, which was shown by Odom *et al.* to completely eliminate the aberrant migration caused by PEG present in the protein samples.[193]

From the results described in Chapter Five, it is clear that there are distinct differences between reduced and oxidised angiotensinogen. The SPR assay using the mouse monoclonal antibody was able to make a distinction between the two redox forms by displaying differential affinity for the two forms, due to differences in both the association and dissociation rates—differences that were shown to be highly significant. As mentioned previously, the epitope of the R & D Systems antibody used in the assay has not been determined, thus it can only be speculated as to the epitope on angiotensinogen that the antibody recognises, since the antibody was raised against a full length glycosylated human angiotensinogen immunogen. Given that the antibody displays differential binding affinity for the two redox forms of angiotensinogen, it is likely that this epitope may lie in the region surrounding the N-terminus or perhaps in one of the other regions that MD simulations revealed had different dynamics in each of the redox states. The antibody has a higher affinity for reduced angiotensinogen ($K_D$ = 103.1 nM compared with 159 nM for oxidised), the redox form that displayed more dynamic regions in the MD simulations, particularly in the regions surrounding the N-terminus and the Cys 18 and Cys 138 residues that form the disulfide bond. It may be that increased dynamics in the epitope region

mean there is less constraint when binding the antibody, and could in fact present the epitope to the antibody in a much more favourable conformation facilitating facile and tighter binding than the more constrained oxidised form of angiotensinogen is capable of. Determining the epitope on angiotensinogen that is bound by the antibody is a further avenue that does need to be addressed in future research, perhaps by methods such as tryptic digest.

The distinct dynamic differences between the two redox forms of angiotensinogen elucidated by MD simulation trajectories reveal a clear mechanistic explanation for the differential binding of the two forms by renin that has been reported,[1] an idea that had already been hinted to in the literature. The increased dynamics in regions of angiotensinogen that form crucial contacts with renin on binding mean that the loss of the Cys 18 and Cys 138 disulfide bond likely disrupts the binding of renin to angiotensinogen. This is because several regions in reduced angiotensinogen are more dynamic and less likely to form the critical interfacial contacts required for binding to renin. It certainly would have been interesting to carry out the MD simulations on renin with reduced or oxidised angiotensinogen to further elucidate the reasoning behind renin's differential binding of the two forms. However, because it would be a much bigger system being simulated, these simulations would require a considerable amount of time and resources that was beyond the scope of this master's project. Further optimisation of the SPR assay using renin, if time had permitted, could have also facilitated the interaction between renin and the two redox forms of angiotensinogen to be studied.

## 6.4 Implications for the Development of a Diagnostic Bioassay for Pre-eclampsia

Finally, the implications of the results presented here need to be considered in light of the development of a diagnostic bioassay for pre-eclampsia. The fact that an SPR-based assay for angiotensinogen now exists that displays differential binding affinity for the two redox states of

angiotensinogen, allowing them to be distinguished experimentally, is a significant step towards the development of a diagnostic bioassay. Because such a diagnostic assay would ideally involve the testing of plasma samples, the results presented here do raise some important considerations. Firstly, the concentration of angiotensinogen in plasma is approximately 0.8 μM,[3] which falls well within the range of angiotensinogen concentrations tested in the SPR assay, making the assay ideal for measuring the plasma levels of angiotensinogen as they fall within the detectable limits of the assay. This assay was only tested on homogeneous reduced or oxidised angiotensinogen however, and whether the subtle differences between the two forms would be still be distinguishable in samples where both reduced and oxidised forms of angiotensinogen are present remains to be elucidated.

In addition, plasma proteins are glycosylated and angiotensinogen is no exception. Human angiotensinogen contains four sites of *N*-glycosylation, and two of which are located at Asn 14 and Asn 137 in close proximity to the two cysteine residues involved in disulfide bond formation.[21] Thus, it remains to be investigated as to whether glycosylated angiotensinogen will have any effect on the developed assay as it was only tested on non-glycosylated angiotensinogen. The immunogen used to raise these monoclonal antibodies in mice was a glycosylated form of human angiotensinogen, and since the antibody has been shown to bind to the non-glycosylated form of angiotensinogen, it is unlikely the epitope encompasses the glycosyl residues on the exterior of the protein. Nonetheless, it is unknown whether these glycosyl residues will mask the differential binding displayed for reduced and oxidised angiotensinogen and hence the sensitivity of the assay, and thus, this will require further enquiry.

Plasma samples are composed of a large variety of proteins, and this assay was developed using pure protein samples, so testing will need to be undertaken to ensure that no non-specific binding from other plasma proteins occurs, which would certainly complicate the binding responses obtained. R & D Systems have already tested the cross-reactivity of the antibody with

other human serpins (product datasheet) and the antibody was not found to cross-react with any of the other proteins that have a similar structure, which is promising but is another consideration that needs to be made, and careful choice of an appropriate reference surface, perhaps by employing the interspot referencing that is a handy feature of the ProteOn$^{TM}$ XPR36, will need to made to ensure accurate and reproducible results are obtained.

Finally a good diagnostic bioassay will only be a viable commercial product if it is low-cost and will continue to generate consistent and reliable results for many samples over a good length of time. The stability of the anti-AGT mAb surface was not tested while this work was being undertaken, but is certainly something that would need to be carried out if this assay was continuing in assay development. However, the assay was reproducible and did give accurate replicable results over several injection runs while data collection was being undertaken. In addition, sensor chips, containing immobilised anti-AGT mAb ligand, that had been removed from the SPR and stored in the refrigerator, still displayed high levels of activity towards angiotensinogen when used again after several months, indicating that the antibody surface is relatively stable and would allow the collection of data for many samples. Although, the initial cost of buying a chip with immobilised antibody would be relatively costly, the cost would be balanced out if many samples could be tested on the same surface without significant loss of activity—it would certainly be a cost-effective method for quickly testing samples, and testing all samples on the same surface would ensure little variation in the results obtained from the entire pool of samples tested. Although the bioassay presented here could be adapted for a number of SPR instruments commercially available, an added bonus of employing the ProteOn$^{TM}$ XPR36 is that up to six samples can be tested simultaneously, greatly increasing the throughput when a large number of blood samples need to be screened in a timely manner.

In conclusion, the antibody-based SPR bioassay for reduced and oxidised angiotensinogen presented here shows good potential as a diagnostic test, but further studies will

need to be conducted to ensure that it is suitable and meets the scrutiny required as a diagnostic bioassay to measure levels of reduced and oxidised angiotensinogen in a clinical diagnostic setting to identify women prone to developing pre-eclampsia.

## 6.5 FINAL REMARKS

With all research there tends to be so many stones left unturned at the conclusion of a given project, and this project is no exception. With more time, it certainly would have been nice to tick off some of the experiments on the list, but this was not so in this case. Perhaps just as important as the results of this project is everything that has been learnt along the way. Many of the experiments underlying the results presented here did not work first time around but, in the end, persistence was the key to success. Looking back, I'm extremely thankful for all the stumbling blocks and learning curves along the way, as it was these experiences that taught me the most, and led me to learn new techniques and take the project into previously unexpected directions—which is, in a sense, exactly what undertaking a thesis is all about.

## *Chapter Seven*

# CONCLUSION

This project began with the main goal of developing a method to experimentally distinguish between the two redox states of angiotensinogen, states that are mediated by the disulfide bridge that exists between Cys 18 and Cys 138. These two forms exist in the plasma pool of healthy individuals in a stable ratio of 60:40 (oxidised to reduced, respectively) regardless of age and gender.[1] Women who develop pre-eclampsia, a pregnancy condition that can be life-threatening for both mother and child and a leading cause of pre-mature births, display an alteration to this tight balance of reduced and oxidised angiotensinogen, and actually have a higher proportion of oxidised angiotensinogen in their plasma. This could have important clinical and physiological implications, especially in light of the findings that renin displays differential binding affinity for the two redox forms in the presence of the (P)RR with a four-fold higher catalytic efficiency for oxidised angiotensinogen.[1] Thus, this alteration of the rate-limiting step of a pathway responsible for the regulation of blood pressure provides a direct mechanistic link as to the exacerbation, or even potentially causative nature, of the pathophysiology of pre-eclampsia.

With this in mind, the undertaking of this thesis aimed from the outset to investigate angiotensinogen's redox switch, and attempt to distinguish between the two forms, which differ only in the presence or absence of a disulfide bond. In order to do this, angiotensinogen was recombinantly expressed using the SUMO fusion system, and an SPR-based assay was developed that made use of a monoclonal antibody to detect angiotensinogen. A second SPR-assay using renin was also developed that served as a proof of concept that the binding between angiotensinogen and renin can be investigated using SPR by utilising a direct coupling method of immobilisation.

The antibody-based SPR assay was reproducible, and was able to generate reliable binding responses over multiple injection cycles, and using this assay it was possible to demonstrate that reduced and oxidised angiotensinogen bind to this antibody with differential affinity, due to significant differences in both the association and dissociation rates of the two forms with the anti-AGT mAb. Further elucidation of the intricate differences existing between the redox states were strikingly revealed by molecular dynamic simulations, which showed that loss of the disulfide bridge between Cys 18 and Cys 138 results in increased dynamics in regions crucial for forming important binding contacts with renin.

The results presented in this thesis are thus a significant step towards the development of a diagnostic assay for angiotensinogen to identify women prone to pre-eclampsia, and provides a sensitive assay capable of distinguishing the redox states of angiotensinogen. More work is still required to be undertaken to assess the viability of this assay in a clinical diagnostic setting, but the work outlined in this thesis thus far certainly highlights its potential.

## *Appendix*

# RECIPES AND BUFFERS

## I SDS-PAGE RECIPES:

### *A) Sample Reducing Dye:*

| SAMPLE REDUCING DYE | VOLUME |
|---|---|
| Bolt™ LDS Sample Buffer (4X) | 25 µL |
| Bolt™ Reducing Agent (10X) | 10 µL |
| MQ water | 15 µL |
| Total Volume | 50 µL |

Mix well, and store aliquots at –20 °C.

### *B) Coomassie Blue Stain:*

| COOMASSIE BLUE STAIN | WEIGHT OR VOLUME |
|---|---|
| MQ water | 225 mL |
| Methanol | 225 mL |
| Glacial Acetic Acid | 50 mL |
| Coomassie Blue | 0.5 g |
| Total Volume | 500 mL |

Mix together with a magnetic stirrer until Coomassie Blue is completely dissolved. Store stain at room temperature.

### *C) Destain Solution (20% Methanol, 10% Acetic Acid):*

| SAMPLE REDUCING DYE | VOLUME |
|---|---|
| MQ water | 700 mL |
| Methanol | 200 mL |
| Glacial Acetic Acid | 100 mL |
| Total Volume | 1000 mL |

Mix well, and store solution at room temperature.

## II DNA Gel Electrophoresis:

### *A) 6X DNA Loading Dye (0.25% w/v bromophenol blue, 30% v/v glycerol)*

| 6X DNA Loading Dye | Weight or Volume |
|---|---|
| Glycerol | 3 mL |
| Bromophenol Blue | 25 mg |
| MQ water | up to 10 mL |
| Total Volume | 10 mL |

Mix well until all bromophenol blue is dissolved. Store solution at 4°C for several weeks or store aliquots at –20 °C.

### *B) 50X Tris Acetate EDTA (TAE) Buffer:*

| 50X TAE Buffer | Weight or Volume |
|---|---|
| Tris Base | 242 g |
| Glacial Acetic Acid | 57.1 mL |
| 0.5 M EDTA pH 8.0 | 100 mL |
| MQ water | up to 1 L |
| Total Volume | 1 L |

Store 50X buffer at 4°C. Prepare 1X TAE buffer by combining 20 mL TAE (50X) with 980 mL MQ water and mixing well. Final 1X TAE buffer is 40 mM Tris acetate and 1 mM EDTA.

## III *o*-Phthalaldehyde (OPA) Assay Reagent:

1.25 g of boric acid was dissolved in approximately 30 mL of MQ water, and then the pH was adjusted to 10.4 with potassium hydroxide. Then, the following were added to the basic boric acid solution:

| OPA ASSAY REAGENT | VOLUME |
|---|---|
| Boric acid solution pH 10.4 (as above) | 30 mL |
| Tween-20 | 150 µL |
| 2-Mercaptoethanol | 150 µL |
| *o*-Phthalaldehyde dissolved in 1 mL methanol | 1 mL |
| MQ water | up to 50 mL |
| Total Volume | 50 mL |

Mix well and keep reagent at room temperature, protected from light. This reagent needs to be used immediately so must be prepared fresh, just before performing the assay. The reagent solution contains 0.4 M boric acid, 0.03% v/v Tween-20, 0.03% v/v 2-mercaptoethanol, 6 mM OPA at pH 10.4.

## IV Media:

### *A) SOC Media*

| SOC RECOVERY MEDIA | WEIGHT OR VOLUME |
|---|---|
| Tryptone | 2 g |
| Yeast Extract | 0.5 g |
| 1 M NaCl | 1 mL |
| 1 M KCl | 0.25 mL |
| 1 M $MgCl_2$ | 1 mL |
| 1 M $MgSO_4$ | 1 mL |
| MQ water | up to 100 mL |
| Total Volume | 100 mL |

Mix well, and then sterilise by autoclaving for 20 minutes at 121 °C. Allow to cool, then aseptically add 2 mL of 1 M glucose solution (filter sterilised), and mix well. Working aseptically, aliquot SOC media out into Eppendorf tubes and store in freezer at –20 °C.

### *B) TB Media*

| TB MEDIA | WEIGHT OR VOLUME |
|---|---|
| Tryptone | 12 g |
| Yeast Extract | 24 g |
| Glycerol | 4 mL |
| MQ water | up to 900 mL |
| Total Volume | 900 mL |

| POTASSIUM PHOSPHATE SOLUTION | WEIGHT OR VOLUME |
|---|---|
| $KH_2PO_4$ | 23.1 g |
| $K_2HPO_4$ | 125.4 g |
| MQ water | up to 1 L |
| Total Volume | 1 L |

Make up the TB media and the potassium phosphate solutions separately, and sterilise each by autoclaving for 20 minutes at 121 °C. Once cool, add 100 mL of the potassium phosphate solution to the TB media aseptically and mix well.

### *C) 2*TY Media*

| TB MEDIA | WEIGHT OR VOLUME |
|---|---|
| Tryptone | 16 g |
| Yeast Extract | 10 g |
| NaCl | 5 g |
| MQ water | up to 1L |
| Total Volume | 1 L |

Dissolve and mix well. Sterilise media by autoclaving for 20 minutes at 121 °C.

## V Buffers

### *A) PBS*

Five PBS tablets (Sigma-Aldrich, St. Louis, Missouri, USA) were dissolved in 1 L of MQ water to give a buffer containing 0.01 M phosphate buffer, 2.7 mM potassium chloride, and 137 mM sodium chloride. For purification, imidazole was added at a concentration of 10 mM (68 mg) for washing or at concentrations of 50 mM (340 mg), and 150 mM (1.02 g) for elution. The pH was altered to either 7.2 or pH 7.4 as required. The buffer was filtered and stored at 4 °C.

### *B) PBST (Phosphate buffered Saline with Tween-20)*

| PBST BUFFER | WEIGHT OR VOLUME |
|---|---|
| NaCl | 8 g |
| KCl | 0.2 g |
| $Na_2HPO_4$ | 1.44 g |
| $KH_2PO_4$ | 0.24 g |
| Tween-20 | 50 µL |
| MQ water | up to 1L |
| Total Volume | 1 L |

Dissolve well in approximately 900 mL MQ water, and adjust pH to 7.4 to give a buffer containing 137 mM NaCl, 3 mM KCl, 10 mM $Na_2HPO_4$, 2 mM $KH_2PO_4$, and 0.005% Tween-20. Make volume up to 1 L with MQ water and mix well. Filter, sonicate for 20 minutes, and store buffer at 4 °C.

### *C) Tris Buffer*

| TRIS BUFFER | WEIGHT OR VOLUME |
|---|---|
| Tris Base | 1.21 g |
| NaCl | 29.22 g |
| MQ water | up to 1L |
| Total Volume | 1 L |

Dissolve well in approximately 900 mL MQ water, and adjust pH to 7.4. Make volume up to 1 L with MQ water and mix well. Filter, and store buffer at 4 °C. Final buffer is 10 mM Tris, and 0.5 M NaCl at pH 7.4.

### *D) Lysis Buffer*

| LYSIS BUFFER | WEIGHT OR VOLUME |
|---|---|
| 1 M $KH_2PO_4$ | 3 mL |
| 1 M $K_2HPO_4$ | 47 mL |
| NaCl | 23 g |
| KCl | 7.5 g |
| Glycerol | 100 mL |
| Triton X-100 | 5 mL |
| Imidazole | 68 mg |
| MQ water | up to 1L |
| Total Volume | 1 L |

Mix well in approximately 800 mL MQ water until completely dissolved. Adjust pH to 7.8 with HCl, and bring volume up to 1 L with MQ water, and mix well. Filter buffer and store buffer at 4 °C. Final buffer is 50 mM potassium phosphate, 400 mM sodium chloride, 100 mM potassium chloride, 10% glycerol, 0.5% Triton X-100, and 10 mM imidazole at pH 7.8.

## *Chapter Eight*

# REFERENCES


1. Zhou A, Carrell RW, Murphy MP, Wei Z, Yan Y, Stanley PLD, Stein PE, Pipkin FB, Read RJ, *A redox switch in angiotensinogen modulates angiotensin release*, Nature 2010, 468: 108-111
2. Turnbull H, *The correspondence of Isaac Newton 1661-1675* Edited by Turnbull H. Cambridge, England, published for the Royal Society by University Press, 1959, p.pp. 416
3. Carrell R, Qi X, Zhou A, *Serpins as hormone carriers: Modulation of release*. Methods in Enzymology 2011, 501: 89-103
4. Sibai B, Dekker G, Kupferminc M, *Pre-eclampsia*, Lancet 2005, 365: 785-799
5. Forest J-C, Charland M, Massé J, Bujold E, Rousseau F, Lafond J, Giguère Y, *Candidate biochemical markers for screening of pre-eclampsia in early pregnancy*, Clinical Chemistry & Laboratory Medicine 2012, 50: 973-984
6. Inoue I, Rohrwasser A, Helin C, Jeunemaitre X, Crain P, Bohlender J, Lifton RP, Corvol P, Ward K, Lalouel JM, *A mutation of angiotensinogen in a patient with preeclampsia leads to altered kinetics of the renin-angiotensin system*, Journal of Biological Chemistry 1995, 270: 11430-11436
7. Langer A, Villar J, Tell K, Kim T, Kennedy S, *Reducing eclampsia-related deaths - a call to action*, The Lancet 2008, 371: 705-706
8. Van Dijk MG, Díaz Olavarrieta C, Zuñiga PU, Gordillo RL, Gutiérrez MER, García SG, *Use of magnesium sulfate for treatment of pre-eclampsia and eclampsia in Mexico*, International Journal of Gynecology and Obstetrics 2013, 121: 110-114
9. Irani RA, Xia Y, *Renin Angiotensin Signaling in Normal Pregnancy and Preeclampsia*, Seminars in Nephrology 2011, 31: 47-58
10. Hirshfeld-Cytron J, Lam C, Karumanchi SA, Lindheimer M, *Late postpartum eclampsia: Examples and review*, Obstetrical and Gynecological Survey 2006, 61: 471-480
11. Valensise H, Novelli GP, Vasapollo B, *Pre-eclampsia, One name, two conditions - The case for early and late disease being different*, Fetal and Maternal Medicine Review 2013, 24: 32-37
12. Huppertz B, *Placental origins of preeclampsia: Challenging the current hypothesis*, Hypertension 2008, 51: 970-975
13. Duley L, T*he Global Impact of Pre-eclampsia and Eclampsia*, Seminars in Perinatology 2009, 33: 130-137
14. Moodley J, *Maternal deaths due to hypertensive disorders in pregnancy: Saving Mothers report 2002-2004*, Cardiovascular Journal of Africa 2007, 18: 358-361
15. Barton JR, Istwan NB, Rhea D, Collins A, Stanziano GJ, *Cost-savings analysis of an outpatient management program for women with pregnancy-related hypertensive conditions*, Disease Management 2006, 9: 236-241
16. Costantine MM, Cleary K, *Pravastatin for the prevention of preeclampsia in high-risk pregnant women*, Obstetrics and Gynecology 2013, 121: 349-353

17. Wilson BJ, Watson MS, Prescott GJ, Sunderland S, Campbell DM, Hannaford P, Smith WCS, *Hypertensive diseases of pregnancy and risk of hypertension and stroke in later life: Results from cohort study*, British Medical Journal 2003, 326: 845-849

18. Giguère Y, Charland M, Thériault S, Bujold E, Laroche M, Rousseau F, Lafond J, Forest JC, *Linking preeclampsia and cardiovascular disease later in life*, Clinical Chemistry and Laboratory Medicine 2012, 50: 985-993

19. Scott BB, *Development in inhibitors of the aspartyl protease renin for the treatment of hypertension*, Current Protein and Peptide Science 2006, 7: 241-254

20. Weber MA, *The 24-hour blood pressure pattern: Does it have implications for morbidity and mortality?*, American Journal of Cardiology 2002, 89: 27A-33A

21. Gimenez-Roqueplo AP, Célérier J, Lucarelli G, Corvol P, Jeunemaitre X, *Role of N-glycosylation in human angiotensinogen*, Journal of Biological Chemistry 1998, 273: 21232-21238

22. Dickson ME, Sigmund CD, *Genetic basis of hypertension: Revisiting angiotensinogen*, Hypertension 2006, 48: 14-20

23. Wood JM, Maibaum J, Rahuel J, Grütter MG, Cohen NC, Rasetti V, Rüger H, Göschke R, Stutz S, Fuhrer W, Schilling W, Rigollier P, Yamaguchi Y, Cumin F, Baum HP, Schnell CR, Herold P, Mah R, Jensen C, O'Brien E, Stanton A, Bedigian MP, *Structure-based design of aliskiren, a novel orally effective renin inhibitor*, Biochemical and Biophysical Research Communications 2003, 308: 698-705

24. Kearney PM, Whelton M, Reynolds K, Muntner P, Whelton PK, He J, *Global burden of hypertension: Analysis of worldwide data*, Lancet 2005, 365: 217-223

25. Cohen P, Badouaille G, Gimenez-Roqueplo AP, Mani JC, Guyene TT, Jeunemaitre X, Menard J, Corvol P, Pau B, Simon D, *Selective recognition of M235T angiotensinogen variants and their determination in human plasma by monoclonal antibody-based immunoanalysis*, Journal of Clinical Endocrinology and Metabolism 1996, 81: 3505-3512

26. Caulfield M, Lavender P, Farrall M, Munroe P, Lawson M, Turner P, Clark AJL, L*inkage of the angiotensinogen gene to essential hypertension*, New England Journal of Medicine 1994, 330: 1629-1633

27. Jeunemaitre X, Soubrier F, Kotelevtsev YV, Lifton RP, Williams CS, Charru A, Hunt SC, Hopkins PN, Williams RR, Lalouel JM, Corvol P, *Molecular basis of human hypertension: Role of angiotensinogen*, Cell 1992, 71: 169-180

28. Dealwis CG, Frazao C, Badasso M, Cooper JB, Tickle IJ, Driessen H, Blundell TL, Murakami K, Miyazaki H, Sueiras-Diaz J, Jones DM, Szelke M, *X-ray analysis at 2.0 Å resolution of mouse submaxillary renin complexed with a decapeptide inhibitor CH-66, based on the 4-16 fragment of rat angiotensinogen*, Journal of Molecular Biology 1994, 236: 342-360

29. Walker WG, Whelton PK, Saito H, Russell RP, Hermann J, *Relation between blood pressure and renin, renin substrate, angiotensin II, aldosterone and urinary sodium and potassium in 574 ambulatory subjects*, Hypertension 1979, 1: 287-291

30. Gardes J, Bouhnik J, Clauser E, Corvol P, Menard J, *Role of angiotensinogen in blood pressure homeostasis*, Hypertension 1982, 4: 185-189

31. Menard J, El Amrani AIK, Savoie F, Bouhnik J, Lynch KR, Peach MJ, *Angiotensinogen: An attractive and underrated participant in hypertension and inflammation*, Hypertension 1991, 18: 705-707

32. Ohkubo H, Kawakami H, Kakehi Y, Takumi T, Arai H, Yokota Y, Iwai M, Tanabe Y, Masu M, Hata J, Iwao H, Okamoto H, Yokoyama M, Nomura T, Katsuki M, Nakanishi S, *Generation of transgenic mice with elevated blood pressure by introduction of the rat renin and angiotensinogen genes*, Proceedings of the National Academy of Sciences of the United States of America 1990, 87: 5153-5157

33. Fejerman L, Bouzekri N, Wu X, Adeyemo A, Luke A, Zhu X, Ward R, Cooper RS, *Association between evolutionary history of angiotensinogen haplotypes and plasma levels*, Human Genetics 2004, 115: 310-318

34. Sarver RW, Peevers J, Cody WL, Ciske FL, Dyer J, Emerson SD, Hagadorn JC, Holsworth DD, Jalaie M, Kaufman M, Mastronardi M, McConnell P, Powell NA, Quin Iii J, Van Huis CA, Zhang E, Mochalkin I, *Binding thermodynamics of substituted diaminopyrimidine renin inhibitors*, Analytical Biochemistry 2007, 360: 30-40

35. Danser AHJ, Deinum J, *Renin, prorenin and the putative (pro)renin receptor*, Hypertension 2005, 46: 1069-1076

36. Gossas T, Vrang L, Henderson I, Sedig S, Sahlberg C, Lindström E, Danielson UH, *Aliskiren displays long-lasting interactions with human renin*, Naunyn-Schmiedeberg's Archives of Pharmacology 2012, 385: 219-224

37. Fisher NDL, Hollenberg NK, I*s there a future for renin inhibitors?*, Expert Opinion on Investigational Drugs 2001, 10: 417-426

38. Hill CC, Pickinpaugh J, *Physiologic changes in pregnancy*, Surgical Clinics of North America 2008, 88: 391-401

39. Dusse LM, Rios DRA, Pinheiro MB, Cooper AJ, Lwaleed BA, *Pre-eclampsia: Relationship between coagulation, fibrinolysis and inflammation*, Clinica Chimica Acta 2011, 412: 17-21

40. Greer IA, *Thrombosis in pregnancy: Maternal and fetal issues*, Lancet 1999, 353: 1258-1265

41. Brown MA, Gallery EDM, Ross MR, Esber RP, *Sodium excretion in normal and hypertensive pregnancy: A prospective study*, American Journal of Obstetrics and Gynecology 1988, 159: 297-307

42. Daniels CR, Eisen V, Slater JD, *Reduced activation and affinity of renin during pregnancy and oral contraception: determination of kinetic parameters by a fully autologous plasma renin assay*, Advances in Experimental Medicine and Biology 1986, 198 Pt B: 463-469

43. Derkx FHM, Stuenkel C, Schalekamp MPA, *Immunoreactive renin, prorenin, and enzymatically active renin in plasma during pregnancy and in women taking oral contraceptives*, Journal of Clinical Endocrinology and Metabolism 1986, 63: 1008-1015

44. Yang J, Shang J, Zhang S, Li H, Liu H, *The role of the renin-angiotensin-aldosterone system in preeclampsia: Genetic polymorphisms and microRNA*, Journal of Molecular Endocrinology 2013, 50: R53-R66

45. Kar M, *Role of biomarkers in early detection of preeclampsia*, Journal of Clinical and Diagnostic Research 2014, 8: BE01-BE04

46. Verdonk K, Visser W, Van Den Meiracker AH, Danser AHJ, *The renin-angiotensin-aldosterone system in pre-eclampsia: The delicate balance between good and bad*, Clinical Science 2014, 126: 537-544

47. Mistry HD, Kurlak LO, Pipkin FB, *The placental renin-angiotensin system and oxidative stress in pre-eclampsia*, Placenta 2013, 34: 182-186

48. Mistry HD, Wilson V, Ramsay MM, Symonds ME, Pipkin FB, *Reduced selenium concentrations and glutathione peroxidase activity in preeclamptic pregnancies*, Hypertension 2008, 52: 881-888

49. Hung TH, Burton GJ, *Hypoxia and reoxygenation: A possible mechanism for placental oxidative stress in preeclampsia*, Taiwanese Journal of Obstetrics and Gynecology 2006, 45: 189-200

50. Redman CWG, Sargent IL, *Pre-eclampsia, the placenta and the maternal systemic inflammatory response - A review*, Placenta 2003, 24: S21-S27

51. Higuchi S, Ohtsu H, Suzuki H, Shirai H, Frank GD, Eguchi S, *Angiotensin II signal transduction through the AT1 receptor: Novel insights into mechanisms and pathophysiology*, Clinical Science 2007, 112: 417-428

52. Boutet M, Roland L, Thomas N, Bilodeau JF, *Specific systemic antioxidant response to preeclampsia in late pregnancy: the study of intracellular glutathione peroxidases in maternal and fetal blood*, American Journal of Obstetrics and Gynecology 2009, 200: 530.e531-530.e537

53. Rogers MS, Wang CCR, Tam WH, Li CY, Chu KO, Chu CY, *Oxidative stress in midpregnancy as a predictor of gestational hypertension and pre-eclampsia*, BJOG: An International Journal of Obstetrics and Gynaecology 2006, 113: 1053-1059

54. Bilodeau JF, Hubel CA, *Current concepts in the use of antioxidants for the treatment of preeclampsia*, Journal of Obstetrics and Gynaecology Canada: JOGC 2003, 25: 742-750

55. Ness RB, Sibai BM, *Shared and disparate components of the pathophysiologies of fetal growth restriction and preeclampsia*, American Journal of Obstetrics and Gynecology 2006, 195: 40-49

56. Zuleta-Tobón JJ, Pandales-Pérez H, Sánchez S, Vélez-Álvarez GA, Velásquez-Penagos JA, *Errors in the treatment of hypertensive disorders of pregnancy and their impact on maternal mortality*, International Journal of Gynecology and Obstetrics 2013, 121: 78-81

57. Abalos E, Duley L, Steyn DW, Henderson-Smart DJ, *Antihypertensive drug therapy for mild to moderate hypertension during pregnancy*, Cochrane Database of Systematic Reviews 2007, CD002252

58. Barton JR, Sibai BM, *Prediction and prevention of recurrent preeclampsia*, Obstetrics and Gynecology 2008, 112: 359-372

59. Conde-Agudelo A, Romero R, Kusanovic JP, Hassan SS, S*upplementation with vitamins C and E during pregnancy for the prevention of preeclampsia and other adverse maternal and perinatal outcomes: A systematic review and metaanalysis*, American Journal of Obstetrics and Gynecology 2011, 204: 503.e501-503.e512

60. Levine RJ, Hauth JC, Curet LB, Sibai BM, Catalano PM, Morris CD, DerSimonian R, Esterlitz JR, Raymond EG, Bild DE, Clemens JD, Cutler JA, Ewell MG, Friedman SA, Goldenberg RL, Jacobson SL, Joffe GM, Klebanoff MA, Petrulis AS, *Trial of calcium to prevent preeclampsia*, New England Journal of Medicine 1997, 337: 69-76

61. Henderson JT, Whitlock EP, O'Connor E, Senger CA, Thompson JH, Rowland MG, *Low-dose aspirin for prevention of morbidity and mortality from preeclampsia: A systematic evidence review for the U.S. Preventive Services Task Force*, Annals of Internal Medicine 2014, 160: 695-703

62. Lin R, Lei Y, Yuan Z, Ju H, Li D, *Angiotensinogen gene M235T and T174M polymorphisms and susceptibility of pre-eclampsia: A meta-analysis*, Annals of Human Genetics 2012, 76: 377-386

63. Song C, Xie S, Wang J, Lian J, Diao B, Tang Y, *Association of angiotensinogen gene polymorphisms and angiogenic factors with preeclampsia in chinese women*, Gynecologic and Obstetric Investigation 2013, 76: 64-68

64. Ward K, Hata A, Jeunemaitre X, Helin C, Nelson L, Namikawa C, Farrington PF, Ogasawara M, Suzumori K, Tomoda S, Berrebi S, Sasaki M, Corvol P, Lifton RP, Lalouel JM, *A molecular variant of angiotensinogen associated with preeclampsia*, Nature Genetics 1993, 4: 59-61

65. Inoue I, Nakajima T, Williams CS, Quackenbush J, Puryear R, Powers M, Cheng T, Ludwig EH, Sharma AM, Hata A, Jeunemaitre X, Lalouel JM, *A nucleotide substitution in the promoter of human angiotensinogen is associated with essential hypertension and affects basal transcription in vitro*, Journal of Clinical Investigation 1997, 99: 1786-1797

66. Cnattingius S, Reilly M, Pawitan Y, Lichtenstein P, *Maternal and fetal genetic factors account for most of familial aggregation of preeclampsia: A population-based Swedish cohort study*, American Journal of Medical Genetics 2004, 130 A: 365-371

67. Esplin MS, Fausett MB, Fraser A, Kerber R, Mineau G, Carrillo J, Varner MW, *Paternal and maternal components of the predisposition to preeclampsia*, New England Journal of Medicine 2001, 344: 867-872

68. Skjærven R, Vatten LJ, Wilcox AJ, Rønning T, Irgens LM, Lie RT, *Recurrence of pre-eclampsia across generations: Exploring fetal and maternal genetic components in a population based cohort*, British Medical Journal 2005, 331: 877-879

69. Lie RT, Rasmussen S, Brunborg H, Gjessing HK, Lie-Nielsen E, Irgens LM, *Fetal and maternal contributions to risk of pre-eclampsia: Population based study*, British Medical Journal 1998, 316: 1343-1347

70. Williams PJ, Pipkin FB, *The genetics of pre-eclampsia and other hypertensive disorders of pregnancy*, Best Practice and Research: Clinical Obstetrics and Gynaecology 2011, 25: 405-417

71. Nishimura H, *Angiotensin receptors — evolutionary overview and perspectives*, Comparative Biochemistry and Physiology Part A: Molecular & Integrative Physiology 2001, 128: 11-30

72. Rankin JC, Watanabe TX, Nakajima K, Broadhead C, Takei Y, *Identification of angiotensin I in a cyclostome, Lampetra fluviatilis*, Zoological Science 2004, 21: 173-179

73. Takei Y, Hasegawa Y, Watanabe TX, Nakajima K, Hazon N, *A novel angiotensin I isolated from an elasmobranch fish*, Journal of Endocrinology 1993, 139: 281-285

74. Takei Y, Joss JMP, Kloas W, Rankin JC, *Identification of angiotensin I in several vertebrate species: its structural and functional evolution*, General and Comparative Endocrinology 2004, 135: 286-292

75. Brown NJ, Vaughan DE, *Prothrombotic effects of angiotensin*, Advances in Internal Medicine 2000, 45: 419-429

76. Guron G, Friberg P, *An intact renin-angiotensin system is a prerequisite for normal renal development*, Journal of Hypertension 2000, 18: 123-137

77. Schieffer B, Schieffer E, Hilfiker-Kleiner D, Hilfiker A, Kovanen PT, Kaartinen M, Nussberger J, Harringer W, Drexler H, *Expression of angiotensin II and interleukin 6 in human coronary atherosclerotic plaques: Potential implications for inflammation and plaque instability*, Circulation 2000, 101: 1372-1378

78. Tamura T, Said S, Harris J, Lu W, Gerdes AM, *Reverse remodeling of cardiac myocyte hypertrophy in hypertension and failure by targeting of the renin-angiotensin system*, Circulation 2000, 102: 253-259

79. Van Kats JP, Danser AHJ, Van Meegen JR, Sassen LMA, Verdouw PD, Schalekamp MADH, *Angiotensin production by the heart: A quantitative study in pigs with the use of radiolabeled angiotensin infusions*, Circulation 1998, 98: 73-81

80. Van Kats JP, Schalekamp MADH, Verdouw PD, Duncker DJ, Danser AHJ, I*ntrarenal angiotensin II: Interstitial and cellular levels and site of production*, Kidney International 2001, 60: 2311-2317

81. Raghavendra V, Chopra K, Kulkarni SK, *Brain renin angiotensin system (RAS) in stress-induced analgesia and impaired retention*, Peptides 1999, 20: 335-342

82. Clausmeyer S, Stürzebecher R, Peters J, *An alternative transcript of the rat renin gene can result in a truncated prorenin that is transported into adrenal mitochondria*, Circulation Research 1999, 84: 337-344

83. Itskovitz J, Rubattu S, Levron J, Sealey JE, *Highest concentrations of prorenin and human chorionic gonadotropin in gestational sacs during early human pregnancy*, Journal of Clinical Endocrinology and Metabolism 1992, 75: 906-910

84. Sealey JE, Goldstein M, Pitarresi T, Kudlak TT, Glorioso N, Fiamengo SA, Laragh JH, *Prorenin secretion from human testis: No evidence for secretion of active renin or angiotensinogen*, Journal of Clinical Endocrinology and Metabolism 1988, 66: 974-978

85. Danser AHJ, Van Den Dorpel MA, Deinum J, Derkx FHM, Franken AAM, Peperkamp E, De Jong PTVM, Schalekamp MADH, *Renin, prorenin, and immunoreactive renin in vitreous fluid from eyes with and without diabetic retinopathy*, Journal of Clinical Endocrinology and Metabolism 1989, 68: 160-167

86. Ganten D, Hermann K, Unger T, Lang RE, *The tissue renin-angiotensin systems: Focus on brain angiotensin, adrenal gland and arterial wall*, Clinical and Experimental Hypertension - Part A Theory and Practice 1983, 5: 1099-1118

87. Hilgers KF, Veelken R, Müller DN, Kohler H, Hartner A, Botkin SR, Stumpf C, Schmieder RE, Gomez RA, *Renin uptake by the endothelium mediates vascular angiotensin formation*, Hypertension 2001, 38: 243-248

88. Larrue J, Demond-Henri J, Daret D, R*enin-angiotensin system in cultured human arterial smooth muscle cells*, Journal of Cardiovascular Pharmacology 1989, 14: S43-S45

89. Shenoy U, Cassis L, C*haracterization of renin activity in brown adipose tissue*, American Journal of Physiology - Cell Physiology 1997, 272: C989-C999

90. Cooper AC, Robinson G, Vinson GP, Cheung WT, Pipkin FB, *The localization and expression of the renin-angiotensin system in the human placenta throughout pregnancy*, Placenta 1999, 20: 467-474

91. Juillerat-Jeanneret L, Celerier J, Bernasconi CC, Nguyen G, Wostl W, Maerki HP, Janzer RC, Corvol P, Gasc JM, *Renin and angiotensinogen expression and functions in growth and apoptosis of human glioblastoma*, British Journal of Cancer 2004, 90: 1059-1068

92. Foundling SI, Cooper J, Watson FE, Pearl LH, Hemmings A, Wood SP, Blundell T, Hallett A, Jones DM, Sueiras J, Atrash B, Szelke M, C*rystallographic studies of reduced bond inhibitors complexed with an aspartic proteinase*, Journal of Cardiovascular Pharmacology 1987, 10: S59-S68

93. Dhanaraj V, Dealwis CG, Frazao C, Badasso M, Sibanda BL, Tickle IJ, Cooper JB, Driessen HPC, Newman M, Aguilar C, Wood SP, Blundell TL, Hobart PM, Geoghegan KF, Ammirati MJ, Danley DE, O'Connor BA, Hoover DJ, *X-ray analyses of peptide-inhibitor complexes define the structural basis of specificity for human and mouse renins*, Nature 1992, 357: 466-472

94. Imai T, Miyazaki H, Hirose S, Hori H, Hayashi T, Kageyama R, Ohkubo H, Nakanishi S, Murakami K, *Cloning and sequence analysis of cDNA for human renin precursor*, Proceedings of the National Academy of Sciences of the United States of America 1983, 80: 7405-7409

95. Tang J, James MNG, Hsu IN, Jenkins JA, Blundell TL, *Structural evidence for gene duplication in the evolution of the acid proteases*, Nature 1978, 271: 618-621

96. Morales R, Watier Y, Böcskei Z, *Human prorenin structure sheds light on a novel mechanism of its autoinhibition and on its non-proteolytic activation by the (pro)renin receptor*, Journal of Molecular Biology 2012, 421: 100-111

97. Van den Eijnden MMED, Saris JJ, De Bruin RJA, De Wit E, Sluiter W, Reudelhuber TL, Schalekamp MADH, Derkx FHM, Danser AHJ, *Prorenin accumulation and activation in human endothelial cells: Importance of mannose 6-phosphate receptors*, Arteriosclerosis, Thrombosis, and Vascular Biology 2001, 21: 911-916

98. Ingelfinger JR, Zuo WM, Fon EA, Ellison KE, Dzau VJ, *In situ hybridization evidence for angiotensinogen messenger RNA in the rat proximal tubule: An hypothesis for the intrarenal renin angiotensin system*, Journal of Clinical Investigation 1990, 85: 417-423

99. Danser JAH, Derkx FHM, Schalekamp MADH, Hense HW, Riegger GAJ, Schunkert H, *Determinants of interindividual variation of renin and prorenin concentrations: Evidence for a sexual dimorphism of (pro)renin levels in humans*, Journal of Hypertension 1998, 16: 853-862

100. Nguyen G, Delarue F, Burcklé C, Bouzhir L, Giller T, Sraer JD, P*ivotal role of the renin/prorenin receptor in angiotensin II production and cellular responses to renin*, Journal of Clinical Investigation 2002, 109: 1417-1427

101. Ellis V, Behrendt N, Dano K, *Plasminogen activation by receptor-bound urokinase: A kinetic study with both cell-associated and isolated receptor*, Journal of Biological Chemistry 1991, 266: 12752-12758

102. Batenburg WW, Krop M, Garrelds IM, De Vries R, De Bruin RJA, Burcklé CA, Müller DN, Bader M, Nguyen G, Danser AHJ, *Prorenin is the endogenous agonist of the (pro)renin receptor. Binding kinetics of renin and prorenin in rat vascular smooth muscle cells overexpressing the human (pro)renin receptor*, Journal of Hypertension 2007, 25: 2441-2453

103. Nabi AHMN, Biswas KB, Nakagawa T, Ichihara A, Inagami T, Suzuki F, *Prorenin has high affinity multiple binding sites for (pro)renin receptor*, Biochimica et Biophysica Acta - Proteins and Proteomics 2009, 1794: 1838-1847

104. Campbell DJ, *Critical Review of Prorenin and (Pro)renin Receptor Research*, Hypertension 2008, 51: 1259-1264

105. Gimenez-Roqueplo AP, Célérier J, Schmid G, Corvol P, Jeunemaitre X, R*ole of cysteine residues in human angiotensinogen: Cys 232 is required for angiotensinogen-pro major basic protein complex formation*, Journal of Biological Chemistry 1998, 273: 34480-34487

106. Van Gent D, Sharp P, Morgan K, Kalsheker N, *Serpins: Structure, function and molecular evolution*, The International Journal of Biochemistry & Cell Biology 2003, 35: 1536-1547

107. Célérier J, Schmid G, Le Caer JP, Gimenez-Roqueplo AP, Bur D, Friedlein A, Langen H, Corvol P, Jeunemaitre X, C*haracterization of a human angiotensinogen cleaved in its reactive center loop by a proteolytic activity from Chinese hamster ovary cells*, Journal of Biological Chemistry 2000, 275: 10648-10654

108. Janciauskiene S, *Conformational properties of serine proteinase inhibitors (serpins) confer multiple pathophysiological roles*, Biochimica et Biophysica Acta - Molecular Basis of Disease 2001, 1535: 221-235

109. Kageyama R, Ohkubo H, Nakanishi S, *Primary structure of human preangiotensinogen deduced from the cloned cDNA sequence*, Biochemistry 1984, 23: 3603-3609

110. Lynch KR, Peach MJ, *Molecular biology of angiotensinogen*, Hypertension 1991, 17: 263-269

111. Gould AB, Green D, *Kinetics of the human renin and human substrate reaction*, Cardiovascular Research 1971, 5: 86-89

112. Poulsen K, Jacobsen J, *Is angiotensinogen a renin inhibitor and not the substrate for renin?*, Journal of Hypertension 1986, 4: 65-69

113. Burton J, Quinn T, *The amino-acid residues on the C-terminal side of the cleavage site of angiotensinogen influence the species specificity of reaction with renin*, Biochimica et Biophysica Acta - Protein Structure and Molecular Enzymology 1988, 952: 8-12

114. Barrett JD, Eggena P, Hidaka H, Sambhi MP, *In vitro inhibition of renin by human des-angiotensin I renin substrate*, Journal of Clinical Endocrinology and Metabolism 1979, 48: 96-100

115. Wilkinson-Berka JL, Tan G, Jaworski K, Ninkovic S, *Valsartan but not atenolol improves vascular pathology in diabetic Ren-2 rat retina*, American Journal of Hypertension 2007, 20: 423-430

116. Anton L, Brosnihan KB, *Systemic and uteroplacental renin--angiotensin system in normal and pre-eclamptic pregnancies*, Therapeutic Advances in Cardiovascular Disease 2008, 2: 349-362

117. Cuddihy SL, Baty JW, Brown KK, Winterbourn CC, Hampton MB, P*roteomic detection of oxidized and reduced thiol proteins in cultured cells*, Methods in Molecular Biology 2009, 519: 363-375

118. Eaton P, *Protein thiol oxidation in health and disease: Techniques for measuring disulfides and related modifications in complex protein mixtures*, Free Radical Biology and Medicine 2006, 40: 1889-1899

119. Rhee SG, Bae YS, Lee SR, Kwon J, *Hydrogen peroxide: a key messenger that modulates protein phosphorylation through cysteine oxidation*, Science"s STKE [electronic resource] : signal transduction knowledge environment 2000, 2000: PE1

120. McDonagh B, D*iagonal electrophoresis for detection of protein disulphide bridges*, Methods in Molecular Biology (Clifton, NJ) 2009, 519: 305-310

121. Hinck AP, Truckses DM, Markley JL, *Engineered disulfide bonds in Staphylococcal nuclease: Effects on the stability and conformation of the folded protein*, Biochemistry 1996, 35: 10328-10338

122. Deshmukh L, Meller N, Alder N, Byzova T, Vinogradova O, *Tyrosine phosphorylation as a conformational switch: A case study of integrin β 3 cytoplasmic tail*, Journal of Biological Chemistry 2011, 286: 40943-40953

123. Ryu SE, *Structural mechanism of disulphide bond-mediated redox switches,* Journal of Biochemistry 2012, 151: 579-588

124. Choi HJ, Kim SJ, Mukhopadhyay P, Cho S, Woo JR, Storz G, Ryu SE, *Structural basis of the redox switch in the OxyR transcription factor*, Cell 2001, 105: 103-113

125. Liu W, Wen W, Wei Z, Yu J, Ye F, Liu CH, Hardie RC, Zhang M, T*he INAD scaffold is a dynamic, redox-regulated modulator of signaling in the Drosophila eye*, Cell 2011, 145: 1088-1101

126. Streatfeild-James RMA, Williamson D, Pike RN, Tewksbury D, Carrell RW, Coughlin PB, *Angiotensinogen cleavage by renin: Importance of a structurally constrained N-terminus*, FEBS Letters 1998, 436: 267-270

127. Bujold E, Roberge S, Lacasse Y, Bureau M, Audibert F, Marcoux S, Forest JC, Giguère Y, *Prevention of preeclampsia and intrauterine growth restriction with aspirin started in early pregnancy: A meta-analysis*, Obstetrics and Gynecology 2010, 116: 402-414

128. Gómez-Arriaga PI, Herraiz I, López-Jiménez EA, Gómez-Montes E, Denk B, Galindo A, *Uterine artery Doppler and sFlt-1/PlGF ratio: Usefulness in diagnosis of pre-eclampsia*, Ultrasound in Obstetrics and Gynecology 2013, 43: 525-532

129. Kolla V, Jenö P, Moes S, Lapaire O, Hoesli I, Hahn S, *Quantitative proteomic (iTRAQ) analysis of 1st trimester maternal plasma samples in pregnancies at risk for preeclampsia*, Journal of Biomedicine and Biotechnology 2012, 2012: 305964

130. Spencer K, Cowans NJ, Stamatopoulou A, *ADAM12s in maternal serum as a potential marker of pre-eclampsia*, Prenatal Diagnosis 2008, 28: 212-216

131. Khosrowbeygi A, Ahmadvand H, *Positive correlation between serum levels of adiponectin and homocysteine in pre-eclampsia*, Journal of Obstetrics and Gynaecology Research 2013, 39: 641-646

132. Zeybek YG, Günel T, Benian A, Aydinli K, Kaleli S, C*linical evaluations of cell-free fetal DNA quantities in pre-eclamptic pregnancies*, Journal of Obstetrics and Gynaecology Research 2013, 39: 632-640

133. Anton L, Olarerin-George AO, Schwartz N, Srinivas S, Bastek J, Hogenesch JB, Elovitz MA, m*iR-210 inhibits trophoblast invasion and is a serum biomarker for preeclampsia*, American Journal of Pathology 2013, 183: 1437-1445

134. Doridot L, Houry D, Gaillard H, Chelbi ST, Barbaux S, Vaiman D, *miR-34a expression, epigenetic regulation, and function in human placental diseases*, Epigenetics 2014, 9: 142-151

135. Southcombe JH, Benton SJ, Hu Y, von Dadelszen P, Child T, Snider JV, Redman CWG, Sargent IL, Granne I, *Measurement of sST2 is comparable to PlGF in the diagnosis of early-onset pre-eclampsia*, Pregnancy Hypertension 2013, 3: 115-117

136. Saboor M, Moinuddin M, Ilyas S, *New horizons in platelets flow cytometry*, Malaysian Journal of Medical Sciences 2013, 20: 63-67

137. Akolekar R, Syngelaki A, Beta J, Kocylowski R, Nicolaides KH, M*aternal serum placental protein 13 at 11-13 weeks of gestation in preeclampsia*, Prenatal Diagnosis 2009, 29: 1103-1108

138. Spencer K, Cowans NJ, Nicolaides KH, *Low levels of maternal serum PAPP-A in the first trimester and the risk of pre-eclampsia*, Prenatal Diagnosis 2008, 28: 7-10

139. Kim SY, Ryu HM, Yang JH, Kim MY, Han JY, Kim JO, Chung JH, Park SY, Lee MH, Kim DJ, *Increased sFlt-1 to PlGF ratio in women who subsequently develop preeclampsia*, Journal of Korean Medical Science 2007, 22: 873-877

140. Zhao M, Yin Y, Guo F, Wang J, Wang K, Chen Q, *Placental expression of VEGF is increased in pregnancies with hydatidiform mole: Possible association with developing very early onset preeclampsia*, Early Human Development 2013, 89: 583-588

141. Kastritis PL, Bonvin AMJJ, *On the binding affinity of macromolecular interactions: Daring to ask why proteins interact*, Journal of the Royal Society Interface 2013, 10: 20120835

142. Rich RL, Myszka DG, *Grading the commercial optical biosensor literature - Class of 2008: 'The Mighty Binders'*, Journal of Molecular Recognition 2010, 23: 1-64

143. Benson JR, Hare PE, *o Phthalaldehyde: Fluorogenic detection of primary amines in the picomole range. Comparison with fluorescamine and ninhydrin*, Proceedings of the National Academy of Sciences of the United States of America 1975, 72: 619-622

144. Roth M, *Fluorescence reaction for amino acids*, Analytical Chemistry 1971, 43: 880-882

145. Myszka DG, Morton TA, *CLAMP©: a biosensor kinetic data analysis program*, Trends in Biochemical Sciences 1998, 23: 149-150

146. Eswar N, Webb B, Marti-Renom MA, Madhusudhan MS, Eramian D, Shen MY, Pieper U, Sali A *Comparative protein structure modeling using MODELLER*, Current Protocols in Protein Science 2007, Chapter 2

147. Hess B, Kutzner C, Van Der Spoel D, Lindahl E, *GROMACS 4: Algorithms for highly efficient, load-balanced, and scalable molecular simulation,* Journal of Chemical Theory and Computation 2008, 4: 435-447

148. Schmid N, Eichenberger AP, Choutko A, Riniker S, Winger M, Mark AE, Van Gunsteren WF, *Definition and testing of the GROMOS force-field versions 54A7 and 54B7*, European Biophysics Journal 2011, 40: 843-856

149. Berendsen HJC, Postma JPM, Van Gunsteren WF, Hermans J, I*nteraction models for water in relation to protein hydration*. Edited by Pullman B. Springer Netherlands, 1981, p. pp. 331-342

150. Berendsen HJC, Postma JPM, Van Gunsteren WF, Dinola A, Haak JR, *Molecular dynamics with coupling to an external bath*, The Journal of Chemical Physics 1984, 81: 3684-3690

151. Tironi IG, Sperb R, Smith PE, Van Gunsteren WF, *A generalized reaction field method for molecular dynamics simulations*, The Journal of Chemical Physics 1995, 102: 5451-5459

152. Heinz TN, Van Gunsteren WF, Hünenberger PH, *Comparison of four methods to compute the dielectric permittivity of liquids from molecular dynamics simulations*, Journal of Chemical Physics 2001, 115: 1125-1136

153. Hess B, Bekker H, Berendsen HJC, Fraaije JGEM, *LINCS: A linear constraint solver for molecular simulations*, Journal of Computational Chemistry 1997, 18: 1463-1472

154. Miyamoto S, Kollman PA, *SETTLE*: *An analytical version of the SHAKE and RATTLE algorithm for rigid water models*, Journal of Computational Chemistry 1992, 13: 952-962

155. Bakan A, Meireles LM, Bahar I, *ProDy:* P*rotein dynamics inferred from theory and experiments*, Bioinformatics 2011, 27: 1575-1577

156. Hunter JD: *Matplotlib*: *A 2D graphics environment*, Computing in Science and Engineering 2007, 9: 99-104

157. DeLano WL, T*he PyMOL molecular graphics system*, 2002

158. Humphrey W, Dalke A, Schulten K, *VMD: Visual molecular dynamics*, Journal of Molecular Graphics 1996, 14: 33-38

159. Bouhnik J, Clauser E, Strosberg D, Frenoy JP, Menard J, Corvol P, *Rat angiotensinogen and des(angiotensin I)angiotensinogen: Purification, characterization, and partial sequencing*, Biochemistry 1981, 20: 7010-7015

160. Grise C, Boucher R, Thibault G, Genest J, *Formation of angiotensin II by tonin from partially purified human angiotensinogen*, Canadian Journal of Biochemistry 1981, 59: 250-255

161. Ebihara A, Kondou T, Mizuno S, Nakagawa T, Nasir UM, Inui Y, Fukamizu A, Suzuki F, Nakamura Y, Murakami K, *Molecular properties of recombinant ovine angiotensinogen*, Biomedical Research 2000, 21: 247-254

162. Kunapuli SP, Prasad GL, Kumar A, *Expression of human angiotensinogen cDNA in Escherichia coli*, Journal of Biological Chemistry 1987, 262: 7672-7675

163. Hall JP, *Applying Fusion Protein Technology to E.coli*, Biopharm International 2007

164. Brondyk WH, *Chapter 11 Selecting an Appropriate Method for Expressing a Recombinant Protein.* Methods in Enzymology 2009, 463: 131-147

165. Pearce MC, Cabrita LD, *Production of recombinant serpins in Escherichia coli*. Methods in Enzymology 2011, 501: 13-28

166. McCarthy AA, Haebel PW, Törrönen A, Rybin V, Baker EN, Metcalf P, *Crystal structure of the protein disulfide bond isomerase, DsbC, from Escherichia coli*, Nature Structural Biology 2000, 7: 196-199

167. Li SJ, Hochstrasser M, *A new protease required for cell-cycle progression in yeast*, Nature 1999, 398: 246-251

168. Saitoh H, Robert T P, Dasso M, *SUMO-1: Wrestling with a new ubiquitin-related modifier*, Trends in Biochemical Sciences 1997, 22: 374-376

169. Pan SH, Malcolm BA, R*educed background expression and improved plasmid stability with pET vectors in BL21 (DE3)*, BioTechniques 2000, 29: 1234-1238

170. Samuelson J, *Bacterial Systems*. Edited by Wiley-VCH Verlag GmbH & Co. KGaA, 2011, p. pp. 11-35

171. Studier FW, *Protein production by auto-induction in high density shaking cultures*, Protein Expression and Purification 2005, 41: 207-234

172. Peternel Š, *Bacterial cell disruption: A crucial step in protein production*, New Biotechnology 2013, 30: 250-254

173. Ulyanov D, Bowler BE, Eaton GR, Eaton SS, *Electron-electron distances in spin-labeled low-spin metmyoglobin variants by relaxation enhancement*, Biophysical Journal 2008, 95: 5306-5316

174. Leslie AG, Moody PC, Shaw WV, *Structure of chloramphenicol acetyltransferase at 1.75-A resolution*, Proceedings of the National Academy of Sciences 1988, 85: 4133-4137

175. Otto A, *Excitation of nonradiative surface plasma waves in silver by the method of frustrated total reflection*, Zeitschrift für Physik 1968, 216: 398-410

176. Daghestani HN, Day BW, *Theory and applications of surface plasmon resonance, resonant mirror, resonant waveguide grating, and dual polarization interferometry biosensors*, Sensors 2010, 10: 9630-9646

177. Abdiche YN, Lindquist KC, Pinkerton A, Pons J, Rajpal A, *Expanding the ProteOn XPR36 biosensor into a 36-ligand array expedites protein interaction analysis*, Analytical Biochemistry 2011, 411: 139-151

178. Billakanti JM, Fee CJ, Lane FR, Kash AS, Fredericks R, S*imultaneous, quantitative detection of five whey proteins in multiple samples by surface plasmon resonance*, International Dairy Journal 2010, 20: 96-105

179. Bravman T, Bronner V, Nahshol O, Schreiber G, *The ProteOn XPR36™ array system—High throughput kinetic binding analysis of biomolecular interactions*, Cellular and Molecular Bioengineering 2008, 1: 216-228

180. Fee C, *Label-free, real-time interaction and adsorption analysis 1: Surface plasmon resonance.* Edited by Gerrard JA. Humana Press, 2013, p. pp. 287-312

181. Van Der Merwe PA, *Surface plasmon resonance*. Edited by Oxford University Press: New York, NY, USA, 2001, p. pp. 137-170

182. Biswas KB, Nabi AN, Arai Y, Nakagawa T, Ebihara A, Ichihara A, Watanabe T, Inagami T, Suzuki F, A*liskiren binds to renin and prorenin bound to (pro)renin receptor in vitro,* Hypertension Research 2010, 33: 1053-1059

183. Cohen P, Simon D, Badouaille G, Mani JC, Portefaix JM, Pau B, *New monoclonal antibodies directed against the propart segment of human prorenin as a tool for the exploration of prorenin conformation*, Journal of Immunological Methods 1995, 184: 91-100

184. Fischer MJ, *Amine coupling through EDC/NHS: a practical approach*, Methods in molecular biology (Clifton, NJ) 2010, 627: 55-73

185. Vacha P, Zuskova I, Bumba L, Herman P, Vecer J, Obsilova V, Obsil T, *Detailed kinetic analysis of the interaction between the FOXO4–DNA-binding domain and DNA*, Biophysical Chemistry 2013, 184: 68-78

186. Christensen LLH, *Theoretical analysis of protein concentration determination using biosensor technology under conditions of partial mass transport limitation*, Analytical Biochemistry 1997, 249: 153-164

187. Li H, Robertson AD, Jensen JH, *Very fast empirical prediction and rationalization of protein pKa values*, Proteins: Structure, Function, and Bioinformatics 2005, 61: 704-721

188. Green DW, Aykent S, Gierse JK, Zupec ME, *Substrate specificity of recombinant human renal renin: effect of histidine in the P 2 subsite on pH dependence*, Biochemistry 1990, 29: 3126-3133

189. O'Shannessy DJ, Wilchek M, *Review. Immobilization of glycoconjugates by their oligosaccharides: Use of hydrazido-derivatized matrices*, Analytical Biochemistry 1990, 191: 1-8

190. Baneyx F, *Recombinant protein expression in Escherichia coli*, Current Opinion in Biotechnology 1999, 10: 411-421

191. Samuelson JC, *Recent developments in difficult protein expression: A guide to E. coli strains, promoters, and relevant host mutations*. Methods in Molecular Biology 2011, 705: 195-209

192. Wong SS, *Chemistry of protein conjugation and cross-linking*. Edited by CRC press, 1991

193. Odom OW, Kudlicki W, Kramer G, Hardesty B, *An effect of polyethylene glycol 8000 on protein mobility in sodium dodecyl sulfate-polyacrylamide gel electrophoresis and a method for eliminating this effect*, Analytical Biochemistry 1997, 245: 249-252

194. Straume M, Johnson ML, *Monte Carlo method for determining complete confidence probability distributions of estimated model parameters*. Edited by Ludwig Brand MLJ. Academic Press, 1992, p. pp. 117-129

195. Hansson T, Oostenbrink C, Van Gunsteren W, *Molecular dynamics simulations*, Current Opinion in Structural Biology 2002, 12: 190-196

196. Meller Ja, *Molecular Dynamics*. Edited by John Wiley & Sons, Ltd, 2001

197. Binder K, Horbach J, Kob W, Paul W, Varnik F, *Molecular dynamics simulations*, Journal of Physics: Condensed Matter 2004, 16: S429

198. Duan Y, Kollman PA, *Pathways to a protein folding intermediate observed in a 1-microsecond simulation in aqueous solution*, Science 1998, 282: 740-744

199. Brás NF, Fernandes PA, Ramos MJ, *Discovery of new sites for drug binding to the hypertension-related renin-angiotensinogen complex*, Chemical Biology and Drug Design 2014, 83: 427-439

200. Green L, *Transgenic mouse strains as platforms for the successful discovery and development of human therapeutic monoclonal antibodies*, Current Drug Discovery Technologies 2014, 11: 74-84

201. Bee C, Abdiche YN, Stone DM, Collier S, Lindquist KC, Pinkerton AC, Pons J, Rajpal A, *Exploring the dynamic range of the kinetic exclusion assay in characterizing antigen-antibody interactions*, PLoS ONE 2012, 7: e36261

202. Kurfürst MM, *Detection and molecular weight determination of polyethylene glycol-modified hirudin by staining after sodium dodecyl sulfate-polyacrylamide gel electrophoresis*, Analytical Biochemistry 1992, 200: 244-248